Engineering and Urology Society

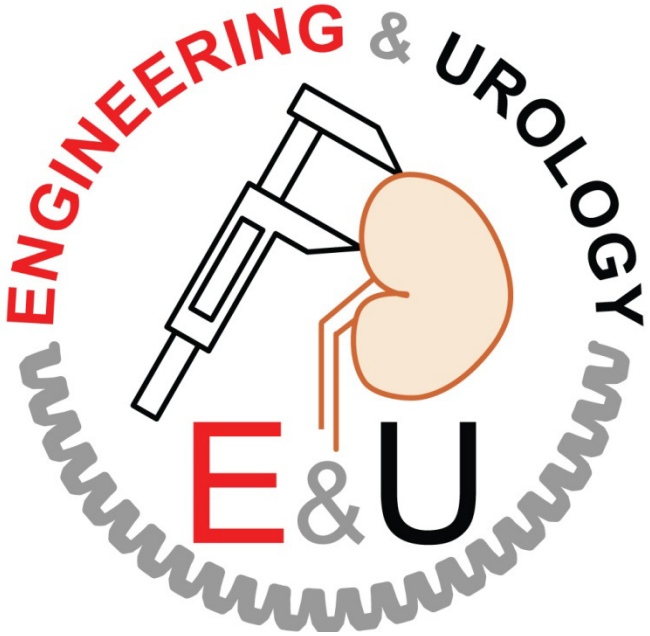

26th Annual Meeting

Saturday May 14th, 2011

Grand Hyatt Washington
Washington, DC

http://engineering-urology.org/

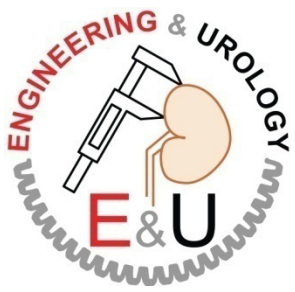

Following a long tradition, the Annual meeting of the Engineering and Urology Society offers the delegates of the American Urological Association an opportunity to present and learn about the latest research developments in urologic technology. Among other medical specialties, Urology has traditionally been at the forefront of technology innovation and continues to adapt or develop novel technologies at a fast pace. The Engineering and Urology Society offers a unique forum where engineering innovation meets clinical demand in a collaboration that leads to unparalleled exchange of ideas.

This year's meeting is organized by the program chairmen Frank Keeley (Bristol, UK) and Evangelos Liatsikos (Patras, Greece). The first session will focus on novel techniques for nephron preservation during laparoscopic partial nephrectomy as well as the application of cooling for robotic radical prostatectomy. Additional talks will discuss a range of topics that are just beyond the horizon including next daVinci instruments, Shark Skin Stents, and innovations in focal therapy. The focus then shifts to quality control in Minimally Invasive Surgery, establishing quality metrics and defining standards for reporting of complications and outcomes. Discussions of novel suturing materials and techniques are also presented. The afternoon sessions highlight advances and debates in the areas of Laparoendoscopic Single Site Surgery and Natural Orifice Translumenal Endoscopic Surgery. Talks present the best approaches, suitable instrumentation and the latest techniques. Additional symposiums will be held for Image Guided Therapy and Stents. Lastly, engineers and clinicians will present their latest research in the two afternoon poster session.

The review of the abstracts for the poster sessions has been performed online by a group of 56 reviewers from around the world. Each paper received between 14 and 19 reviews. We would like to thank the reviewers, listed at the end of this program book, for their constructive comments and essential contribution to the quality of the meeting.

Based on the peer review, the Best Paper Award goes to abstract "Modeling of magnetic tools for use with superparamagnetic particles for magnetic stone extraction" from the University of Texas, and the Outstanding Paper Award to abstract "Computer Simulations of Thermal Damage to the Human Vas Deferens During Noninvasive Laser Vasectomy" from the University of North Carolina at Charlotte.

We gratefully thank all reviewers for their hard work, objective scoring, and contribution to the success of the meeting. The society presents Best Reviewer Awards for the online review process, based on the grading performance and the number of reviews performed. The Best Reviewer Awards are presented to Drs. Thorsten Bach, Brian Eisner, Mohamed Elkoushy, Avinash Kambadakone, Watid Karnjanawanichkul, Bodo Knudsen, Thomas Lawson, Sutchin Patel, Cristian Surcel, Hessel Wijkstra, and Kevin Zorn.

We congratulate all award winners and welcome all urologists, engineers, and scientists to join us for this unique multi and interdisciplinary experience. As always, we are grateful to Dr. George Nagamatsu, the founder and first president of the society for setting the foundations based upon which we meet.

Please visit the website http://engineering-urology.org for a complete version of this program including the abstracts presented. These abstracts will also be published in the Journal of Endourology. Previous years abstracts appeared in the December 2010 (pp. 2093-2157), June 2009 (pp. 1025-1082), and November 2008 (2583-2640) issues.

Thank you for your continued scientific support,

Manoj Monga
Hessel Wijkstra
Dan Stoianovici

CONTINUING MEDICAL EDUCATION

Accreditation: The American Urological Association Education & Research, Inc. (AUAER) is accredited by the Accreditation Council for Continuing Medical Education (ACCME) to provide continuing medical education for physicians.

Credit Designation: The American Urological Association Education & Research, Inc. designates this live activity for a maximum of 7.75 AMA *PRA Category 1 Credit(s)™*. Physicians should claim only the credit commensurate with the extent of their participation in the activity.

The AUAER takes responsibility for the content, quality, and scientific integrity of this CME activity.

AUAER Disclosure Policy: As a provider accredited by the ACCME, the AUAER must ensure balance, independence, objectivity and scientific rigor in all its activities.

All faculty and program planners participating in an educational activity provided by the AUAER are required to disclose to the provider any relevant financial relationships with any commercial interest. The AUAER must determine if the faculty's relationships may influence the educational content with regard to exposition or conclusion and resolve any conflicts of interest prior to the commencement of the educational activity. The intent of this disclosure is not to prevent faculty with relevant financial relationships from serving as faculty, but rather to provide members of the audience with information on which they can make their own judgments.

Off-label or Unapproved Use of Drugs or Devices: It is the policy of the AUAER to require the disclosure of all references to off-label or unapproved uses of drugs or devices prior to the presentation of educational content. The audience is advised that this continuing medical education activity may contain reference(s) to off-label or unapproved uses of drugs or devices. Please consult the prescribing information for full disclosure of approved uses.

Disclaimer: The opinions and recommendations expressed by faculty, authors, and other experts whose input is included in this program are their own and do not necessarily represent the viewpoint of the AUAER.

Evidence Based Content: As a provider of continuing medical education accredited by the ACCME, it is the policy of the AUAER to review and certify that the content contained in this CME activity is valid, fair, balanced, scientifically rigorous, and free of commercial bias.

Special Assistance/Dietary Needs
The American Urological Association Education & Research, Inc. (AUAER), an organization accredited for Continuing Medical Education (CME), complies with the Americans with Disabilities Act §12112(a). If any participant is in need of special assistance or has any dietary restrictions, a written request should be submitted at least one month in advance. For additional assistance with your request please call 800-908-9414.

FACULTY DISCLOSURES:

Abbou, Clement-Claude: Nothing to disclose
Ahlering, Thomas E.: Intuitive Surgical: Meeting Participant or Lecturer, Consultant or Advisor
Best, Sara: Nothing to disclose
Cadeddu, Jeffrey Anthony: Ethicon Endosurgery, Inc.: Scientific Study or Trial, Other: Intellectual property licensing: MedTrials, Inc: Consultant or Advisor
Cherullo, Ed: Nothing to disclose
Clayman, Ralph: Applied Urology: Investment interest; Boston Scientific: Other: royalties; Cook Urological: Consultant or Advisor; Greenwald, Inc. Other: royalty, Orthopedic Services Inc. (OSI): Other: royalty; Vascular Technology, Inc.: Other: royalty
de la Rosette, Jean: BSC: Consultant or Advisor
Desai, Mihir: Baxter, Inc.: Consultant or Advisor; Hansen Medical: Consultant or Advisor
Droupy, Stephane: Bayer Shering: Consultant or Advisor; Hansen Medical: Consultant or Advisor
Gettman, Matthew Thomas: Nothing to disclose
Gill, Inderbir Singh: Hansen Medical: Investment Interest
Goezen, A.: ESUT/EULIS Session of 26th Annual Engineering & Urology Meeting: Meeting Participant or Lecturer
Herrell, III, S. Duke: Aesculap, Inc.: Consultant or Advisor; Covidien Surgical Devices: Consultant or Advisor; Galil Medical: Consultant or Advisor; Veran Medical Technologies: Other: Stockholder; Wilex, Investigator
Humphreys, Mitchell R.: Lumenis, Inc. Consultant or Advisor; Boston Scientific Inc.: Consultant or Advisor
Hruza, Marcel: Nothing to disclose
Irwin, Brian Hilbert: Nothing to disclose
Kaouk, Jihad H: Covidien: Meeting Participant or Lecturer; Endocare: Meeting Participant or Lecturer; Intuitive Surgical: Other: proctoring surgery
Keeley, Francis: Nothing to disclose
Kim, Hyung-Joo: Johns Hopkins Medical Institute, Urology-Robotics Lab: Investigator
Klein, Jan-T: Nothing to disclose
Knoll, Thomas: Nothing to disclose
Laguna, Pilar: Nothing to disclose
Landman, Jaime: Cook Urological: Consultant or Advisor; Scientific Study or Trial; Meeting Participant or Lecturer, Other: Royalty Agreement; Galil Medical: Scientific Study or Trial; Consultant or Advisor
Liatsikos, Evangelos N: Nothing to disclose
Marberger, Michael: Focus Surgery: Scientific Study or Trial; GP-Pharma Barcelona:Consultant or Advisor: GSK: Consultant or Advisor, Meeting Participant or Lecturer, Scientific Study or Trial, Meeting Participant or Lecturer, Scientific Study or Trial, Meeting Participant or Lecturer, Consultant or Advisor; R. Wolf: Consultant or Advisor; R. Wolf, Germany: Consultant or Advisor
Osther, Palle: Nothing to disclose
Pini, Giovannalberto: Nothing to disclose
Ponsky, Lee Evan: Accuray: Scientific Study or Trial, Other: Data Safety Monitoring Board; Tengion Inc.: Other: Data Safety Monitoring Board; US Endoscopy: Consultant or Advisor, Varian Medical System: Consultant or Advisor
Rao, Pradeep Prabhakar.: Nothing to disclose
Raman, Jay D.: Nothing to disclose
Rane, Abhay: Nothing to disclose
Rassweiler, Jens: Nothing to disclose
Shalhav, Arieh Leib: Nothing to disclose
Stein, Robert Jeffrey: Applied Medical: Meeting Participant or Lecturer
Stoianovici, Dan: Nothing to disclose
van Velthoven, Roland F.P.: Nothing to disclose
White, Wesley Matthew: Pfizer: Meeting Participant or Lecturer

SPONSORS

The Engineering and Urology Society thanks the following companies for their support of this course:

Boston Scientific Corp, Inc.

C.R. Bard, Inc.

Minimally Invasive Devices, Inc.

Minimally Invasive Devices, Inc. (MID) was founded by a Urologist in 2007, and is a venture backed early stage medical device company. MID has developed the FloShield laparoscopic visualization system, the first device that prevents debris and condensation formed during laparoscopic surgery from settling on the lens of the laparoscope. FloShield creates a "vortex" of CO2 using gas from the insufflator to keep particles and fluid away from the lens surface so surgeons can operate continuously without removing the lens for cleaning. The FloShield franchise consists of FloShield-10mm, FloShield-5mm, FloPort access system, and the Flo-X biocompatible wash.

Percutaneous Systems, Inc.

PercSys® develops, manufactures, and commercializes innovative medical devices designed to make kidney stone procedures easier, less traumatic, and more effective. The company's PercSys Accordion® and Accordion CoAx® stone management devices are designed to prevent migration of stones and fragments during lithotripsy and to facilitate fragment removal following the treatment.

EXHIBITORS

Cook Medical

Cook Medical was one of the first companies to help popularize interventional medicine, pioneering many of the devices now commonly used worldwide to perform minimally invasive medical procedures. Today, the company integrates minimally invasive medical device design, biopharma, gene and cell therapy, and biotech to enhance patient safety and improve clinical outcomes in the fields of aortic intervention; interventional cardiology; critical care medicine; gastroenterology; radiology, peripheral vascular, bone access and oncology; surgery and soft tissue repair; urology; and assisted reproductive technology, gynecology and high-risk obstetrics. Founded in 1963 and operated as a family-held private corporation, Cook is a past winner of the prestigious Medical Device Manufacturer of the Year Award from Medical Device & Diagnostic Industry magazine.

Gyrus ACMI, Inc.

Olympus, which incorporates surgical market leader Gyrus ACMI, is transforming the future of healthcare to help Urologists improve outcomes and enhance quality of life for their patients by enabling less invasive procedures with innovative diagnostic and therapeutic solutions. We offer advanced HD visualization with Narrow Band Imaging (NBI), best-in-class, advanced bipolar energy tissue treatment and comprehensive stone management solutions including laser and ultrasonic technologies with a broad line of access, retrieval and drainage single-use devices. Our Laparo-Endoscopic Single-Site (LESS) surgery platform of products includes single-port access devices, deflectable tip scopes with HD visualization and versatile bipolar and ultrasonic energy.

PROGRAM

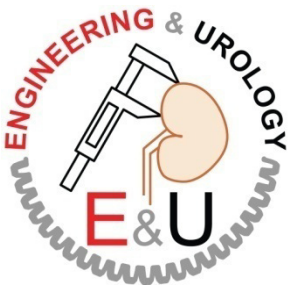

26th Annual Meeting
Saturday May 14th, 2011
Grand Hyatt Washington
Room: Constitution A & B
Washington, DC

Program Chairmen: Evangelos Liatsikos and Francis Keeley

7:00 – 7:15	**Stryker Fellow Report**	Hyung-Joo Kim
7:20 –8:20	**Session 1: ORGAN PRESERVATION**	**Evangelos Liatsikos** **Francis Keeley**
7:20 AM	"Zero-Ilschemia" Partial Nephrectomy: Robotic & Laparoscopic Technique	Inderbir Gill
7:35 AM	Pharmacological Protection during Laparoscopic Partial Nephrectomy	Evangelos Liatsikos
7:50 AM	Cooling during Laparoscopic Partial Nephrectomy	Arieh Shalhav
8:05 AM	Cooling during Robotic Radical Prostatectomy	Thomas Ahlering
8:30 – 9:30	**Session 2:**	**Evangelos Liatsikos** **Francis Keeley**
8:30 AM	Beyond daVinci	Ralph Clayman
8:45 AM	Shark Skin Stents and Catheters	Jaime Landman
9:00 AM	Holmium Laser Radical Prostatectomy	Mitchell Humphreys
9:15 AM	Innovations in Focal Therapy	Michael Marberger
9:40 – 11:40	**Session 3: ESUT SESSION – QUALITY CONTROL IN MIS**	**Evangelos Liatsikos** **Francis Keeley** **Palle Osther**
9:40 AM	What is the Role of the Clavien System in Endourology?	Jean de la Rosette Marcel Hruza
9:55 AM	How far should Live Surgery Session be part of Scientific Meetings?	Roland van Velthoven
10:10 AM	Auditing & Quality Indicators in Endourology & Laparoscopy	Thomas Knoll
10:25 AM	Objective and Subjective Scar Assessment	Giovannalberto Pini
10:40 AM	3D/CT analysis of neurovascular anatomy	Stephane Droupy
10:55 AM	New Suturing Devices (Endosew/Terumo)	Roland van Velthoven Jan Klein
11:10 AM	Barbed Suture in Urology	Ali Goezen Pilar Laguna Claude Abbou
11:25 AM	ETHOS Platform for Laparoscopy	Jens Rassweiler
11:45–12:00	**AWARDS PRESENTATION**	**Dan Stoianovici**
11:50AM	Best Paper Award: Modeling of Magnetic Tools for use with Superparamagnetic Particles for Magnetic Stone Extraction	Raul Fernandez Yung Khan Tan
12:00 –1:00 PM	**LUNCH** Room Constitution CDE & Corridors	

1:00-2:30 PM **Session 4: LAPAROENDOSCOPIC SINGLE SITE SURGERY AND NATURAL ORIFICE TRANSLUMENAL ENDOSCOPIC SURGERY (LESS AND NOTES)**

1:00-1:30 PM	**DEBATES**	**Abhay Rane**
1:00 PM	Robotic LESS is Better than Conventional LESS	Pro: Jihad Kaouk Con: Pradeep Rao
1:10 PM	LESS for Cancer Makes Sense	Pro: Lee Ponsky Con: Jaime Landman
1:20 PM	Small Port Surgery is Better than LESS	Pro: Duke Herrell Con: Wesley White
1:30-1:50 PM	**PANEL DISCUSSION: SUCCESSFUL LESS NUANCES**	**Lee Ponsky**
1:30 PM	Access: Reusable vs. Custom Built Trocars. Pros & Cons.	Mihir Desai
1:35 PM	Instruments	Francis Keeley
1:40 PM	Optics	Robert Stein
1:45 PM	Dissection/Retraction	Sara Best
1:50-2:25 PM	**TALKS**	**Matthew Gettman**
1:50 PM	Little LESS	Ed Cherullo
1:57 PM	Pitfalls in LESS	Jay Raman
2:04 PM	What's New in LESS	Inderbir Gill
2:11 PM	What's New in NOTES	Mitchell Humphreys
2:18 PM	White paper on LESS trials, Inclusion Criteria	Brian Irwin

WORKING GROUPS

2:35-4:30 PM Urology NOTES Working Group Business Meeting
Room: Constitution A & B

2:00-4:00 PM Image Guided Therapy Working Group
Room: Constitution CDE & Corridors

4:00-5:00 PM Stent Working Group
Room: Constitution CDE & Corridors

POSTER SESSIONS:

1:00–2:30PM	**Poster Session 1**	Session 1A Room: Cabin John & Arlington	Jean de la Rosette Peter Pinto
		Session 1B Wilson & Roosevelt	Arthur Smith Pierre Mozer
3:00–4:30PM	**Poster Session 2**	Session 2A Room: Cabin John & Arlington	Jens Rassweiler Jihad Kaouk
		Session 2B Wilson & Roosevelt	Mohamad Allaf Vipul Patel

POSTER SESSION 1A

1:00 PM – 2:30 PM
Cabin John & Arlington Room

Jean de la Rosette
Peter Pinto

No.	Title	Presenting Author
1	PROSTATE CANCER LOCALIZATION BY ASSESSMENT OF ULTRASOUND-CONTRAST-AGENT DISPERSION	Massimo Mischi
2	TRANSURETHRAL PROSTATE RESECTION (TURP) BEFORE HIGH INTENSITY FOCUSED ULTRASOUND (HIFU) THERAPY OF PROSTATE CANCER (PCA) IS THERE AN ADVANTAGE IN IMMEDIATE OR DELAYED HIFU TREATMENT ?	Christian Chaussy
3	PILOT STUDY EVALUATION OF STANDARD LAPAROSCOPIC SUTURING AND A NOVEL PARENCHYMAL APPOSITION MECHANISM FOR MINIMALLY INVASIVE RENAL RECONSTRUCTION	Allison Polland
4	DO SAFETY WIRES INCREASE THE RISK OF URETERAL INJURY DURING DEPLOYMENT OF URETERAL ACCESS SHEATHS? EVALUATION USING AN *EX VIVO* PORCINE MODEL	Joseph Graversen
5	THE EFFECT OF BARBED SUTURE ON THE POSTERIOR RECONSTRUCTION AND URETHROVESICAL ANASTOMOSIS DURING ROBOTIC ASSISTED LAPAROSCOPIC PROSTATECTOMY	Joseph Graversen
6	MULTI-INSTITUTIONAL REVIEW: DOES FOLEY CATHETER VERSUS SUPRAPUBIC TUBE DRAINAGE IMPACT THE RISK OF POST-OPERATIVE COMPLICATIONS IN PATIENTS UNDERGOING CRYOABLATION OF THE PROSTATE?	Jonathan Melquist
7	ROBOTIC RADICAL PROSTATECTOMY USING A 3-DIMENSIONAL FLAT-SCREEN MONITOR FOR THE SURGICAL ASSISTANTS	Kazushi Tanaka
8	THE ONE STEP PERCUTANEOUS NEPHROLITHOTOMY "MICROPERC": THE INITIAL CLINICAL REPORT.	Shashikant Mishra
9	THE FIBRE TOW TECHNIQUE: A NOVEL MANEUVER TO RETRIEVE URETERIC CALCULI	A V Rawandale
10	HISTOTRIPSY OF THE PROSTATE: ENDOSCOPIC PREDICTION OF URETHRAL DISINTEGRATION	George Schade

11	PREVALENCE OF ORTHOPEDIC PROBLEMS AMONG ENDOUROLOGISTS AND THEIR COMPLANCE WITH RADIATION SAFETY MEASURES	Mohamed Elkoushy
12	RENAL CAPSULE INTERFACE IN RCC - A FRACTAL ANALYSIS	Cristian Surcel
13	ACTIVE STENT MIGRATION WITH MULTI-LENGTH URETERAL STENTS	Joseph V. DiTrolio
14	**BEST PAPER AWARD** MODELING OF MAGNETIC TOOLS FOR USE WITH SUPERPARAMAGNETIC PARTICLES FOR MAGNETIC STONE EXTRACTION.	Yung Khan Tan
15	REAL TIME DIAGNOSIS OF BLADDER CANCER WITH PROBE-BASED CONFOCAL LASER ENDOMICROSCOPY, A PROSPECTIVE DIAGNOSTIC ACCURACY STUDY	Jen-Jane Liu
16	A NOVEL LAPAROSCOPIC CAMERA FOR CHARACTERIZATION OF RENAL ISCHEMIA USING DLP® HYPERSPECTRAL IMAGING; INITIAL EXPERIENCE IN A PORCINE MODEL	Ephrem Olweny
17	SPIDER™ SURGICAL SYSTEM FOR UROLOGIC LESS: FROM INITIAL LABORATORY EXPERIENCE TO FIRST CLINICAL APPLICATION	Autorino Riccardo
18	BALL-TIP HOLMIUM:YAG OPTICAL FIBER	Bodo Knudsen
19	VARIABLE POWER INPUT MICROWAVE ABLATION OF *EX VIVO* PORCINE KIDNEY WITH SIMULATED INTRACORPOREAL TEMPERATURE ENVIRONMENT	Castle Scott
20	PNEUMODISSECTION: A NEW CRYOABLATIVE TECHNIQUE	Matthew Maurice
21	PREDICTION OF WARM ISCHEMIA TIME AND POSTOPERATIVE RENAL FUNCTION BY THE RENAL NEPHROMETRY SCORE IN PATIENTS UNDERGOING ROBOTIC PARTIAL NEPHRECTOMY	Fatih Altunrende

POSTER SESSION 1B

1:00 PM – 2:30 PM
Wilson & Roosevelt Room

Arthur Smith
Pierre Mozer

22	MEASUREMENT OF SPATIAL DISTRIBUTION IN SEXTANT PROSTATE BIOPSY	Misop Han
23	INCIDENTAL PROSTATE CANCER TREATED WITH ROBOTIC TRANSRECTAL HIGH INTENSITY FOCUSED ULTRASOUND (HIFU)	Stefan Thueroff
24	ROBOTIC VERSUS LAPAROSCOPIC PARTIAL NEPHRECTOMY FOR BILATERAL SYNCHRONOUS KIDNEY TUMORS: COMPARATIVE ANALYSIS AT A SINGLE INSTITUTION	Shahab Hillyer
25	HIGH FREQUENCY ULTRASOUND IMAGING DURING NONINVASIVE LASER COAGULATION OF THE CANINE VAS DEFERENS, IN VIVO	Christopher Cilip
26	SPARKER ARRAY FOR LITHOTRIPSY	Raymond Schaefer
27	THREE-DIMENSIONAL IMAGING OF URETER WITH ENDOSCOPIC OPTICAL COHERENCE TOMOGRAPHY	Hui Zhu
28	COMPARISON OF TENSILE BEHAVIOR OF BLADDER, KIDNEY, URETER TO A LATEX “4-IN-1” SUTURE MODEL	Phillip Mucksavage
29	A NOVEL STEREOTACTIC PROSTATE BIOPSY SYSTEM INTEGRATING PREINTERVENTIONAL MRI WITH LIVE US FUSION	Timur H Kuru
30	JACKHAMMER NEPHROSCOPY (JN): AN AID TO FRAGMENT EVACUATION DURING PERCUTANEOUS NEPHROLITHOTOMY	A V Rawandale
31	*IN VIVO* EVALUATION OF A NOVEL BIPOLAR RADIOFREQUENCY ABLATION DEVICE IN PATIENTS UNDERGOING LAPAROSCOPIC PARTIAL NEPHRECTOMY: A PILOT STUDY	Ornob Roy

32	BOX COUNTING FRACTAL ANALYSIS IN THE MANAGEMENT OF SMALL RENAL MASSES	Cristian Surcel
33	BOX COUNTING ANALYSIS IN RETROPERITONEAL FIBROSIS-5-YEARS OF EXPERIENCE WITH 19 PATIENTS	Cristian Surcel
34	NERVE COMPRESSION STUDY FOR BETTER UNDERSTANDING URINARY INCONTINENCE	Angela Forrest
35	EVALUATION OF A NEW 240 μM SINGLE-USE HOLMIUM:YAG OPTICAL FIBER FOR FLEXIBLE URETEROSCOPY	David Shore
36	NOVEL INSTRUMENTATION FOR DAVINCI™ ROBOTIC LAPAROENDOSCOPIC SINGLE-SITE SURGERY: EARLY LABORATORY EXPERIENCE	Autorino Riccardo
37	LASER PROBE FOR LAPAROSCOPIC NEPHRON SPARING SURGERY	Timothy Munuhe
38	ENDOSCOPIC SNARE RESECTION OF BLADDER TUMORS	Matthew Maurice
39	MR-TRUS REGISTRATION ACCURACY FOR TARGETED BIOPSY OF THE PROSTATE	Shyam Natarajan
40	*EX VIVO* MODEL FOR RENAL FRACTURE IN CRYOABLATION	Cervando Ortiz-Vanderdys
41	LAPAROENDOSCOPIC SINGLE-SITE SURGERY FOR RENAL CANCER: ONCOLOGICAL OUTCOMES	Humberto Laydner
42	PREDICTION OF WARM ISCHEMIA TIME AND POSTOPERATIVE RENAL RENAL NEPHROMETRY SCORE IS ASSOCIATED WITH COMPLICATION RATE AFTER ROBOTIC PARTIAL NEPHRECTOMY	Fatih Altunrende

POSTER SESSION 2A

3:00 PM – 4:30 PM
Cabin John & Arlington Room

Jens Rassweiler
Jihad Kaouk

43	EARLY TREATMENT OF HORMONE-REFRACTORY NON-METASTASIZED PROSTATE CANCER (HRPCA) WITH ROBOTIC HIGH INTENSITY FOCUSED ULTRASOUND (RHIFU)	Christian Chaussy
44	INTRAPROSTATIC CANCER TOPOGRAPHY AND DETECTION RATE IN 963 CASES	Christian Chaussy
45	DEFINING OPTIMAL LASER-FIBER SWEEPING ANGLE FOR EFFECTIVE TISSUE VAPORIZATION USING 180 W 532 NM LITHIUM TRIBORATE LASER	Jin Ko Woo
46	PROSPECTIVE, RANDOMIZED USE OF THE BARBED VLOC SELF-RETAINING SUTURE TO FACILITATE VESICOURETHRAL ANASTAMOSIS DURING ROBOT ASSISTED RADICAL PROSTATECTOMY: TIME REDUCTION AND COST BENEFIT	Kevin Zorn
47	**OUTSTANDING PAPER AWARD** COMPUTER SIMULATIONS OF THERMAL DAMAGE TO THE HUMAN VAS DEFERENS DURING NONINVASIVE LASER VASECTOMY	Gino Schweinsberger
48	DECREASED OPERATIVE INTERRUPTION USING FLOSHIELD TO KEEP THE LAPAROSCOPE CLEAN	Wayne Poll
49	SUBMILISIEVERT COMPUTED TOMOGRAPHY FOR THE EVALUATION OF UROLITHIASIS	Brian Eisner
50	SPEAR-HEADED LITHOTRIPTOR: AN INEXPENSIVE ALTERNATIVE FOR HARD STONES	A V Rawandale
51	“STAGHORN MORPHOMETRY”: A NEW TOOL FOR CLINICAL CLASSIFICATION AND PREDICTION MODEL FOR PCNL MONOTHERAPY.	Shashikant Mishra
52	WEB-ACCESSIBLE 3D ANATOMY SOFTWARE OF UROLOGIC PATHOPHYSIOLOGICAL CONDITIONS AND PROCEDURES FOR PATIENT EDUCATION	Daniel Burke

53	FACTORS DERERMINING STONE FREE RATE IN SHOCK WAVE LITHOTRIPSY USING THE STORZ MODULITH SLX-F2 LITHOTRIPTER	Mohamed Elkoushy
54	*IN VIVO* TESTING OF THE SECOND GENERATION SPIDER LAPAROENDOSCOPIC SINGLE-SITE SURGICAL SYSTEM	Gorbatiy Vladislav
55	NOVEL OFFICE-BASED RAPID UTI DETECTION SYSTEM	Joseph V. Ditrolio
56	COST ANALYSIS OF METAL URETERAL STENTS WITH 12 MONTHS OF FOLLOW-UP	Eric Taylor
57	3D-TRUS MAPPING FUSION FOR SECOND LOOK PROSTATE BIOPSIES	Pierre Mozer
58	RADIOSURGICAL ABLATION OF RENAL TUMORS: EVALUATION OF SAFETY	Oussama Darwish
59	TRUS PROSTATE BIOPSIES PIERCED AREA CAN IMPACT ON CANCER RATE DETECTION	Grégoire Coffin
60	HUMAN LAPAROENDOSCOPIC SINGLE SITE PYELOPLASTY USING THE SPIDER SURGICAL SYSTEM: FEASIBILITY AND SAFETY	Scott Castle
61	A 3D ELASTROGRAPHY-GUIDED SYSTEM FOR LAPAROSCOPIC PARTIAL NEPHRECTOMY	Phillip Pierorazio
62	DEVELOPMENT OF A RENAL PHANTOM MODEL FOR IMAGE-GUIDED LAPAROSCOPIC PARTIAL NEPHRECTOMY	Phillip Pierorazio
63	FLOW CHARACTERISTICS IN A NOVEL SPIRAL CUT URETERAL STENT.	Phillip Mucksavage

POSTER SESSION 2B

3:00 PM – 4:30 PM
Wilson & Roosevelt Room

Mohamad Allaf
Vipul Patel

64	LOCALLY ADVANCED NON METASTATIC PROSTATE CANCER (T3-4, N0, M0) TREATED WITH ROBOTIC HIGH INTENSITY FOCUSED ULTRASOUND (RHIFU)	Stefan Thueroff
65	5 PART PERCUTANEOUS ACCESS NEEDLE WITH GLIDEWIRE (5-PANG) TECHNIQUE FOR PERCUTANEOUS NEPHROLITHOTOMY: TECHNIQUE AND OUTCOMES	A V Rawandale
66	"5-PART PERCUTANEOUS ACCESS NEEDLE OVER GLIDEWIRE - SUPRAPUBIC ACCESS TECHNIQUE (5-PANG-SAT): A MINIMALLY INVASIVE SOLUTION FOR SUPRAPUBIC VESICAL ACCESS: OUR INITIAL EXPERIENCE"	A V Rawandale
67	ABLATION OF SMALL RENAL MASSES: PRACTICE PATTERNS AT ACADEMIC INSTITUTIONS IN THE UNITED STATES	Sutchin Patel
68	PROSPECTIVE RANDOMIZED EVALUATION OF GELMAT FOOT PADS IN THE ENDOSCOPIC SUITE	Joseph Graversen
69	NOVEL ROBOT FOR TRANS-PERINEAL PROSTATE NEEDLE INTERVENTION: PHANTOM STUDY	Andrew Hung
70	A NOVEL 3.0 FR URETERAL STENT WITH DRAINAGE CHARACTERISTICS OF A 4.7 FR JJ STENT	Dirk Lange
71	MINNESOTA ONLINE SURGICAL LEARNING MANAGEMENT PLATFORM FOR MULTI-INSTITUTIONAL VALIDATION STUDIES AND SKILLS ASSESSMENT	Yunhe Shen
72	INFLUENCE OF HO:YAG PULSE MODIFICATION ON *IN VITRO* STONE DISINTEGRATION.	Felix Pohl
73	DETERMINATION OF RENAL STONE COOPSITION IN PHANTOM AND PATIENTS USING SINGLE SOURCE DUAL-ENERGY CT	Brian Eisner

74	JET EVACUATION TECHNIQUE (JET) FOR CALCULI EXTRACTION DURING URETEROSCOPY	A V Rawandale
75	COMBINING SUBJECT-SPECIFIC PELVIC MODELING AND AMBULATORY MONITORING APPROACHES IN ASSESSING FEMALE SUI	Yingchun Zhang
76	TARGETED IMAGING OF BLADDER CANCER WITH CANCER-SPECIFIC MOLECULAR CONTRAST AGENTS	Jen-Jane Liu
77	PROSTATE TUMOUR IDENTIFICATION USING A FORCE-SENSITIVE ROLLING INDENTATION PROBE	Pardeep Kumar
78	NOVEL ROBOTIC-ASSISTED PERCUTANEOUS ABLATION SYSTEM	Julien Guillotreau
79	INFLUENCE OF ULTRASOUND SYSTEM SETTINGS ON KIDNEY STONE DETECTION	John Kucewicz
80	FREEHAND 3D-TRUS PROSTATE BIOPSY MAPPING: FIRST CLINICAL RESULTS	Pierre Mozer
81	RAPIDLY DEPLOYABLE TELEROBOTIC SLAVE FOR TRANSURETHRAL EXPLORATION AND INTERVENTION	Lara K. Suh
82	USE OF THE ROBOTIC BOWEL CLAMP FOR RENAL HILAR CONTROL	Aria Razmaria
83	VISUAL MEASUREMENT OF SUTURE STRAIN FOR ROBOTIC SURGERY	Aria Razmaria

ABSTRACT 1

PROSTATE CANCER LOCALIZATION BY ASSESSMENT OF ULTRASOUND-CONTRAST-AGENT DISPERSION

M. Mischi[1], M.J.P. Kuenen[1], M.P. Laguna Pes[2], H. Wijkstra[1,2]

[1] *Eindhoven University of Technology, Electrical Engineering Department, the Netherlands*
[2] *Academic Medical Center University of Amsterdam, Urology Department, the Netherlands*

Introduction: In the United States, prostate cancer (PCa) accounts for 28% and 11% of all cancer diagnoses and deaths in 2010, respectively. Although efficient focal therapies are available, their applicability is hampered by a lack of imaging solutions; despite their invasiveness and poor spatial accuracy, systematic biopsies remain the most reliable option for PCa localization. Contrast-enhanced ultrasound imaging has recently opened new possibilities for PCa localization. Based on a proven correlation between cancer aggressiveness and angiogenesis, several imaging methods have been proposed that are based on blood-perfusion assessment. However, no method has yet produced reliable results. We propose contrast-ultrasound dispersion imaging (CUDI) as a new alternative method. Different from perfusion, whose relation with angiogenesis is affected by opposing effects, the intravascular dispersion of ultrasound contrast agents is directly influenced by angiogenic changes in the microvascular architecture.

Methods: CUDI is performed after an intravenous injection of a 2.4-mL SonoVue® (Bracco, Milan) bolus. The bolus passage through the prostate is imaged by an iU22 ultrasound scanner (Philips Healthcare, Bothell). Contrast-specific imaging is adopted to increase contrast sensitivity. After data linearization, an indicator dilution curve (IDC) is obtained at each video pixel. Local dispersion can be estimated by IDC modeling or derived by analysis of shape variations in neighbor IDCs. As shown in Figure 1, a dispersion image can then be generated evidencing angiogenic areas and, therefore, cancer growth. A preliminary validation was performed at the Academic Medical Center University of Amsterdam by comparing the obtained dispersion images with the histology results after radical prostatectomy (see Figure 1) in four patients.

Results: In all patients, the dispersion images showed a good agreement on a pixel level with the histology. The resulting average ROC curve area was 0.91, higher than by any perfusion parameter.

Conclusion: Our preliminary results evidence a promising value of CUDI for PCa localization and motivate towards an extensive validation to optimize and compare the method with other techniques. Once validated, CUDI could support targeting of both biopsy and focal-therapy.

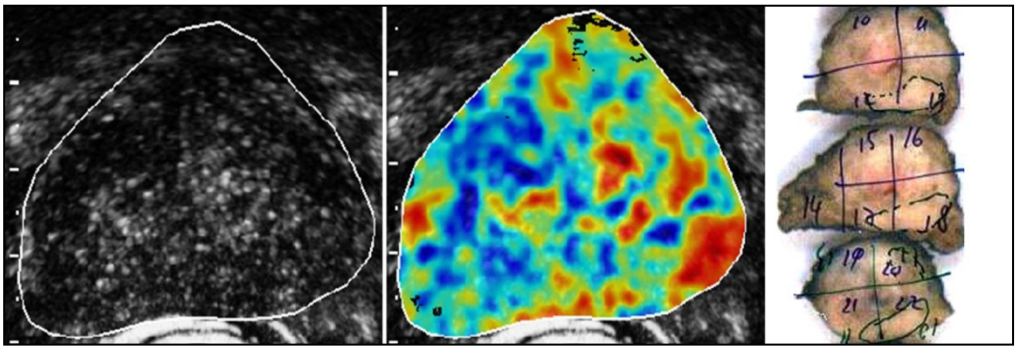

Figure 1: Gray level, dispersion, and histology images.

ABSTRACT 2

TRANSURETHRAL PROSTATE RESECTION (TURP) BEFORE HIGH INTENSITY FOCUSED ULTRASOUND (HIFU) THERAPY OF PROSTATE CANCER (PCA) IS THERE AN ADVANTAGE IN IMMEDIATE OR DELAYED HIFU TREATMENT ?

Chaussy Christian[1,3] , Thueroff Stefan[2,3]
[1]*Dept. of Urology University of Regensburg,*
[2]*Dept. of Urology Klinikum Muenchen,* [3]*Harlachinger Krebshilfe e.V.*

OBJECTIVE: TURP before HIFU is mandatory in order to adjust each prostate to the maximum penetration depth (30mm) and for movement of the longitudinal transrectal applicator. Only a prostate volume of < 25 cc can be treated completely. We studied the influence of immediate or delayed (1 month) HIFU after TURP. HIFU application dose, treatment time, and side effect induction, as well as changes in TURP technology (mono-/bipolar), were analyzed.

MATERIAL AND METHOD: A total of 1,529 patients have been treated with TURP & HIFU since 2000; 1,346 of these patients were included into the analysis with their complete data set. Our prospective data collection includes 140 data points/HIFU treatment since 1996, subgrouped into annual cohorts. TURP from 2000-2007 was performed as monopolar, and since 2008 as bipolar resection. The HIFU device used was Ablatherm® (EDAP-TMS,Lyon).

RESULTS: In 2001, only 10% delayed treatments were performed; in 2010 54% HIFU treatments were performed with a one month delay. Treatment time was not influenced by this strategy: 1,105 combined TURP & HIFU lasted 94 minutes (range of 72-115 minutes), with a month delay the HIFU treatment lasted 92 minutes (range 65-119 minutes). HIFU dose showed equal data: 562 (433-682) lesions applied in the combined and 549 (391-717) lesions applied in the split group. Resected tissue was 53% (range 48%-63%) until 2006 and increased by 25% to 66% (range 63%-70%) by introduction of bipolar TURP. Side effect analysis clearly showed that HIFU one month after TURP reduces typical side effects by 50%. Efficacy (PSA Nadir) did not show differences between the two groups.

CONCLUSION: Since the treatment goal is complete prostate coagulation by HIFU, neoadjuvant TURP is necessary in order to increase efficacy and to minimize side effects. Whether TURP and HIFU are performed in one or two sessions does not influence efficacy (according to Nadir), but side effects decreased by 50% with delayed treatment.

Source of funding:
Harlachinger Krebshilfe e.V.; Lingen Stiftung
Thanks to Ms. Regina Nanieva for database management and analysis.

ABSTRACT 3

PILOT STUDY EVALUATION OF STANDARD LAPAROSCOPIC SUTURING AND A NOVEL PARENCHYMAL APPOSITION MECHANISM FOR MINIMALLY INVASIVE RENAL RECONSTRUCTION

Allison R. Polland[1], Adam C. Mues[1], Joseph A. Graversen[1], and Jaime Landman[1,2]
[1]*Columbia University, Department of Urology, New York, NY*
[2]*University of California Irvine, Department of Urology, Orange, CA*

Introduction: Despite advances, reconstructive components of laparoscopic procedures remain challenging. This limits the application of a minimally invasive access approach in many procedures. In an effort to minimize the extensive reconstructive efforts, associated particularly with laparoscopic partial nephrectomy, we have developed a parenchymal apposition mechanism (PAM). The objectives of this project were to evaluate whether the PAM device would increase the efficiency and efficacy of renal defect closure when compared with standard laparoscopic suturing, and to evaluate whether a PAM closure would cause less traumatic injury to adjacent renal parenchyma than standard laparoscopic closure.

Methods: In this pilot study, medical students, residents, fellows, and attending physicians performed reconstruction of a standardized renal defect with a standardized laparoscopic technique (SLT) and with the PAM technique. The PAM prototype was engineered using two salmon egg hooks connected with 5 inches of 4-0 vicryl suture, placed within a V-shaped foam delivery mechanism. Use of the PAM requires laparoscopic deployment of each hook separately into the renal parenchyma on either side of a defect, and tensioning by placement of a Weck Clip in the center of the connecting suture over a force-vector-directing bead. Each participant performed a single closure with SLT and with the PAM device of a standardized defect in *ex vivo* porcine kidneys. Time required to close the renal defect, tissue trauma/damage during closure and the intra-parenchymal pressure after defect closure were measured.

Results: A total of 13 subjects, 7 medical students, 3 residents, 2 fellows and 1 attending, were enrolled. There was no statistical difference between the two methods of closure in average time for closure. In a subgroup analysis of subjects who had performed laparoscopic reconstructive procedures as the primary surgeon, SLT was significantly faster than PAM ($p = 0.036$). Mean pressures achieved in attempted closure using SLT and PAM were not significantly different, 0.38N (range 0.000 to 0.77N) and 0.38N (range 0.006 to 0.80N) respectively ($p = 0.99$). The mean parenchymal trauma rating was not significantly different between the groups, however the upper limit of the range of trauma ratings was greater in the standard closures.

Conclusion: This pilot study demonstrated the feasibility of PAM parenchymal closure in an *ex vivo* kidney model. There was no difference in time to closure, pressure of closure or parenchymal trauma between SLT and PAM for laparoscopic closure of a renal parenchymal defect. Additional testing of the PAM is necessary to explore its use in laparoscopic reconstruction of the kidney and other organs.

ABSTRACT 4

DO SAFETY WIRES INCREASE THE RISK OF URETERAL INJURY DURING DEPLOYMENT OF URETERAL ACCESS SHEATHS? EVALUATION USING AN *EX VIVO* PORCINE MODEL

Joseph A. Graversen,[a,b] Oscar M. Valderrama,[b] Ruslan Korets,[a] Adam C. Mues,[b] Ketan K. Badani,[b] Jaime Landman,[c] Mantu Gupta[b]

[a]*Designated Presenter*
[b]*Department of Urology, Columbia University Medical Center, New York, NY, USA*
[c]*Department of Urology, University of California in Irvine, Orange, CA, USA*

Introduction: Ureteral access sheaths are used routinely to facilitate ureteroscopy, but concerns have been raised regarding the force necessary to insert them, potential ureteral injury, and whether the presence of a safety wire (SW) outside the sheath increases or decreases the likelihood of ureteral injury. In response to these concerns a modified balloon expandable ureteral access sheath (BEUAS) (Onset Medical, Pathway™ Expandable Ureteral Access Sheath, Irvine, CA) has been redeveloped and made available commercially. The purpose of this study is to compare the insertion force required and the rate of ureteral injury engendered by standard (sUAS) and balloon expandable ureteral access sheaths with and without the presence of a SW.

Methods: Forty intact porcine kidney-ureter units were divided into groups of 10. In each group, either a BEUAS or a sUAS was passed with and without a SW. Insertion force was determined by securing each unit to a spring-loaded digital scale and recording tensile force at various points along the ureter. The average force for each group was calculated and analyzed. After UAS removal, retrograde injection of water was used to distend and identify ureteral lacerations.

Results: Regardless of the presence or absence of a SW, the mean force to insert a sUAS was significantly greater than the force required to insert a BEUAS (1.23 vs. 0.21 kg, $p<0.0001$, respectively). The use of a SW significantly increased the force required to insert a sUAS ($p=0.0003$); however, this was not observed with the BEUAS ($p=0.2605$). There were a total of 19 lacerations, but there was no correlation between the type of sheath or the presence of a SW and the number of lacerations.

Conclusion: The mean insertion force of the BEUAS is significantly less than that of the sUAS both with and without a SW. SW use significantly increases the force required to insert a sUAS but not a BEUAS. SW use does not cause a significant increase in ureteral injuries in an *ex vivo* porcine model.

Ureteral Access Sheath Mean Force Insertion With and Without SafetyWire		
Group	Mean Force (kg)	p value
Total BEUAS	0.21	<0.0001
Total sUAS	1.23	
With Safety Wire		
BEUAS	0.24	<0.0001
sUAS	1.79	
Without Safety Wire		
BEUAS	0.17	0.0002
sUAS	0.67	
Expandable Sheath		
With SW	0.24	0.2605
Without SW	0.172	
Standard Sheath		
With SW	1.79	0.0003
Without SW	0.67	

ABSTRACT 5

THE EFFECT OF BARBED SUTURE ON THE POSTERIOR RECONSTRUCTION AND URETHROVESICAL ANASTOMOSIS DURING ROBOTIC ASSISTED LAPAROSCOPIC PROSTATECTOMY

Joseph A. Graversen,[1] Adam C. Mues,[1] Mantu Gupta, Jaime Landman,[2] Ketan K. Badani[2]
[1]*Department of Urology, Columbia University Medical Center, New York, NY, USA*
[2]*Department of Urology, University of California in Irvine, Orange, CA, USA*

Introduction and Objective: Robotic assisted laparoscopic prostatectomy (RALP) rapidly is becoming the primary technique for performing radical prostatectomy. The posterior rhabdosphincter reconstruction (RSR) and urethrovesical anastomosis (UVA) are time-consuming steps essential to the procedure. Currently, a 3-0 monofilament synthetic absorbable suture (SAS) is the most popular suture utilized. A polyglyconate, unidirectional barbed SAS (V-Loc™ Wound Closure Device, Covidien, Mansfield, MA) has been re-developed recently and made available commercially. The design includes a looped free-end that allows for knotless stitch initiation and unidirectional barbs that allow for slippage- free tensioning. The purpose of this study was to determine whether the advantages of the V-Loc™ translate into improvements in the efficiency and efficacy of the RSR and UVA.

Methods: Forty-two patients underwent RALP using V-Loc™ SAS for the RSR and UVA. A control group underwent RALP using standard 3-0 monofilament SAS and consisted of 24 consecutive patients who underwent RALP just prior to the V-Loc™ group, and 18 patients treated concurrently with the study group. In both groups, the RSR was performed in two layers and the UVA was performed using the principles of the Van Velthoven stitch. Upon completion, a Foley catheter was placed and the bladder was filled with 60 cc to check the integrity of the UVA. The time to complete the RSR and the UVA was recorded in each group and analyzed.

Results: There were 42 patients in each of the 2 groups. The RSR in the control and V-Loc™ groups were 9 and 6 minutes respectively ($p<0.01$). Similarly, the UVA in the control and V-Loc™ groups were 18 and 12 minutes respectively ($p<0.01$). The mean total time saved with the V-Loc™ was 9 minutes ($p<0.001$). In the cohort, there were no anastomotic leaks during both intraoperative UVA testing or clinically during postoperative follow-up.

Conclusions: The use of the V-Loc™ barbed suture significantly decreased the time to complete the RSR, the UVA, and the total time for anatomic reconstruction without compromising short-term efficacy. Long-term effects, such as bladder neck contracture rates, require further investigation.

	Patients (*n*)	RSR (min)	UVA (min)	Total Time	Anastomotic Leaks
Control	42	9 (6-19)	18 (11-28)	27	0/42
V-Loc™	42	6 (5-16)	12 (8-18)	18	0/42
Difference		3	6	9	0
p-value		<0.01	<0.01	<0.001	

ABSTRACT 6

MULTI-INSTITUTIONAL REVIEW: DOES FOLEY CATHETER VERSUS SUPRAPUBIC TUBE DRAINAGE IMPACT THE RISK OF POST-OPERATIVE COMPLICATIONS IN PATIENTS UNDERGOING CRYOABLATION OF THE PROSTATE?

J. Melquist[1], S. Tannenbaum[2], C. Johnson[3], D. Schulsinger[1]

[1]Stony Brook University Medical Center, Stony Brook, NY[1]
[2]Alliance Urology Specialists, Greensboro, NC[2]
[3]Mountain View Urological Associates, Hendersonville, NC[3]

Introduction: Known complications following cryosurgery include erectile dysfunction, incontinence, transient urinary retention, rectal-urethral fistula, urethral sloughing, and infection. We present a multi-institutional review of 207 cryoablation procedures. The purpose of this study was to review patients with postoperative complications following cryoablation of the prostate and to see if the type of urinary drainage impacted these complications.

Methods: A total of 207 patients underwent cryoablation of the prostate from 2006 to 2010, at three institutions using the Galil Medical (Arden Hills, MN) cryoablation system. All patients underwent a double freeze-double thaw treatment using 17-gauge needles. Foley catheter drainage alone was implemented in 119 cases. The remaining 88 patients had a suprapubic tube placed using a cystoscopically-guided percutaneous method. All patients received a short course of post-operative antibiotics. Fluoroquinolones were used unless contraindicated. Patients were followed for a minimum of one year.

Results: Ten (4.8%), with a mean of 74 years age, PSA 9.8 ng/mL, Gleason 6.3, of the 207 patients were found to have post-operative genitourinary infections (2 epididymo-orchitis, 7 epididymitis, 1 UTI). Nine (10.2%) of the 88 patients receiving SP drainage had post-operative infections. Meanwhile, one of 119 patients (0.8%) with Foley catheter drainage had a post-operative infection. The infection rate in those patients who received an SP tube was greater significantly than patients given Foley catheterization ($p=0.0023$, two-tailed Fischer's exact test). There is an absolute risk reduction of 9.4% when comparing Foley catheter drainage to the more standard SP placement. This represents a preventive fraction of 92% with the use of Foley catheter over SP drainage. There were no statistical differences in other variables between the two groups: age, pre-operative PSA, number of freezing rods utilized, and prostate size.

Conclusions: There is a greater risk of acute genitourinary infections following cryosurgery when patients are drained by SP tube placement when compared to Foley catheterization. Based on these data, one may consider the use of Foley catheter over SP tube drainage of the bladder following cryotherapy of the prostate.

ABSTRACT 7

ROBOTIC RADICAL PROSTATECTOMY USING A 3-DIMENSIONAL FLAT-SCREEN MONITOR FOR THE SURGICAL ASSISTANTS

Kazushi Tanaka, Masato Fujisawa
Division of Urology, Department of Surgery Related, Kobe University Graduate School of Medicine

Objectives: 3-Dimensional (3-D) visualization for the surgeon is considered to be one of the major advantages of robotic prostatectomy. Paired optical systems and cameras provide the surgeon at the console with a 3-D perspective of the field. However, the assistants working on the side of the patient still have to depend upon 2-D images projected onto a flat-screen monitor. On this monitor, they often have to rely on motion parallax and judge depth by observing the spatial relationship of objects in the field of vision. We created a new 3-D system on a flat screen for the da Vinci Robot System. We undertook this study to see if passing on this technology to surgical assistants would improve their efficiency.

Materials and Methods: The da Vinci stereoscopic visualization system has a custom-designed endoscope with two separate optic channels; thus, it recreates the most important aspect of stereopsis: binocular disparity. The image is displayed on the surgeon's console through the Vision cart. We made a control box that can convert the da Vinci 3-D signals to 3-D signals on a flat screen. It is connected to the da Vinci system and a 3-D monitor. We receive a 3-D view though polarized 3-D glasses. The study was conducted with patients undergoing robotic radical prostatectomy in Kobe University Hospital. The assistant wore polarized glasses for a flat screen 3-D monitor and used the 3-D system throughout the entire procedure. The efficiency of the 3-D system for assistance was evaluated on a scale of 0 to100 subjectively.

Results: All 13 cases were achieved with 3-D assistance. The polarized glasses were comfortable to wear, and direct vision seldom was influenced. Overall satisfaction was scored +94. Vision provided by the 3-D flat screen monitor was described to be "as good as the surgeon's console."

Conclusion: The use of 3-D visualization seems to improve the efficiency of assistance during robotic radical prostatectomy. Vision provided by the 3-D flat screen with special glasses is very similar to the robot's console.

ABSTRACT 8

THE ONE STEP PERCUTANEOUS NEPHROLITHOTOMY "MICROPERC": THE INITIAL CLINICAL REPORT

Mishra S[1], Sabnis RB[2], Desai MR[1]
[1] *Muljibhai Patel Urological Hospital, Nadiad, Gujarat, India. Pin 387001*

Introduction: Bader M described the first 4.85 Fr "All Seeing needle™" which provides optical confirmation during initial calyceal access for standard PCNL. We utilised the same concept for performing one-step PCNL through the same 4.85 Fr sheath in order to perform the first clinical feasibility and safety study of PCNL through the smallest sheath available. We define the term "Microperc" as a modified PCNL where renal access and one-step PCNL is performed through the same "All Seeing needle."

Methods: Microperc was performed in 10 cases using a 16 G (4.85 Fr) "All Seeing needle" under direct vision and with a three-way connector allowing irrigation, passage of flexible telescope, and 200 μm Holmium:YAG laser fiber for stone fragmentation. Pre, intra-, and post-operative parameters were analyzed prospectively.

Results: The mean calculus size was 13 mm (range 6-23 mm). There were 1 patient each with ectopic pelvic kidney, pediatric kidney, chronic kidney disease, and obesity. The Microperc was feasible in all cases, with a mean visual analogue score (VAS) by the surgeon for access of 4.4 ± 2.0 (range 2-8), hemoglobin drop of 0.95 ± 0.58 (range 0.3-2.3 gm/dl) in the patients, and a mean length of hospital stay of 1.5 ± 1.3 days (range 1-5 days). The stone-free rate at 1 month post-procedure was 90%. One patient had intra-operative bleeding, which required conversion to a standard PCNL procedure. There were no post-operative complications in these 10 cases and no auxiliary procedures were required.

Conclusion: Microperc is technically feasible, safe, and efficacious for small burden renal calculus disease. The "All Seeing needle" permitted optimal vision during our initial 10 cases. Further feasibility studies and head-to-head comparison with the available modalities for defining the place of microperc in treatment of small bulk renal calculus disease are required.

ABSTRACT 9

THE FIBRE TOW TECHNIQUE: A NOVEL MANEUVER TO RETRIEVE URETERIC CALCULI

Rawandale AV, Kurane CS, Patni LG
Institute of Urology, Dhule, India.

Introduction: Retrograde stone migration during ureteroscopic lithotripsy poses a problem. We describe the "Fibre Tow technique," a novel maneuver to retrieve such stones in order to facilitate pulverization.

Methods: The technique can be described in the following steps

- Step 1: Patient position: Reverse Trendelenberg
- Step 2: Ureter distended with irrigation
- Step 3: Stop irrigation
- Step 4: Pass the laser fibre or lithotripsy probe by the side of the calculus (Fig 1)
- Step 5: Move circumferentially below the calculus so that the calculus sits on the fibre (Fig 2)
- Step 6: Withdraw the fibre and scope with the calculus sitting on it
- Repeat as and when required.
- Pre "Tow" hydration and diuretic help

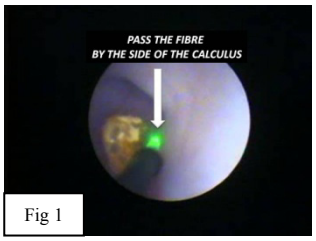

Fig 1

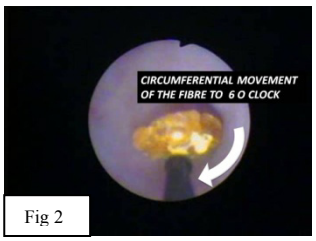

Fig 2

Results: The calculus cannot slide down the ureteral mucosa due to high inertia of the stone at rest. It has to be lifted off the ureteral mucosa in order for it to move down the ureter. The technique prevents the repeated exchange of stone retrieval devices, reduces cost of the accessories, and saves time as the same fibre is used for to tow the stone as well as pulverization. It is easily reproducible and can be used in any part of the ureter.

Conclusion: The "Fibre Tow" allows fast and safe manipulations of calculi during ureteroscopy. It is cost effective, saves time, is easily reproducible, and can be used for any ureteric stone

ABSTRACT 10

HISTOTRIPSY OF THE PROSTATE: ENDOSCOPIC PREDICTION OF URETHRAL DISINTEGRATION

George R. Schade[1], Nicholas R. Styn[1], Timothy L. Hall[2], William W. Roberts[1,2]
[1] *University of Michigan, Department of Urology*
[2] *University of Michigan, Department of Biomedical Engineering*

Introduction: Histotripsy is a non-invasive, non-thermal, pulsed, focused ultrasound technology that uses controlled acoustic cavitation to homogenize tissue. Successful histotripsy treatment for BPH is based upon the principle of early drainage of treated homogenate via the urethra to produce a TURP-like defect. However, the prostatic urethra is more resistant to cavitational effects than benign prostatic hypertrophy (BPH) adenoma. We utilized immediate post-histotripsy cystoscopy to characterize urethral appearance in a canine model and devised a novel damage scale in order to predict the successful evolution of urethral disintegration.

Methods: Prostate histotripsy or a sham procedure was performed on 17 and 1 canine subjects, respectively. Dependent on gland size, 1-3 histotripsy treatments/prostate were delivered, each targeting a single transverse line, including urethra and adjacent glandular tissue, using an extracorporeal 750 kHz, 16-element piezoelectric focused ultrasound transducer. Serial cystoscopy was performed with an 8.2 Fr flexible ureteroscope on post-operative day (POD) 0, 1, 3, 7, and 14, and urethral damage was assessed using a grading scale (0=normal, 1=bleeding/hyperemia, 2=roughened/shedding urothelium, 3=tissue flap, 4=necrotic urethral wall, 5=complete urethral disintegration). Cystoscopy findings from POD0 and POD1 were evaluated as predictors for the development of frank urethral disintegration by POD14. Findings were confirmed histologically.

Results: A total of 35 treatments were delivered to 17 prostates of mean volume 20.6 ± 6.0 cc. While frank urethral disintegration was visualized in only 2/35 (5.7%) treatment zones on endoscopic assessment immediately following treatment (POD0), urethral disintegration developed in 25/35 (71.4%) treatment zones by POD14. Cystoscopically observing at least grade 1 damage at the time of treatment was associated with a positive predictive value (PPV) and negative predictive value (NPV) of 0.75 and 1.00, respectively, for developing frank urethral fragmentation by POD14. Observing at least grade 2 damage improved PPV to 0.91 while decreasing NPV to 0.89. The utility of cystoscopy on POD1 did not differ significantly from POD0.

Conclusion: The finding of urothelial shedding on cystoscopy at the time of histotripsy of the prostate indicates high likelihood of progression to urethral disintegration in the canine model. Routine cystoscopy may be helpful at the time of treatment to allow administration of the minimal effective dose while allow drainage of the fractionated BPH adenoma through the fragmented urethra.

Funding: NIH RO1DK087871

Figure 1:

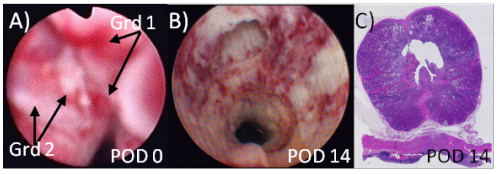

D)

Time of Cystoscopy	Urethral Appearance	Sensitivity	Specificty	PPV	NPV	Accuracy
POD 0	≥Grade 1	1.00	0.30	0.75	1.00	0.77
	≥Grade 2	0.95	0.80	0.91	0.89	0.90
POD 1	≥Grade 1	1.00	0.20	0.76	1.00	0.77
	≥Grade 2	1.00	0.70	0.89	1.00	0.91

Cystoscopic appearance of grade (Grd) 1 and 2 damage on POD0 (A) with subsequent evolution to disintegration on POD14 (B and C). Grd 1 and 2 damage as predictors of urethral distintegration by POD 14 (D).

ABSTRACT 11

PREVALENCE OF ORTHOPEDIC PROBLEMS AMONG ENDOUROLOGISTS AND THEIR COMPLANCE WITH RADIATION SAFETY MEASURES

Mohamed A. Elkoushy and Sero Andonian

Division of Urology, Department of Surgery, McGill University Health Center, McGill University, Montreal, Quebec, Canada

Introduction: The advent of fluoroscopically-guided interventional procedures has resulted in dramatic rise in radiation exposure for both patients and interventionalists with their distinct occupational health hazards. Radiation safety measures such as ALARA or "As Low As Reasonably Achievable" principles of reducing exposure time, maximizing distance, and shielding have been recommended to reduce radiation exposure to patients and operating room personnel. Shielding consists mainly of wearing heavy, lead-impregnated chest and pelvic aprons, in addition to thyroid shields, lead-impregnated glasses, and gloves. Exposure to radiation and subsequent orthopedic complaints secondary to heavy radiation protection measures are important occupational hazards that endourologists face. The aim of the present study was to assess the compliance of endourologists with radiation safety measures and determining the prevalence of orthopedic complaints among practicing endourologists.

Methods: An internet-based survey was sent to all members of the Endourological Society. The website remained open for six weeks (November 1st till December 15th, 2010) to allow members an opportunity to visit and complete the online survey. Baseline characteristics on practice pattern (geographical region, age, years of practice, days per week of endourology, and number of cases in the previous year), compliance with various radiation protection measures (thyroid, chest and pelvic aprons, gloves, glasses, and dosimeters), and prevalence of various orthopedic complaints (neck, back, hand and joint problems) were assessed. Furthermore, open-ended questions assessed reasons for non-compliance.

Results: Out of 160 surveys returned, 24 were excluded because of incomplete data. There was good compliance with chest and pelvic shields, with 97% of endourologists reported wearing these; however, compliance with thyroid shields was only 68%. Furthermore, only 34.3%, 17.2%, and 9.7% of endourologists reported using dosimeters, lead-impregnated glasses, and gloves, respectively. Overall, 86 (64.2%) respondents complained of orthopaedic problems. Specifically, 51 (38.1%) complained of back problems, 37 (27.6%) complained of neck problems, 23 (17.2%) complained of hand problems, and 19 (14.2%) complained of hip and knee problems. Furthermore, the prevalence of orthopaedic complaints were significantly higher among African endourologists, older endourologists (>40 years), longer duration of practice (>10 years), and combined annual caseload of ureteroscopies (URS) and percutaneous nephrolithotomies (PCNL).

Conclusion: There was lack of compliance among endourologists in the use of certain radiation protection measures, such as thyroid shield, dosimeter, lead-impregnated glasses, and gloves. Orthopaedic complaints among practicing endourologists are common and correlate with the annual caseload of combined URS and PCNL.

ABSTRACT 12

RENAL CAPSULE INTERFACE IN RCC - A FRACTAL ANALYSIS

C. Surcel[1], C. Mirvald[1], C. Chibelean[1], C. Gîngu[1], S. Najjar, V. Cerempei[1], C. Savu[2], A. Udrea [3], I. Sinescu[1]

[1]*Center of Urological Surgery, Dialysis and Renal Transplantation, Fundeni Clinical Institute, Bucharest, Romania*
[2] *Department of Intensive Care and Anesthesiology, Fundeni Clinical Institute, Bucharest, Romania*
[3] *"Politehnica" University, Bucharest, Romania*

Introduction: The TNM/ UICC stadialization of RCC is used widely and has a major impact in prognosis and treatment. It is best assessed by CT spiral scan, which became the gold standard. The main impediment is the differentiation between intracapsular and extracapsular tumours. In order to differentiate intrarenal from extrarenal tumours, we use a fractal analysis of renal capsule interface.
Material and methods: We studied 32 cases of RCC operated in our Center of Urological Surgery, Dialysis and Renal Transplantation, "Fundeni" Clinical Institute, and 3 normal tissues used as controls. All of them were evaluated by CT spiral scan preoperatively and the preliminary results ranked 6 tumors as T3a and 26 as T1-T2. After video capture and video processing the outline of renal parenchyma and perirenal tissue represented by renal capsule was traced. This limit was analyzed by estimating the global fractal dimension, the local fractal dimension, and local connected fractal dimension. The results were evaluated statistically using Kolmogorv-Smirnof and ξ^2 and Student test. Postoperatively the specimens were evaluated histopathologically, and the results correlated with the fractal analyses.
Results: The analysis of global fractal dimension preoperatively revealed 12 tumors with greater complexity then normal tissue and 20 tumors with lack of complexity. Postoperatively the histhopathological result were that 18 tumors were intracapsular (pT1-T2) and 14 tumors had capsular invasion and perirenal extension (pT3a). Comparing statistically the CT scan results before and after fractal analysis with pathological specimens, we noticed a significant difference among the preoperatively CT scan results and the pathological specimens (T value 2.23 and p = 0,05 with 95% results validity) and no statistically difference between fractal CT scan analysis and pathological specimens (t value-0,51).
Conclusion: An increase in fractal dimension expressed by greater complexity may correlate with a higher risk of renal capsule invasion with implications in outcome and orientation of therapeutic strategies.

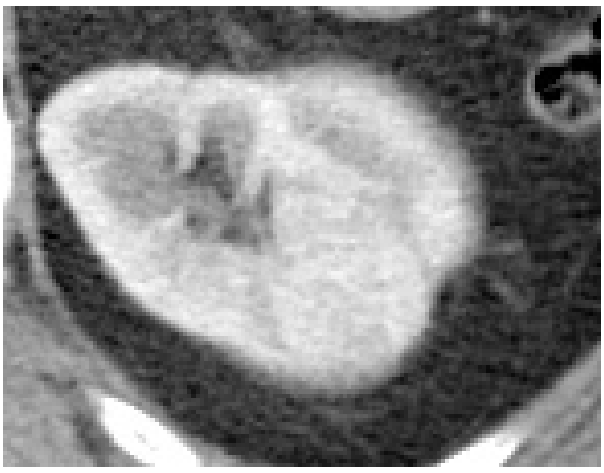

Figure 1. Left RCC in corticomedular phase

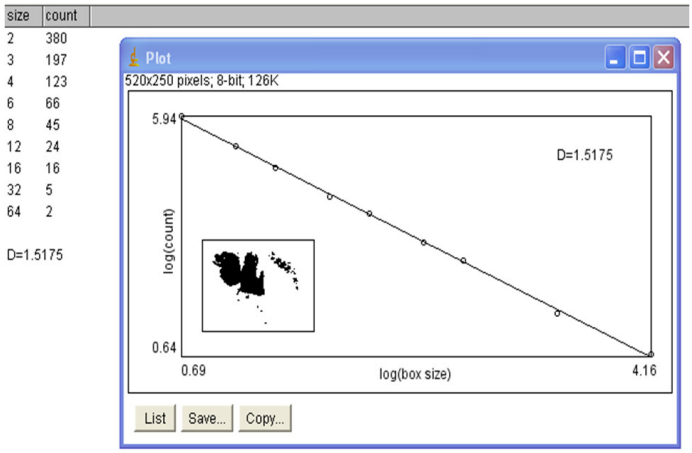

Figure 2. Image analysis by box counting algorithm

ABSTRACT 13

ACTIVE STENT MIGRATION WITH MULTI-LENGTH URETERAL STENTS

Joseph V. DiTrolio, MD[1], Michael D. LaSalle[2], MD, Rahuldev Bhalla, MD[3]

[1] Department of Urology, UMDNJ/New Jersey Medical School, Newark, New Jersey [2]Department of Urology, St. Barnabas Medical Center, Livingston, New Jersey[3] Department of Urology, Stony Brook University Medical Center, Long Island, New York

Introduction: Contributing agents in the fragmentation of stones by extracorporeal shockwave lithotripsy (SWL) are ureteral stents, which allow for better fragmentation of ureteral calculi and assistance of passing those fragments, as well as avoiding ureteral obstruction. Variable length ureteral stents have the luxury of one size fits all. The object of this study was to determine whether removal of the renal portion of the stent in a variable length device would naturally recoil in the bladder, which in turn can be utilized to motivate stone fragment passage actively when incorporated with a partially occlusive proximal device.

Methods: Utilizing the Cook Sof-Flex multiple length stent 4.7Fr, the renal portion of the stent was removed. The stent then was inserted to its maximum length, with a small coil remaining in the bladder, and monitored under direct observation via the cystoscope.

Results: Direct observation of the bladder portion of the multi-length stent revealed a natural tendency for the stent to actively migrate caudally in the ureter and recoil to its natural pre-insertion form in the bladder. This migration was assisted during respiratory motion. Speed of the migration was variable, but motion was persistent.

Conclusion: Distally coiled stents have the capability to be an active assistant in the progression of ureteral calculus or fragments when incorporated with a cephalad semi-occlusive device. Further studies are warranted to convert double-J stents from a static stone passage device to an active assistant in the management of ureteral calculi disease.

ABSTRACT 14 **BEST PAPER AWARD**

MODELING OF MAGNETIC TOOLS FOR USE WITH SUPERPARAMAGNETIC PARTICLES FOR MAGNETIC STONE EXTRACTION

Yung K Tan[1], Raul Fernandez[2], Sara L Best[1], Ephrem O Olweny[1],Stacey L McLeroy[3], Bruce E Gnade[3], Margaret S Pearle[1], Jeffrey A Cadeddu[1]

[1]University Texas Southwestern, [2]University of Texas at Arlington, [3]University of Texas at Dallas

Introduction: Complete stone removal is important in upper tract stone surgery. Unfortunately, even with the latest technological advances, current methods only achieve 50-80% complete clearance of upper tracts stones at the time of primary treatment. Our group has explored the novel use of peptide coated iron oxide superparamagnetic microparticles that bind to calcium stones allowing for extraction of these stones with magnetic tools. We have achieved binding of the particles to stone and pick up of the coated stones with magnets as a proof of concept. This study focused on the analytical and experimental work carried out to predict capture thresholds for feasible magnetic tool sizes and kidney stone magnetization, aimed at understanding the theoretical limits of this technology.

Methods: Magnetostatics equations were applied to a simplified, one-dimensional scenario of a spherical target coated with a variable amount of superparamagnetic particles, placed under the influence of a magnetic field aimed at vertical attraction of the target. Equations were parameterized in terms of (a) target size, ranging from 0.5 mm to 3 mm to represent stone sizes of interest, (b) effective emu per surface area delivered by the particle binding chemistry, and (c) distance to the field source. The field is generated by a fixed, axially-magnetized, high-energy rare earth barrel taking up the maximum diameter of the ureteroscope when backloaded and tethered through the instrument port (2.54 mm diameter x 12.7 mm long). Actual magnetometer data for coated stones was numerically fit and used to synthesize magnetization curves for varying surface-loading chemistries (emu/mm^2). The estimated magnetic dipole was then multiplied by the spatial derivative of the magnetic field projected by the tool to predict the net force acting upon the stone.

Results: Figure 1 depicts a distance-to-capture performance envelope, consisting of a family of curves for various stone sizes tracing the predicted attractive range as a function of available magnetization. The range of emu per unit area resulting from microparticle loading is order-of-magnitude representative of current research standards and commercially available magnetophoretic particles. Experimental testing for known magnetic loading corroborates the low single-digit centimeter range for magnetic stone capture.

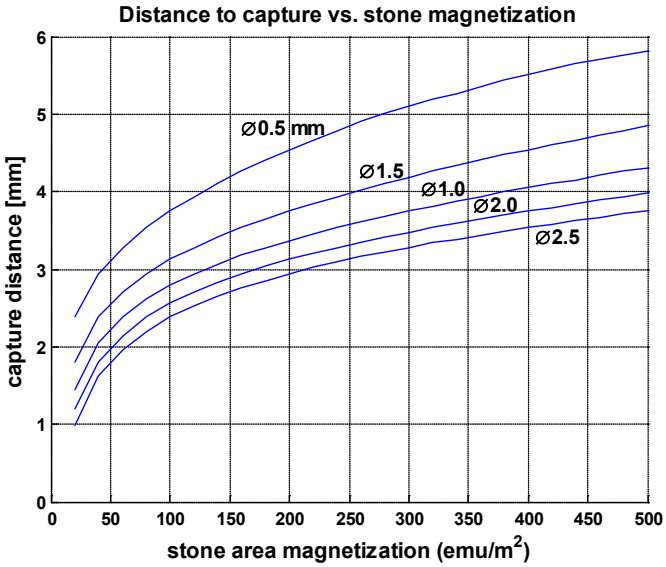

Conclusion:
The use of paramagnetic particles in combination with magnetic tools to extract stones continues to be a promising area of research. Enhanced superparamagnetic micro-particle binding chemistry stands to extend this range, albeit along an asymptotic trendline.

ABSTRACT 15

REAL TIME DIAGNOSIS OF BLADDER CANCER WITH PROBE-BASED CONFOCAL LASER ENDOMICROSCOPY: A PROSPECTIVE DIAGNOSTIC ACCURACY STUDY

Jen-Jane Liu,[1,2] Shelly T. Hsiao,[2] Ying Pan,[1] Katherine E. Mach,[1,2] Alex McMillan,[3] Kristin Jensen,[2] Joseph C. Liao[1,2]

[1] Department of Urology, Stanford University, USA [2] Veterans Affairs Palo Alto Health Care System-Palo Alto, USA, [3] Department of Health Research and Policy, Stanford University, USA

Introduction: Confocal laser endomicroscopy (CLE) is an emerging technology for *in vivo* optical biopsy of the urinary tract that enables micron scale resolution reminiscent of histology using probes that fit in standard cystoscopes/resectoscopes. White light cystoscopy (WLC) has well-recognized shortcomings in bladder cancer diagnosis, particularly in differentiating nonpapillary urothelial carcinoma from inflammation. Accuracy for cancer is reported to be 70-80% for WLC. We previously established suggested criteria to differentiate normal, benign, and neoplastic urothelium with CLE. We report the results of our ongoing prospective diagnostic accuracy study of CLE for bladder cancer diagnosis.

Methods: Patients scheduled to undergo transurethral resection of bladder tumor were recruited. Patients first went WLC, followed by CLE with intravesical fluorescein, tumor resection/biopsy, and histologic confirmation. Suspicious (targeted) areas were marked with electrocautery, imaged with CLE, and resected/biopsied. Normal-appearing areas also were imaged and biopsied as controls. Diagnostic accuracy is determined during cystoscopy by the surgeon and offline in a blinded fashion after image processing. Using histology as the standard, the diagnostic accuracy of WLC and WLC + CLE was calculated.

Results: To date, 35 patients and 118 areas were able to be imaged with CLE; 58 of these areas were deemed suspicious by WLC, and 62 classified as "normal." Of the 58 suspicious lesions, 41 were confirmed to be urothelial carcinoma, and the remainder were benign or normal. Ninety-eight percent of normal-appearing lesions were confirmed to be normal on histopathology, and one area had CIS. For targeted lesions, accuracy for cancer diagnosis by WLC+CLE was 88%, compared to 84% for WLC alone. For normal-appearing lesions, accuracy for cancer diagnosis for both WLC alone and WLC+CLE was 98%. Representative CLE images of normal, benign, and cancer areas are shown in Figure 1.

Conclusion: CLE is a promising adjunct to WLC in the diagnosis of bladder cancer. Preliminary results suggest that the addition of CLE to WLC may improve accuracy of bladder cancer diagnosis compared to WLC alone, although additional data is required to show whether CLE offers a clinically significant benefit.

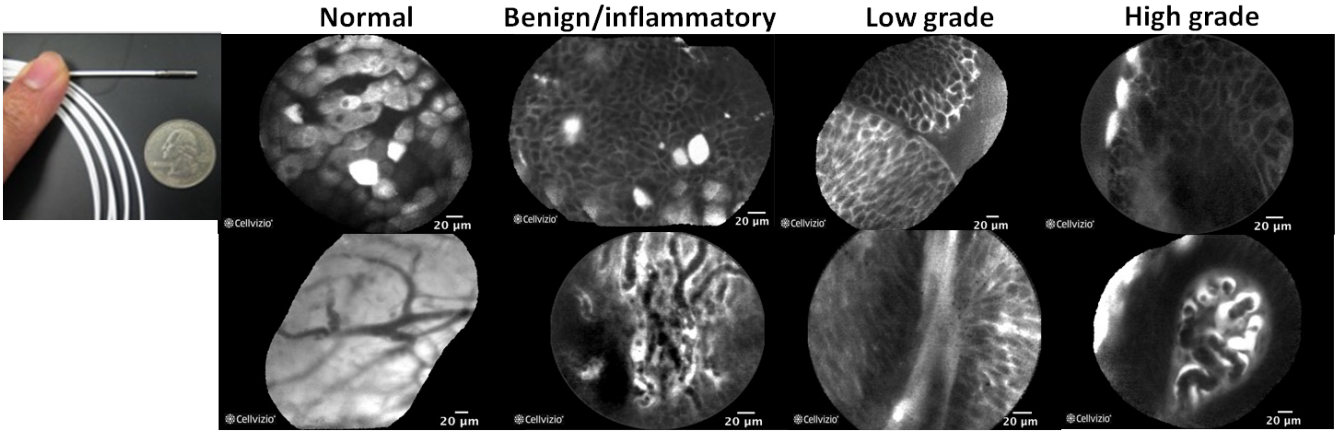

Figure 2: CLE probe and representative CLE images of normal, benign/ inflammatory, low grade, and high grade lesions

ABSTRACT 16

A NOVEL LAPAROSCOPIC CAMERA FOR CHARACTERIZATION OF RENAL ISCHEMIA USING DLP® HYPERSPECTRAL IMAGING: INITIAL EXPERIENCE IN A PORCINE MODEL

Ephrem O. Olweny[1], Sara L. Best[1], Neil Jackson[1], Eleanor F. Wehner[1], Samuel K. Park[1], Yung K. Tan[1], Abhas Thapa[1], Karel J. Zuzak[2], Jeffrey A. Cadeddu[1]

[1]*Dept of Urology, University of Texas Southwestern Medical Ctr., Dallas, TX*
[2]*Digital Light Innovations, Austin, TX*

Introduction: Digital light processing (DLP®) hyperspectral imaging is a non-invasive means of visualizing the chemical composition of *in vivo* tissues using reflectance spectroscopy. It is able to provide a real-time map of surface tissue oxygenation. Using a CoolSNAP HQ_2™ CCD camera (Photometrics, Tucson, AZ), we have previously used this system to characterize renal ischemia during open partial nephrectomy in pigs and humans. By incorporating a light guide, 0^0 laparoscope, and a DVC 1200M CCD camera (DVC, Austin, TX), DLP® hyperspectral imaging was adapted for use during laparoscopic surgery.

Methods: Two adult female pigs underwent DLP hyperspectral imaging using the laparoscopic system, before, during, and after clamping the renal hilum for 90 minutes. Imaging during ischemia was obtained at several intervals. The relative percentage of oxygenated hemoglobin (relative $\%HbO_2$) was determined at each imaging interval using previously described methodology. Data were compared to those for 3 pigs imaged over a similar interval using the open HQ_2™ camera.

Results: For Lap *vs*. Open, relative $\%HbO_2$, was 68.7 *vs*. 72.9% pre-clamp respectively, dropping by an average of 27% *vs*. 26% within 10 minutes after clamping, and rapidly rising to baseline after clamp removal, with similar trends for the two imaging systems.

Conclusion: The laparoscopic DLP hyperspectral imaging system performs similarly to the open system and has excellent spectral imaging capabilities.

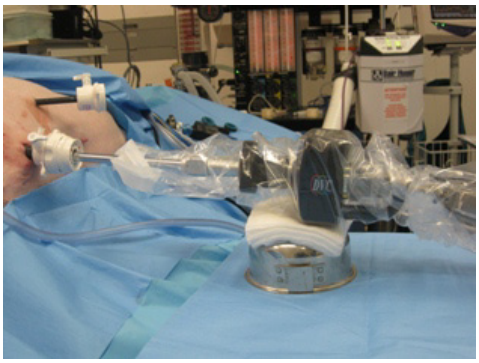

Fig 1. Laparoscopic HSI

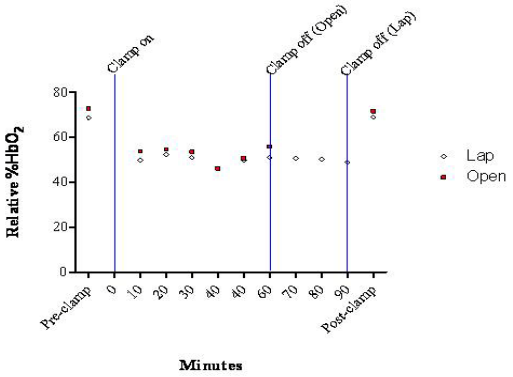

Fig 2. $\%HbO_2$ *versus* time

ABSTRACT 17

SPIDER™ SURGICAL SYSTEM FOR UROLOGIC LESS FROM INITIAL LABORATORY EXPERIENCE TO FIRST CLINICAL APPLICATION

Riccardo Autorino, Michael A. White, Humberto Laydner, Bo Yang, Fatih Altunrende, Rakesh Khanna, Shahab Hillyer, Gregory Spana, Wahib Isaac, Julien Guillotreau, Raschid Yakoubi, Robert J. Stein, Jihad H. Kaouk and Georges-Pascal Haber

Glickman Urological and Kidney Institute, Cleveland Clinic, Cleveland, OH

Introduction: Aim of this study was to describe initial laboratory experience using the SPIDER™ platform for LESS urologic procedures and to report its first clinical application.

Methods: The SPIDER system was tested in a laboratory setting and used for a clinical case of renal cyst decortication. Three tasks were performed during the dry lab session, and different urologic procedures were conducted in a porcine model. The time to complete the tasks and penalties was registered during the dry lab session. Perioperative outcomes and subjective assessment by the surgeons were registered.

Results: The surgeons had a positive experience with the SPIDER system, with a mean overall score of 3.6 (on a scale of 1–5), and they were able to gain proficiency in performing tasks regardless of their level of expertise. The highest scores recorded were for ease of device insertion, instrument insertion and exchange, and triangulation. During the clinical case, the platform provided good triangulation without instrument clashing. However, retraction was challenging because of the lack of strength and precise maneuverability with the tip of the instruments fully deployed.

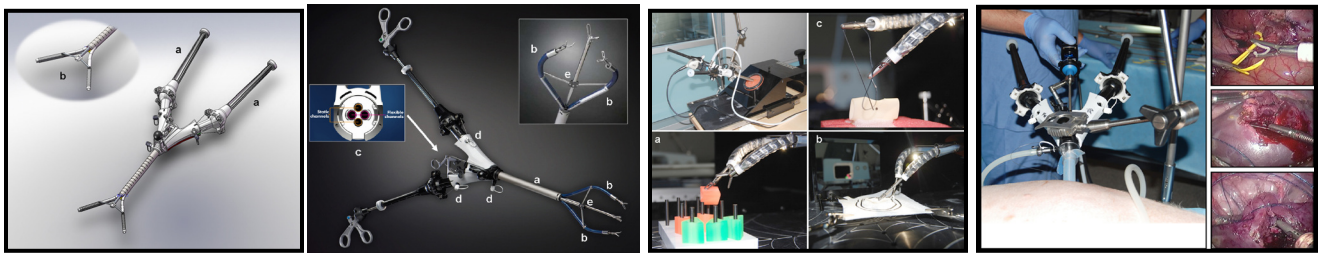

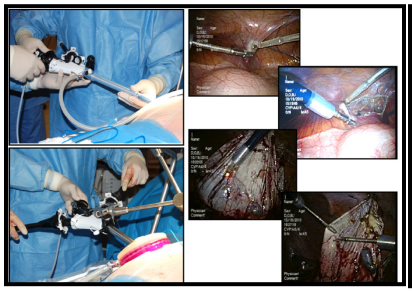

Procedure	Surgeon's level of expertise*	Side	OR time, min	Suturing time, min	EBL, ml	Complications	Addition of an extra port	Time to hilar control, min	WIT, min
Nephrectomy	Low	L	90	–	100	Bleeding	Yes (1 × 5 mm)	60	–
	Medium	R	75	–	0	No	No	35	–
	High	L	45	–	0	No	No	20	–
PN	High	R	67	24	0	No	No	19	29
	Medium	R	65	22	0	No	No	25	29
	Medium	R	90	21	80	Bleeding	No	60	28
Pyeloplasty	High	R	45	30	0	No	No	–	–
	Low	L	60	38	0	No	No	–	–
PC	Medium	–	85	20	0	No	No	–	–

OR = operating room; EBL = estimated blood loss; WIT = warm ischemia time; L = left side; R = right side; PN = partial nephrectomy; PC = partial cystectomy; LESS = laparoendoscopic single-site surgery.
* Low: early laparoscopic experience; medium: advanced laparoscopic experience and limited LESS experience; high: advanced LESS experience.

Conclusion: The SPIDER™ surgical system represents a new concept in the field of the LESS armamentarium, offering intuitive maneuverability of instruments in the abdominal cavity, restored triangulation without external instrument clashing, and no significant gas leakage. Drawbacks of the first generation system include its challenging clinical application, and further refinements are awaited to define the role of the system.

ABSTRACT 18

BALL-TIP HOLMIUM:YAG OPTICAL FIBER

Bodo Knudsen
The Ohio State University Medical Center

Introduction: The holmium:YAG optical laser should be advanced through the working channel of a flexible endoscope in a straight (*i.e.,* non-deflected) configuration. The fiber usually will not pass through the channel with the scope deflected and damage to the working channel may occur as the sharp tip cuts into it and lead to leaks and costly repair. We tested the hypothesis that a ball-tipped fiber allows for safer passage through a flexible ureteroscope in the deflected configuration.

Methods & Results: A 240 µm core sized holmium:YAG optical laser fiber (Boston Scientific, Natick, MA) was prepared with a ball-tip and passed through the working channel of seven flexible ureteroscopes (Wolf Viper, Stryker U-500, Olympus URF-V x2, Olympus URF-P5, ACMI Dur-8 Elite, Storz Flex-X2). The following measurements were recorded: pre- and post-visual assessment of the screen image, resistance to passing fiber in both a 180 degree and maximally deflected configuration (Scale 1- 5), visualization of aiming beam (Scale 1 – 3), and visualization of the stone before and during ablation (1.0J 10z, Scale 1 – 3). Three different fibers were tested for each ureteroscope.

Conclusion: The ball-tipped fiber passed through all scope channels but required greatest force in the two ureteroscopes that had active secondary deflection (DUR-8 Elite, U-500). No visible damage to the ureteroscopes occurred. The ball-tip allowed the fiber to pass through a deflected ureteroscopy and may reduce endoscope damage during holmium:YAG laser lithotripsy.

SCOPE	OPTICS PRE	OPTICS POST	RESISTANCE TO FIBER PASSAGE: 180°	RESISTANCE TO FIBER PASSAGE: FULLY DEFLECTED	AIMING BEAM QUALITY	FIBER VISUALIZATION: PRE-ABLATION	FIBER VISUALIZATION: DURING-ABLATION
Wolf Viper	No damage	No damage	2, 2, 2	2, 2, 2	2, 2, 2	2, 2, 2	2, 2, 2
Stryker U-500	Lens damaged prior to testing	No new damage	2, 4, 4	3, 4, 4	NA	NA	NA
Olympus URF-V #1	No damage	No damage	1, 2, 2	2, 2, 2	2, 2, 2	2, 2, 2	2, 2, 2
Olympus URF-V #2	No damage	No damage	3, 2, 2	2, 1, 2	2, 2, 2	2, 2, 2	2, 2, 2
Olympus URF-P5	No damage	No damage	2, 2, 2	2, 2, 2	2, 2, 2	2, 2, 2	2, 2, 2
ACMI DUR-8 Elite	No damage	No damage	3, 4, 3	3, 4, 3	2, 2, 2	2, 2, 2	2, 2, 2
Storz Flex-X2	No damage	No damage	1, 1, 1	1, 1, 1	2, 2, 2	2, 2, 2	2, 2, 2

ABSTRACT 19

VARIABLE POWER INPUT MICROWAVE ABLATION OF *EX VIVO* PORCINE KIDNEY WITH SIMULATED INTRACORPOREAL TEMPERATURE ENVIRONMENT

Scott M. Castle[1], Kenneth D Fernandez-Prada[1,2], Oscar Villalon[1,2], Lukas Ramcharran[1,2], Raymond J. Leveillee[1,2], Nelson Salas[1,2]

[1]*Joint Bioengineering and Endourology Developmental Surgical (JBEDS) Laboratory, Division of Endourology, Laparoscopy, and Minimally Invasive Surgery, Department of Urology, University of Miami Miller School of Medicine , Miami, Florida*

[2]*Department of Biomedical Engineering, University of Miami, Coral Gables, Florida*

Introduction: Thermal ablation currently has widespread use for the treatment of small renal masses with radio-frequency and cryoablation being used most frequently. Microwave (MW) ablation is a new modality with limited clinical experience in the kidney. Manufacturer parameter recommendations for treatment endpoint are not directed specifically and may not be suitable for renal ablations. We aimed to study the effect of incremental MW power settings on renal tissue temperatures surrounding the MW probe in an *ex vivo* porcine experiment when using the ValleyLab Evident® 915 MHz MW ablation system (Covidien Inc, Boulder, CO).

Methods: Fresh frozen porcine kidneys were thawed and placed in a 37°C water bath for 30-60 minutes prior to experimentation. A six-sided acrylic box was designed with a real-time electrical thermocouple feedback system with heating pads (Omega, Stamford CT), allowing ambient air temperatures to be maintained at 37°C. Kidneys were placed atop approximately 1.0 – 1.5 cm thick bovine muscle samples. The acrylic box contained holes to allow placement of the MW probe along the coronal plane of the kidney. Non-conducting peripheral fiber-optic thermal sensors (Lumasense, Santa Clara, CA) were deployed into the anterior surface of the kidney perpendicular to the probe axis on a pre-made grid to enable temperature measuring at discrete distances (Figure 1). A total of 15 ablations were performed for 10 minutes at 20W (5), 40W (5), and 45W (5) with a single 2.0 cm exposed tip probe. Temperatures were recorded at 1Hz during and post-ablation.

Results: Mean kidney parenchymal starting temperatures ranged from 31 to 38°C prior to ablation start. Deployments at 20, 40, and 45W showed mean peak temperatures of 70.9, 83.4, and 94.3°C at location 1 (45W>20W, p = 0.001), respectively. At location 2, mean peak temperatures were 85.6, 95.6, and 100.0°C (Figure, 45W>20W, p = 0.03), respectively. At location 3, mean peak temperatures were 51.8, 51.4, and 58.5°C (45W=40W=20W, p>0.05), respectively. At location 4, mean peak temperatures were 62.1, 72.9, and 84.3°C (45W>20W, p = 0.04), respectively.

Conclusion: Treatment endpoint for renal tissue will be affected by the output power and irradiation time during microwave ablation. Our *ex vivo* normal tissue experiments suggest that a 10 min ablation interval at different power settings creates different heating patterns. In the future, power adjustments may be used to optimize cancer control, along with renal preservation, in renal MW ablation.

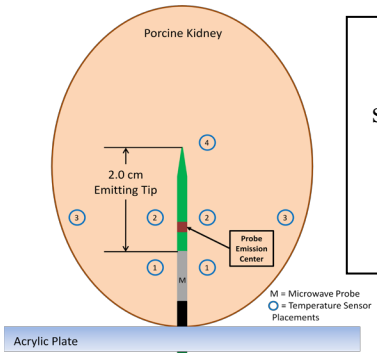

Figure 1. Temperature sensor schematic during MWA in *ex vivo* porcine kidneys.

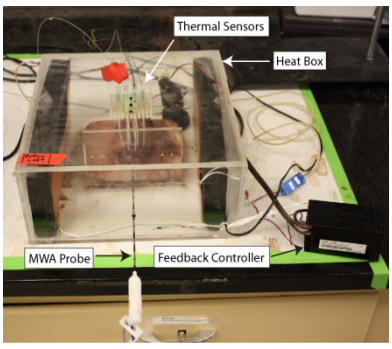

Figure 2. Acrylic box with thermocouple feed-back system during MWA irradiation of *ex vivo* porcine kidneys

ABSTRACT 20

PNEUMODISSECTION: A NEW CRYOABLATIVE TECHNIQUE

Maurice MJ[1,2], Haaga JR[2], Ponsky LE[2]
[1]Case Western Reserve University, [2]University Hospitals Case Medical Center

Introduction: While typically reserved for poor surgical candidates, percutaneous cryoablation (PCA) is emerging as a safe and effective alternative to partial nephrectomy for treating the small renal mass (SRM). PCA poses a risk of thermal injury to adjacent tissues, limiting its application. Various protection techniques aimed at minimizing this risk have been described without widespread success or acceptance. We describe pneumodissection (PD), a novel technique for preventing unintended thermal tissue injury during PCA. We present our initial experience with 3 patients.

Methods: Using a Yueh needle, a sufficient quantity of air was injected into the perirenal space under CT guidance until the resulting air pocket separated the kidney mass from the adjacent bowel. PCA was completed as previously described. Safety was evaluated by analyzing post-procedural and follow-up CT imaging for bowel injury and by clinical assessment.

Results: Three patients with SRMs with overlying bowel, with a mean age of 65 years, mean tumor size of 1.8cm, and with tumors located in the right (2) or left (1) kidney, and being lateral (2) or medial (1), were studied. PD mechanically separated the bowel from tumor (mean distance 1.3cm), permitting successful PCA. There were no immediate or late complications (median follow up 7 months) by CT imaging or clinical assessment.

Conclusion: We have shown that PD is a safe and effective technique for preventing bowel injury in patients undergoing PCA. PD physically separates and thermally insulates vulnerable structures from the ice ball, making previously inaccessible tumors amenable to PCA. Unlike other dissection techniques, PD employs room air, an excellent thermal insulator, which does not freeze or conduct thermal energy as readily as water. Since room air is available widely and is dispensed easily, PD requires no special equipment. Given our success, we support the widespread adoption of PD. In the future, PD may broaden the application of PCA and revolutionize therapy for the SRM. Further study is needed to validate these results.

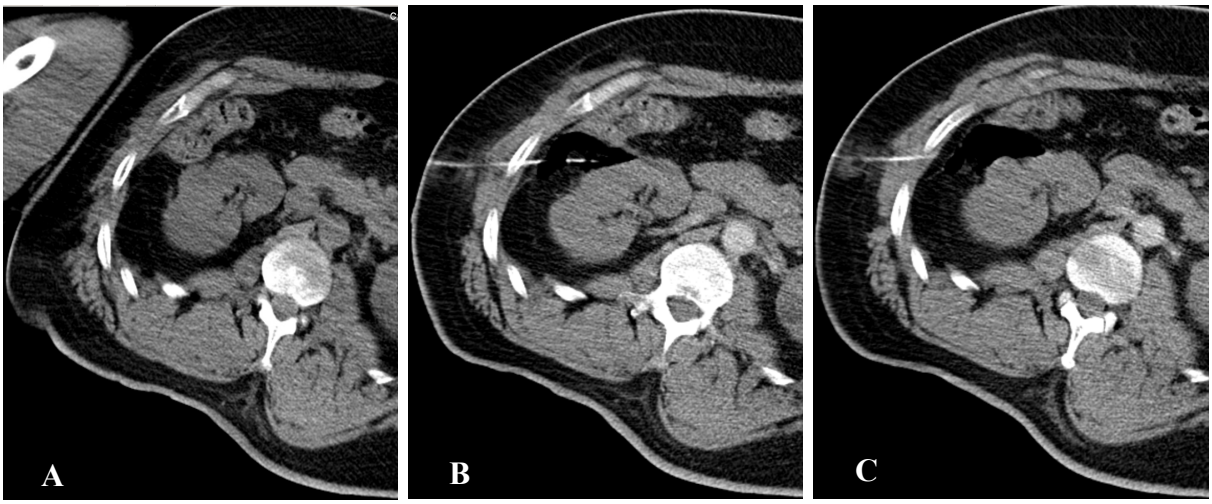

Figure 1: CT images pre- (A) and post- (B, C) PD.

ABSTRACT 21

PREDICTION OF WARM ISCHEMIA TIME AND POSTOPERATIVE RENAL FUNCTION BY THE RENAL NEPHROMETRY SCORE IN PATIENTS UNDERGOING ROBOTIC PARTIAL NEPHRECTOMY

Fatih Altunrende, Humberto K Laydner, Riccardo Autorino, Yang Bo, Michael A White, Rakesh Khanna, Wahib Isac, Shahab Hillyer, Gregory Spana, Sylvain Forrest, Adrian Hernandez, Julien Guillotreau, Rachid Yakoubi, Georges-Pascal Haber, Jihad H Kaouk, Robert J Stein

Cleveland Clinic, Cleveland, OH

Introduction: Prolonged warm ischemia time (WIT) is associated highly with renal damage during partial nephrectomy. Recently, the RENAL nephrometry score (RNS) was developed to standardize the description of renal tumor anatomy in a quantifiable manner. We analyzed preoperative factors as well as individual categories of the RNS to identify those predicting a longer WIT and affecting postoperative renal function.

Methods: Medical records and imaging exams of 187 consecutive patients who underwent robotic partial nephrectomy at our institution were reviewed. Total RNS and its individual categories were determined. Multivariable linear regression analysis was performed to identify factors significantly associated with WIT and late postoperative glomerular filtration rate (GFR).

Results: Mean patient age, body mass index (BMI), and tumor size were 59.6 years, 30.6 Kg/m^2, and 3.15 cm, respectively. The overall RNS was categorized as low complexity (4-6) in 84 patients (45%), moderate complexity (7-9) in 80 (43%), and high complexity (10-12) in 23 (12%). There was no association between gender (p=0.6), BMI (p=0.3), or anterior/posterior location (p=0.8) with WIT. A longer WIT was associated with tumor size > 4cm (p<0.0001), entirely endophytic properties (p=0.005), tumor $\leq$ 4mm near the collecting system/sinus (p<0.0001), and location of the tumor > 50% across the polar line, or crossing the axial renal midline, or entirely between the polar lines (p=0.004). The total RNS and WIT correlated highly (Spearman correlation coefficient=0.54, p<0.0001). There was a very significant trend of higher WIT by the increase of the complexity of the renal tumor (p for trend <0.0001). Late postoperative GFR could be predicted by the following equation: $GFR_L = 36 + 0.7 \times GFR_{pre} - 0.6 \times WIT - 0.2 \times age + 0.4 \times RNS$, where GFR_L: late postoperative GFR and GFR_{pre}: preoperative GFR.

Conclusion: WIT is affected highly by the RNS and its categories, except anterior/posterior location. Increased complexity of the tumor leads to a very significant trend of higher WIT. Prediction of late postoperative renal function could help in the decision-making process for nephron sparing surgery. Further validation of our late postoperative equation is warranted.

$$GFR_L = 36 + 0.7 \times GFR_{pre} - 0.6 \times WIT - 0.2 \times age + 0.4 \times RNS$$

GFR_L: late postoperative GFR

GFR_{pre}: preoperative GFR

Figure 3: Equation predictive of late postoperative GFR

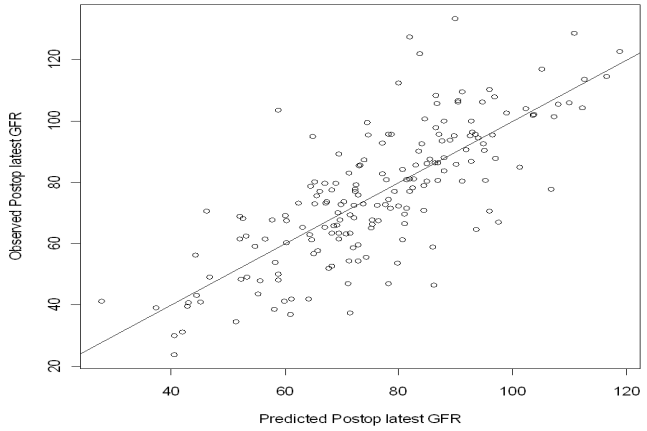

Figure 2: Performance of the equation to predict GFR

*The dots represent the actual values, while the 45° line represents what would be the perfect model

ABSTRACT 22

MEASUREMENT OF SPATIAL DISTRIBUTION IN SEXTANT PROSTATE BIOPSY

Doyoung Chang, Chunwoo Kim, Hyungjoo Kim, Yihe Zuo, Doru Petrisor, Misop Han, Dan Stoianovici
Urology Robotics Lab, Johns Hopkins University
http://urobotics.urology.jhu.edu/

Introduction: Prostate biopsy typically is performed under transrectal ultrasound (TRUS) guidance. In clinical practice, it is difficult to determine the accuracy of the geometric distribution of TRUS-guided sextant biopsy within the gland.

Methods: A biopsy simulation system was built to measure *in vitro* biopsy locations accurately. This system consists of a custom-made pelvic mockup with precisely defined geometry and an optical tracking system (Polaris®, NDI, Ontario, Canada) used to measure the relative location of the mockup, TRUS probe, and biopsy needle (Figure 1). The pelvic mockup includes a prostate model and rectal cavity. Special molds were made for building the mockup so that the geometry, size, and position of the prostate within the mockup is consistent and invariant from one mockup to another. An active (6-DOF) optical tracking marker was assembled precisely on the mockup box. Since the location of the prostate within the box is known, this marker can be used to measure the exact location of the prostate. Two other active markers were mounted on the handle of the TRUS probe to measure its location. Finally, a point (3-DOF) marker was mounted on the shaft of the biopsy needle to measure the depth of needle insertion. Overall, this system measures the locations where biopsies are sampled. Calibration and verification tests showed that the measurement errors of the instrument are within 1 mm. We defined the gold standard using a common 12-core sextant biopsy plan, and then determined how closely an experienced urologist can perform a biopsy compared to the gold standard.

Results: A preliminary result from a simulated biopsy is represented graphically in Figure 2. The simulated biopsy cores are clustered and a large portion of the prostate gland remains under-sampled. Targeting errors are defined as the distance from the gold standard to the core center of each sample. The average error was 8.86 mm.

Conclusion: TRUS-guided prostate biopsies may not closely follow sextant biopsy plans. A study with multiple experienced urologists is in progress.

Acknowledgement: Study partially supported by the Sidney Kimmel Comprehensive Cancer Center at Johns Hopkins, Award CA141835 from the National Cancer Institute, Award PC101984 form the Prostate Cancer Research Program (PCRP), and Hitachi Medical Systems America.

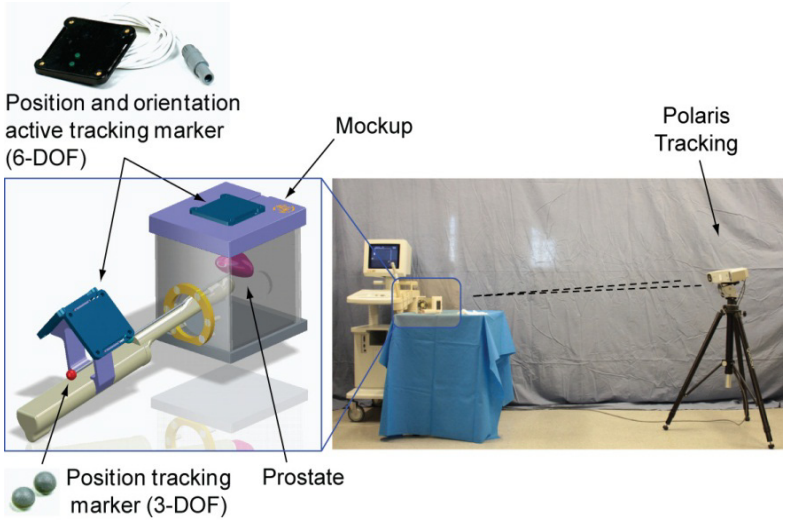

Figure 1: Optical tracking of probe and prostate mockup

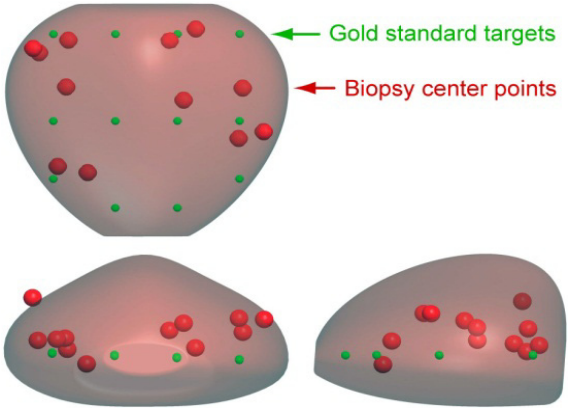

Figure 2: Gold standard biopsy locations (green marks) and actual center of core samples acquired (red marks) in three orthogonal views of the prostate.

ABSTRACT 23

INCIDENTAL PROSTATE CANCER TREATED WITH ROBOTIC TRANSRECTAL HIGH INTENSITY FOCUSED ULTRASOUND (HIFU)

Thueroff Stefan[2,3], Chaussy Christian[1,3]

[1]Dept. of Urology University of Regensburg,
[2]Dept. of Urology Klinikum Muenchen, [3]Harlachinger Krebshilfe e.V.

OBJECTIVE: In 8% of the patients who undergo TURP because of symptomatic BPH, histological examination shows PCa. Consequently, these patients need a therapeutic approach for their PCa. We treated these patients with HIFU as a local therapy and analyzed efficacy and side effects.

MATERIAL AND METHODS: Since 2000 we identified 65 patients with incidental PCa out of our prospective monocentric HIFU database (n = 2,300). Their mean age was 70 years (range 57-87 years), the mean PSAi was 4.9 (range 1-32), mean prostate volume 39 cc (range 16-130 cc), and a median of 20 grams (range 1-95 g) had been resected. Histology showed median 5% (5-50%) positive chips and a Gleason of 5 (3-9). Patients were treated completely with transrectal HIFU (robotic Ablatherm® integrated imaging, EDAP-TMS, Lyon) in spinal anesthesia in a single session.

RESULTS: A PSA Nadir of 0.07 (0-3.67) was measured after 1.8 months (range 0.7-5.9 months), including 62% <0.1 / 81% <0.5 ng/ml). A median PSA of 0.13 (0-8.3), equivalent to a median PSA velocity of 0.01 ng/ml/year, was found after a mean follow-up of 48 months (range of 3-110 months).
Intra- and post-operative side effects were minimal-- Clavien: < 15% I-III. Long-term follow-up showed 45% of secondary obstructions caused by necrotic tissue or bladder neck stenosis. Other long- term side effects were mild: intermediate urinary stress incontinence Grade I (11%), and UTI (14%). Median disease-free survival was 31 months in a median 33 month follow-up. There was no cancer- specific mortality.

CONCLUSION: The PSA nadir of 0.07 ng/ml, as well as the PSA velocity of 0.01 ng/ml/year, indicates that HIFU can be used as a curative therapy for patients with incidental PCa. The psychological burden of the patients who are confronted either with untreated cancer disease in cases of "wait & see," or with fear of significant side effects in cases of radical surgery or radiation, can be avoided by this non-invasive transrectal therapy with High Intensity Focused Ultrasound.

Source of Funding: Harlachinger Krebshilfe e.V, Lingen Stiftung
Thanks to Ms. Regina Nanieva for HIFU database management and analysis

ABSTRACT 24

ROBOTIC VERSUS LAPAROSCOPIC PARTIAL NEPHRECTOMY FOR BILATERAL SYNCHRONOUS KIDNEY TUMORS: COMPARATIVE ANALYSIS AT A SINGLE INSTITUTION

Shahab P. Hillyer, Riccardo Autorino , Humberto Laydner, Bo Yang, Fatih Altunrende, Michael White, Gregory Spana, Rakesh Khanna, Wahib Isac, Adrian V. Hernandez, Matthew Simmons, Robert Stein, Georges-Pascal Haber, and Jihad Kaouk

Section of Laparoscopic and Robotic Surgery, Glickman Urological and Kidney Institute
Cleveland Clinic, Cleveland, Ohio

Introduction: Robotic Partial Nephrectomy (RPN) is emerging as an attractive minimally invasive nephron-sparing approach for renal tumors. The aim of this study was to compare intra-operative and early post-operative outcomes of RPN to Laparoscopic Partial Nephrectomy (LPN) outcomes in patients with bilateral synchronous renal tumors.

Methods: Our ongoing IRB-approved prospectively maintained kidney cancer database was used to identify the study population. Medical records of patients who underwent minimally invasive nephron-sparing surgery at our institution from January 2001 and March 2010, were used. A cohort of 9 patients undergoing bilateral RPN was identified and compared to 17 consecutive patients who underwent sequential bilateral LPN. Demographic, intra-operative, post-operative, and short-term renal functional data were retrospectively compared between the 2 groups.

Results: A total of 18 procedures were performed in the RPN group and 32 procedures in the LPN group. Mean warm ischemia time was shorter in the RPN group than the LPN group (23 vs. 29.5 minutes, respectively; p=0.059). Median tumor size was 3.7 cm and 2.7 cm in the RPN and LPN groups, respectively (p=0.03). Final post-op GFR mean was 68.7±9.8 and 51.2±6.6 in the RPN and LPN groups, correspondingly (p=0.004). No difference was found in terms of complications in the RPN group (n=2) versus the LPN group (n=4).

Conclusion: RPN is a safe and effective minimally invasive nephron-sparing treatment for bilateral synchronous kidney tumors. There is a trend towards shorter warm ischemia time and less impact on postoperative renal function compared to the laparoscopic approach.

Table I: Outcomes

	RPN	LPN	p value
Number of Procedures	18	32	
Mean estimated blood loss (mL)	333±138.6	225±54.7	0.14
Average warm ischemia time (min)	23±5.2	29.5±37.5	0.056
Average length of time to discharge (days)	4.7±1.5	3.7±0.4	0.16
Number of follow up Months	13.4±4.5	22.1±14.5	0.24
Latest post-op GFR (mean, std)	68.7±9.8	51.2±6.6	0.004
Average % decrease in GFR	-18.6±8.6	-32.2±9.6	0.03
Number of patients with postoperative complications (%)	2 (11%)	4 (12.5%)	0.73
% with positive margins (# of patients)	0	0	

*Group comparison p-value performed using two-tailed T test

ABSTRACT 25

HIGH FREQUENCY ULTRASOUND IMAGING DURING NONINVASIVE LASER COAGULATION OF THE CANINE VAS DEFERENS, *IN VIVO*

Christopher M. Cilip[1], Phillip M. Pierorazio[2], Ashley E. Ross[2], Mohamad E. Allaf[2], Nathaniel M. Fried[1]
[1] *Department of Optical Science and Engineering, University of North Carolina at Charlotte, NC*
[2] *Department of Urology, Johns Hopkins Medical Institutions, Baltimore, MD*

Introduction: Approximately 500,000 vasectomies are performed annually in the United States, making it the most common urological procedure in the U.S. Although more effective and less likely to have complications than tubal ligation, the number of men undergoing surgical sterilization is approximately three-fold less than women. A safer, less invasive approach to vasectomy may eliminate male fears associated with surgery and reverse these trends. Our laboratory has recently demonstrated successful noninvasive laser coagulation and thermal occlusion of the canine vas deferens, *ex vivo* and *in vivo*, with the goal of developing a completely noninvasive vasectomy procedure. During conventional surgical vasectomy, occlusion of the vas is confirmed visually. However, during noninvasive laser vasectomy, a noninvasive diagnostic method may be helpful to confirm successful targeting and closure of the vas to insure consistent and reproducible results. High frequency ultrasound (HFUS) imaging has been shown previously to quantify the anatomical dimensions of the human *vas* accurately, *in vivo*. The objective of this study was to use HFUS to confirm successful targeting and thermal coagulation of the canine *vas* during noninvasive laser vasectomy.

Methods: Bilateral noninvasive laser coagulation of the vas deferens was performed in a total of 6 dogs using an Ytterbium fiber laser with a wavelength of 1075 nm, output power of 9.0 W, 500 ms pulse duration, pulse rate of 0.5 Hz, and 3 mm diameter spot. A cryogen spray cooling device was used to cool the treatment area during the procedure and prevent the formation of scrotal skin burns. A standard clinical US system with 13.2 MHz transducer was used to image the canine vas before and after the procedure. Simultaneous application of Doppler US at a frequency of 6.15 MHz helped to distinguish between the *vas* and the spermatic cord. Burst pressure measurements were recorded for the excised thermally coagulated *vas* samples to quantify the degree of closure.

Results: Acute burst pressures averaged 291 $\pm$ 31 mmHg, significantly greater than previously reported normal ejaculation pressures of 136 $\pm$ 29 mmHg. Representative HFUS images of the canine vas deferens both before and after the procedure are shown in Figure 1, demonstrating the ability to distinguish native from thermally coagulated *vas*. Doppler US indicated normal blood flow through the testicular artery and no detectable collateral damage to proximal structures.

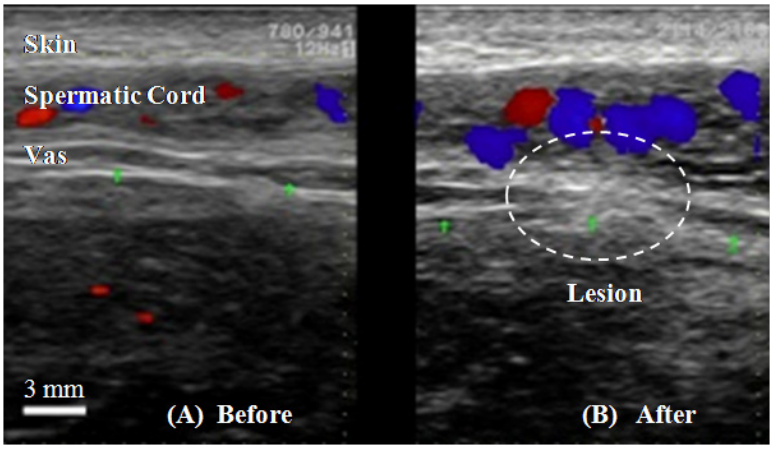

Figure 4. Representative ultrasound images showing (A) native *vas* before the procedure and (B) thermal lesion in *vas* after the procedure.

Conclusion: High frequency ultrasound can be used as a diagnostic method to confirm successful targeting and thermal coagulation of the canine vas during noninvasive laser vasectomy.

ABSTRACT 26

SPARKER ARRAY FOR LITHOTRIPSY

Raymond Schaefer, Michael Grapperhaus
Phoenix Science & Technology, Inc.

Introduction: Despite the positive clinical outcomes (greater than 90% success rate) of early electro-hydrodynamic lithotripters (EHLs), such as the Dornier HM3, the use of shock wave lithotripsy (SWL) has decreased in the last 20 years. This is attributable to several factors, including the short lifetime of sparker electrodes in the HM3, which prompted a move to non-sparker shock-wave sources in 2nd and 3rd generation lithotripters. As a result, the success rate of SWL has decreased to less than 50% in recent years, while the success rate of invasive techniques, such as flexible ureteroscopy, have success rates greater than 90%. We have developed a new shock wave source using an array of small sparker sources for use in SWL that can resolve lifetime and other issues of sparker based SWL.

Methods: Two arrays of 7 sparkers were built and operated simultaneously, with the sparkers arranged along the circumference of a circle in a single plane (Figure 1). The pressure field was measured with PVDF hydrophones (Onda HGL-0400 at low pressure and Onda HNS-0500 at higher levels) both at focus and along three axes around focus. The pressure field from a single sparker also was measured and used in a simulation to estimate the pressure field from different array configurations and operating conditions. The sparker arrays also were used to break artificial stones made with Ultracal-30 gypsum.

Results: The sparker array produced a pressure pulse that delivered a peak pressure of 40 MPa with a pulse width of 0.7 μsec to the focus. The planar sparker array produced a pressure field with a focal spot (50% of peak) that is 38 mm long the direction normal to the plane of the array, but narrow, only 2.5 mm, within the plane of the array and perpendicular to the direction of propagation and 15 mm long in the direction of propagation. Simulation of the pressure field reproduced this, and also predicted a more symmetric focal region for a compact 3-dimenstional arrangement with the sparkers on a spherical surface. The model predicts that this configuration will produce a focal region between 4.2 and 6.4 mm in the plane perpendicular to propagation and 50 mm long in the direction of propagation. The

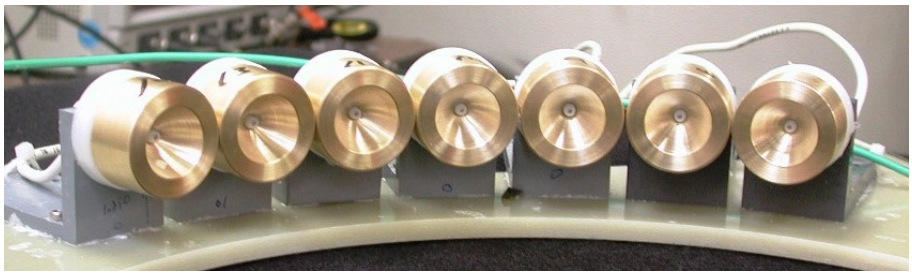

Figure 1: Seven element sparker array

simulations also suggest that the physical pulse width is proportional to the temporal pulse width of the pulse, which provides greater flexibility in the design of the pressure field.

The sparker array was used to break artificial stones in 7 tests using 2400 shock wave pulses in each test. Additional testing resulted in the array delivering more than 20,000 pulses without a decrease in output pressure.

Conclusion: The sparker array provides a consistent, configurable electro-hydrodynamic shock wave source for use in shock wave lithotripsy.

ABSTRACT 27

THREE-DIMENSIONAL IMAGING OF URETER WITH ENDOSCOPIC OPTICAL COHERENCE TOMOGRAPHY

Hui Wang, Wei Kang, Hui Zhu, Gregory MacLennan, Andrew Rollins,
Case Western Reserve University, Cleveland, OH

INTRODUCTION AND OBJECTIVES: To verify the ability of identifying the layered structures of ureteral wall and imaging a segment of ureter in three dimensions with a high speed endoscopic optical coherence tomography (EOCT).

METHODS: We imaged a porcine ureter *ex vivo* using a spectral domain EOCT with an optimally designed circumferential scanning fiber catheter. The images were correlated with the histological images to identify corresponding structures. Three-dimensional images and enface images at different radical depths were reconstructed from the multiple cross-sectional images to show the layered structure of a segment of the ureter from different views.

RESULTS: EOCT images can clearly reveal all layers of the ureteral wall, as shown in the histological images. Especially with the optimally designed fiber catheter, the light beam was well centered during the rotation and pull back, which allowed constant acquisition of high fidelity images and unambiguous identification of the smooth muscle layers in all images. With significantly improved imaging speed, a segment of ureter (20 mm) can be imaged in a short period of time.

CONCLUSIONS: With its capability to image all layers of the ureteral wall, EOCT offers the potential to stage urothelial cancers that have infiltrated the muscular wall (stage T2). This information will be complimentary to the diagnostic information obtained through ureteroscopic biopsy and CT urogram.

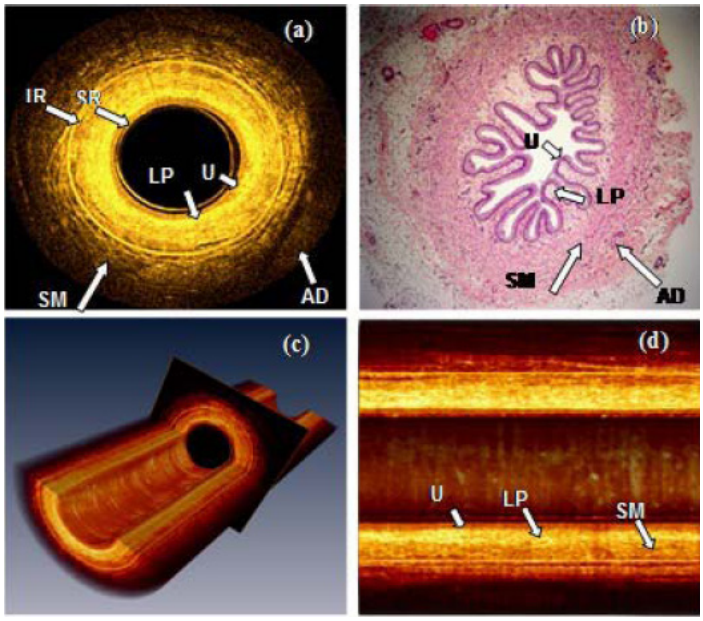

ABSTRACT 28

COMPARISON OF TENSILE BEHAVIOR OF BLADDER, KIDNEY, AND URETER TO A LATEX "4-IN-1" SUTURE MODEL

Phillip Mucksavage[1], Kevin I. Ruzics[1], Peter Vu Bui[2], , Donald L. Pick[1], Jason Lee[1], Adam Kaplan[1], Elspeth M. McDougall[1],Albert F. Yee[2], and Michael K Louie[1]

[1]Department of Urology, [2]Department of Chemical Engineering and Materials Science, University of California, Irvine, USA

INTRODUCTION: Creating a suturing model for training purposes often is hampered by the inability to recreate a realistic feel for placing sutures or knot-tying. We compared the tensile strength of the latex 4-in-1 suture model (a training model for suturing bladder, vesicourethral anastomosis, ureter and UPJ), with the tensile behavior of porcine bladder, kidney and ureter.

METHODS: Fresh porcine bladder, kidneys, and ureters were compared to the 4-in-1 model. A mechanical tester (Test Resources model 800LE) was used to pull a 0 vicryl suture out of the sample at a constant velocity, while measuring force (N) vs. displacement (mm). The 4-in1 model, kidney, and bladder tissue was torn in various directions, while the ureter was torn longitudinally. Bladder muscle fiber orientation also was used to compare tensile strengths in the parallel and perpendicular fiber orientation.

RESULTS: The bladder and ureter had similar tensile strengths to the 4-in-1 model but were not similar to the kidney (Figure 1). For the bladder, the difference between tearing according to observed parallel or perpendicular fibers was not statistically significant (p=0.08).

CONCLUSIONS: The 4-in-1 model was similar to ureteral and bladder tissue, but did not realistically model kidney tissue.

Figure 1. Tensile Strengths of Each Material Tested

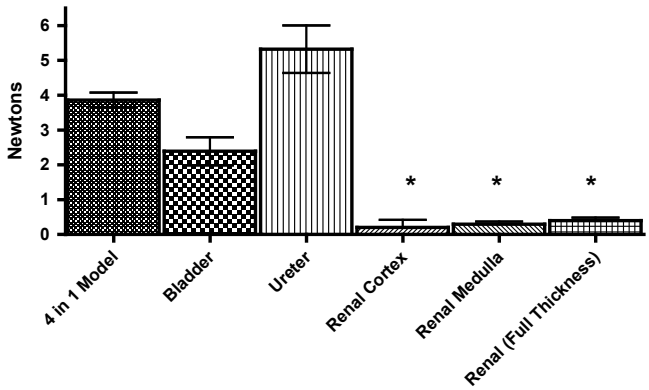

** = significantly different when compared to 4-in-1 model. All samples were compared to the 4-in-1 model using an unpaired Student's t-Test with p < 0.05 considered significant.*

ABSTRACT 29

A NOVEL STEREOTACTIC PROSTATE BIOPSY SYSTEM INTEGRATING PREINTERVENTIONAL MRI WITH LIVE US FUSION

Kuru TH, Hadaschik BA, Hohenfellner M

Department of Urology, Universityhospital Heidelberg, Heidelberg, Germany

Introduction: A key challenge for prostate cancer therapy is to diagnose tumor lesions precisely. Here we describe a novel stereotactic prostate biopsy system which integrates preinterventional MRI with peri-interventional ultrasound for perineal prostate biopsies.

Methods: 50 men with suspicion of prostate cancer underwent multiparametric 3T-MRI (median age 67 years, mean PSA 8.9 ng/ml, mean prostate volume 51 ml). Suspicious lesions were marked before the obtained data were transferred to the stereotactic biopsy system. Using a custom-made biplane TRUS probe mounted on a stepper, 3D-ultrasound data were generated and fused with the MRI. As a result, suspicious MRI-lesions were superimposed onto the TRUS-data. Next, 3D biopsy planning was performed including systematic biopsies from the peripheral and transition zones of the prostate. Perineal biopsies were taken under live US imaging, and the location of each biopsy was documented in 3D. Feasibility, safety, target registration error and cancer detection were evaluated.

Results: Prostate cancer was detected in 27 out of 50 patients (54%). A positive correlation between MRI findings and histopathology was found in 72%. In MRI-lesions marked as highly suspicious, the detection rate was 100% (13/13). Target registration error of the first 1159 biopsy cores was 1.7 mm. Regarding adverse effects, one patient experienced urinary retention and one patient a perineal hematoma. Urinary tract infections did not occur.

Conclusion: Perineal stereotactic prostate biopsies guided by the combination of MRI and ultrasound allow effective examination of suspicious MRI-lesions. Each biopsy core taken is documented accurately for its location in 3D enabling MRI-validation and tailored treatment planning. The morbidity of the procedure was minimal.

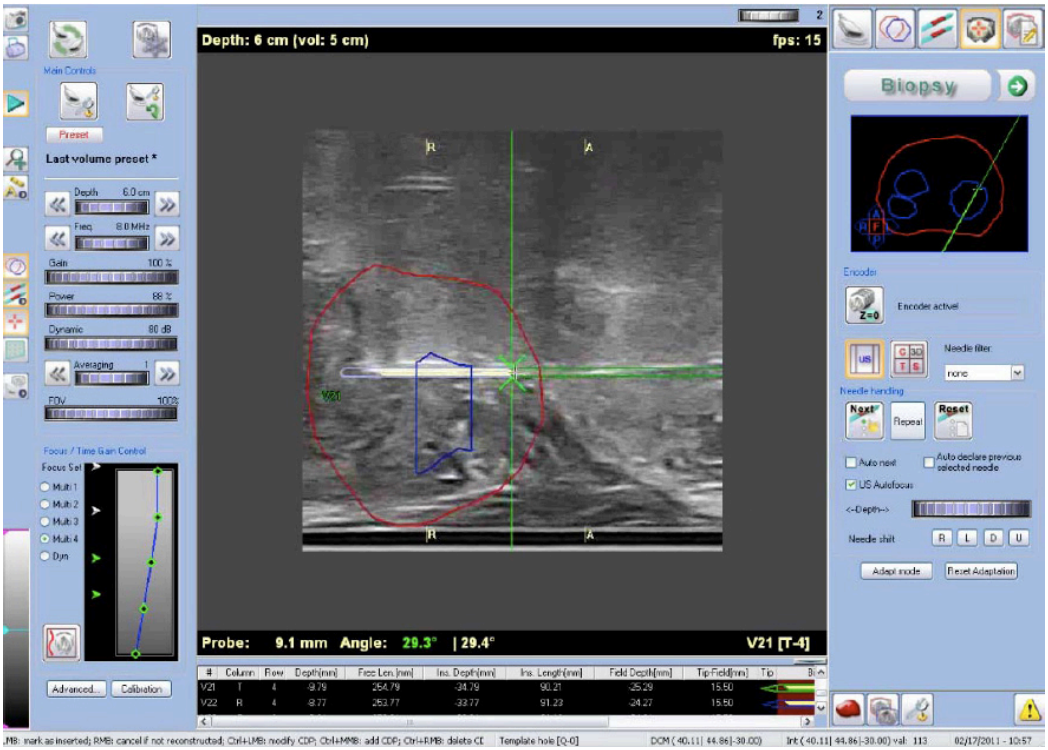

ABSTRACT 30

JACKHAMMER NEPHROSCOPY (JN): AN AID TO FRAGMENT EVACUATION DURING PERCUTANEOUS NEPHROLITHOTOMY

Rawandale AV, Kurane CS, Patni LG
Institute of Urology, Dhule, India.

Objective: Evacuation of small fragments poses a problem during Percutaneous nephrolithotomy (PCNL). We describe and evaluate an innovative "Jackhammer nephroscopy" to overcome this problem.

Methods: Jackhammer nephroscopy (JN) was designed and the safety, advantages and weaknesses evaluated in 15 cases.

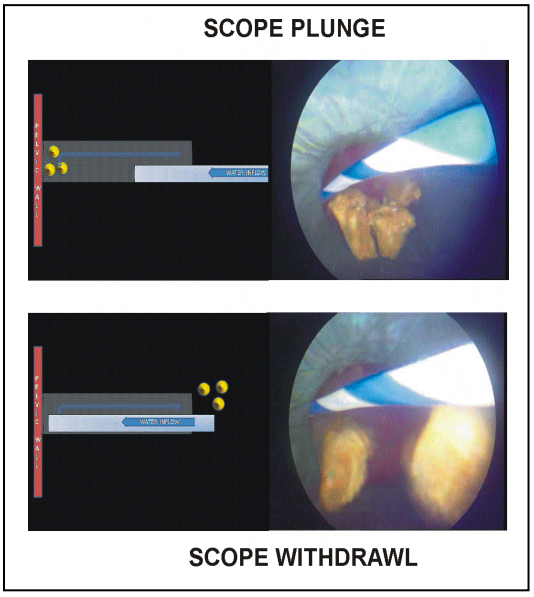

Steps of JN:

1. Trap fragments in the sheath holding the sheath against the pelvic wall, creating a closed water column in the sheath.
2. Hold the scope along one wall of the Amplatz Sheath.
3. Keep inflow open.
4. Perform rapid controlled longitudinal to and fro Jackhammer movements of the scope.
5. Archimedes principle displaces the water column – with the fragments.

Results: The JN was used for all punctures, stones, renal anatomies, and for second time surgeries. JN helps fast and easy extraction of the stone fragments. We never had to abandon the technique. No intra-operative or post-operative complications were observed. Larger fragments need accessory devices. Collecting evacuated fragments may need a sieve drape. Some learning curve should be expected

JN DATA

Renal units	15
Mean age (yrs)	35.20 (11-65)
Male: Female	4:1
History of surgeries	1 (6.67%)
Fragments evacuated	15 (100%)
Calyx	
Upper	3 (20%)
Middle	3(20%)
Lower	9 (60%)
Tract Size	
24 Fr	4 (20%)
26 Fr	1 (9%)
28 Fr	6 (54.5%)
30 Fr	4 (36.4%)

Conclusion: We recommend the Jackhammer nephroscopy as safe, fast, effective and cheap technique to evacuate small fragments during percutaneous nephrolithotomy.

ABSTRACT 31

IN VIVO EVALUATION OF A NOVEL BIPOLAR RADIOFREQUENCY ABLATION DEVICE IN PATIENTS UNDERGOING LAPAROSCOPIC PARTIAL NEPHRECTOMY: A PILOT STUDY

Ornob P Roy, Zhamshid Okhunov, Louis R Kavoussi
The Smith Institute for Urology, Hofstra University, New Hyde Park, NY

Introduction: Ablative therapies have become increasingly attractive in the treatment of small renal masses (SRMs). Radiofrequency ablation (RFA) is a well-established technology routinely employed in ablative treatment of hepatic and pulmonary masses. Traditional RFA is performed using monopolar probes inserted into targeted tissue that conduct energy through a circuit completed by a grounding pad. This approach has several limitations, most notable for small ablative zones with irregular shapes and borders, skip lesions of viable tissue within targeted ablation zones, and skin burns at the grounding pad sites. These problems may be avoided by using bipolar RFA probes, which have been successfully tested in animal *in vivo* and *ex vivo* models.

Methods: We evaluated a novel bipolar RFA device (Encage™, Trod Medical®) which employs a probe within coil technique to contain all ablative energy within the margins of the outer coil (Figure 1). In an IRB-approved study, we used this to ablate renal masses in 10 patients undergoing laparoscopic partial nephrectomy. The probe was placed percutaneously and laparoscopically guided into the tumor after laparoscopic exposure. Electrical current was adjusted continuously by the generator to overcome disruption from increasing impedance created from desiccated tissue. The specimens then were excised in routine fashion of laparoscopic partial nephrectomy, and analyzed by a single pathologist. We recorded lesion size, shape, and size of transition zone to viable tissue (via NADH staining).

Results: Ablation was successful in all 10 patients. Duration of ablation was 200 seconds. Average time to set up and place probe was between 2 and 4 minutes. All ablated tissue showed no sign of viable cells as per histologic examination and NADH staining. Size of ablation zone averaged 6.26 cm^3, with regular borders and a tapered cylindrical shape similar to the shape of the outer coil (Figure 2). The width of the transition zone, or area spanning complete tissue ablation to the first viable cells, ranged from 10 to 60 microns. There were no complications during the ablations.

Conclusion: This pilot study demonstrates the safety and efficacy of a novel bipolar RFA device. The area of ablated tissue not only exhibits completely devitalized cells, but also a very precise target zone. With these characteristics, potential advantages of this new technology during RFA ablation of SRMs include less collateral damage, more complete ablation without skip lesions leading to lower rates of local recurrence, and reduced incidence of skin burns. Although successful with laparoscopic guidance, further studies are needed to evaluate image-guided percutaneous application of this device.

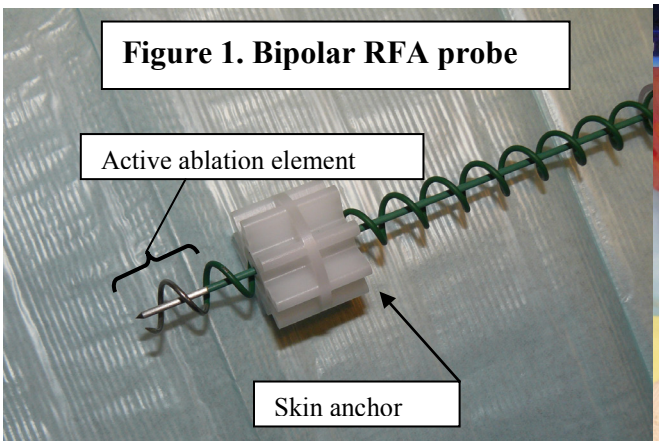

Figure 1. Bipolar RFA probe

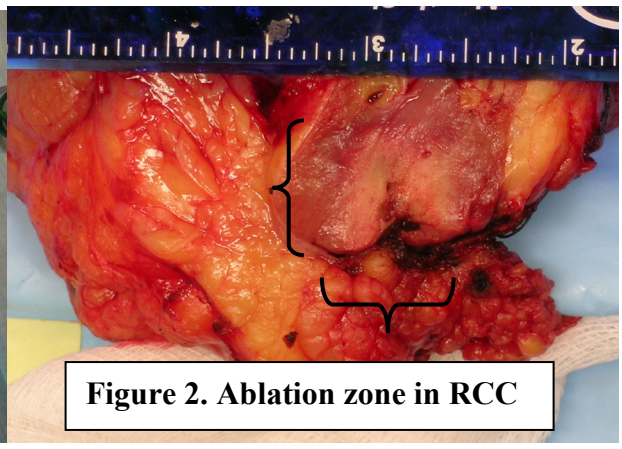

Figure 2. Ablation zone in RCC

ABSTRACT 32

BOX COUNTING FRACTAL ANALYSIS IN THE MANAGEMENT OF SMALL RENAL MASSES

C. Surcel[1], C. Mirvald[1], C. Chibelean[1], C. Gîngu[1], S. Najjar[1], V. Cerempei[1], C. Savu[2], A. Udrea [3], I. Sinescu[1]

[1]*Center of Urological Surgery, Dialysis and Renal Transplantation, Fundeni Clinical Institute, Bucharest, Romania*

[2] *Department of Intensive Care and Anesthesiology, Fundeni Clinical Institute, Bucharest, Romania*

[3] *"Politehnica" University, Bucharest, Romania*

Objective: The purpose of this article is to establish the validity of fractal analysis in the evaluation of capsular invasion of small RCC based on contrast enhanced computed tomographic (CT) images.

Materials and Methods: Between January 2007 and January 2011, 183 consecutive patients (age range, 19–95 years; 102 men, 81 women) with small renal masses <4cm considered T1a and T3a respectively, underwent total or partial nephrectomy. The pattern and degree of enhancement, lesion contour and calcifications were evaluated on the preoperative renal CT. Renal capsule contour was extracted by removing the interior points of the object during each phase of the CT scan and analyzed by estimating the global fractal dimension, the local fractal dimension and local connected fractal dimension using a box counting algorithm. T3a stage was considered to be a reduction of more than 0.2 units in the global fractal dimension. The imaging stage and fractal analysis results were compared to the histological results using Fisher tests, Pearson χ^2 tests, multivariate logistic regression and Wilcoxon rank sum tests.

Results: Of the 183 renal tumors (median size, 3.4 cm; range,1.1–4.0 cm) included in this study, 98 (54%) were clear cell renal cell carcinomas (RCCs); 20 (11%), papillary RCC; 24 (13%), chromophobe RCC; 21 (12%), oncocytomas; six (3%), lipid-poor angiomyolipomas; and 14 (8%), other or unclassified renal tumors. Clear cell RCC most commonly manifested with a mixed enhancement pattern of both hypervascular soft-tissue components and low-attenuation areas that corresponded to necrotic or cystic changes. The imagistic parameters suggesting clear RCC were correspondent to 88% of all clear cell tumors, while the fractal analysis was correspondent to 79% respectively. The sensibility of the imaging parametres and global fractal dimension in predicting T3a stage were 67% and 89% respectively, when compared to the histological result. Even more, the fractal dimension seems to slightly variate between the CT evaluations of oncocytomas (1.30 ±0.1), suggesting a non aggressive pattern of extension characteristic for benign lesions.

Conclusions: The fractal analysis improves the accuracy of preoperative staging in RCC and can be a useful tool in diagnosing benign lesions that require active surveillance.

Figure 1. Right T1a RCC (corticomedular phase)

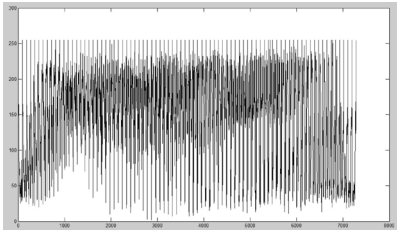

Figure 2. The time (spatial) series - *x(t)* - is generated by computing either the mean value or the maximal (dominant) value of each columns of pixels within the strip.

ABSTRACT 33

BOX COUNTING ANALYSIS IN RETROPERITONEAL FIBROSIS – 5 YEARS OF EXPERIENCE WITH 19 PATIENTS

C. Surcel[1], C. Mirvald[1], C. Chibelean[1], C. Gîngu[1], S. Najjar[1], V. Cerempei[1], C. Savu[2], A. Udrea [3], I. Sinescu[1]
[1]*Center of Urological Surgery, Dialysis and Renal Transplantation, Fundeni Clinical Institute*
[2] *Department of Intensive Care and Anesthesiology, Fundeni Clinical Institute*
[3] *"Politehnica" University, Bucharest, Romania*

Introduction: The aim of this study is to evaluate effective prognostic factors in the evolution of patients with retroperitoneal fibrosis and to establish the validity of fractal analysis in determining the disease severity in these patients.

Material and Methods: This study included 19 patients (M/F: 5/14) treated for idiopathic retroperitoneal fibrosis and bilateral obstructive renal failure between Jan 2004-Dec 2008. Patients were identified retrospectively, searching for patients diagnosed with IRF, after retroperitoneal biopsy or, in most cases the diagnosis rested on radiological findings, especially CT, with identification of a retroperitoneal mass, the absence of other demonstrable renal or ureteric disease or any other pathology that could explain the findings. CT was useful in describing the retroperitoneal mass around the aorta and inferior vena cava, the extent of the lesion and for monitoring the response to surgical treatment during the follow-up. The data were evaluated about medical history, physical examination findings, laboratory tests (serum urea and creatinine, blood sugar, sodium, potassium, bicarbonate levels, serum pH, uric acid, haematocrit, white blood cell count), imaging methods (renal echography, abdominal CT-scan, MRI). At admission, all patients had active disease with obstructive renal failure and underwent bilateral ureteric stenting in order to normalize the BUN levels. After normalizing of BUN levels, ureterolysis and omental wrapping was performed. Postoperatively, ureteric stents were removed after 1 month and remission of renal disfunction was obtained in approximately 5 months (range 2-10 months). All patients were followed for at least 1 year. Patients were checked regularly every 3 months.

Results: Of the 19 patients, there were 5 men and 14 women. The median age at diagnosis of RF was 50 years (range 42–64 years). The most frequent presenting symptoms were back or abdominal pain, weakness, weight loss, oligoanuria, arterial hypertension and mild fever. The duration of symptoms before diagnosis ranged from 6 to 18 months. At presentation all patients had active disease, presenting renal dysfunction with a median serum creatinine of 5,18 mg/dl (range 1-15.4 mg/dl). Most of the patients had moderate bilateral hydronephrosis (2nd degree hydronephrosis). In our study, all patients had excellent prognosis, with full recovery of renal function in 15 patients (78%). The fractal dimension of the fibrosis mass contour correlates with level of renal function impairment. Even more, the fractal dimension seems to variate slightly between CT evaluations (1.30 ±0.1), suggesting a non-aggressive pattern of extension of the fibrotic mass characteristic for benign lesions.

Figure: Retroperitoneal fibrotic mass involving the 2 ureters + ureteral stents (native CT scan)

Conclusions: The imaging parameters did not predict the disease severity, except the increase in fractal dimension of fibrosis surface area. Efficacy of bilateral ureteric stenting in improving renal function is limited in most of the cases. Despite the level of renal function impairment at admission, full recovery can be achieved after bilateral ureteric stenting/nephrostomy and ureterolysis.

ABSTRACT 34

NERVE COMPRESSION STUDY FOR BETTER UNDERSTANDING URINARY INCONTINENCE

Angela J Forrest[1], Yingchun Zhang[2], Gerald W Timm[2]
[1]*Electrical Engineering,* [2] *Urologic Surgery, University of Minnesota*

Introduction: The lower urinary tract is controlled by the central and peripheral nervous systems. We have designed a well-controlled animal model to investigate the effects of repetitive compression on the amplitude and velocity of nerve conduction in the pudendal and pelvic nerve using the femoral nerve as a model.

Methods: New Zealand Rabbits were used in our animal experiments. All animals were managed in accordance with Institutional Animal Care and Use committee (IACUC) within the University of Minnesota. Each rabbit was anesthetized and its thigh was cut open to expose the femoral nerve. A balloon-sleeve compression system (Fig. 1(a)) was used to generate pressure on the femoral nerve. A stimulus isolator was employed to stimulate the nerve and a needle electrode was used to capture the compound nerve action potentials (CNAPs). Compression pressure was increased gradually and the amplitude of CNAPs was recorded. The nerve conduction velocity (NCV) was calculated as $Velocity = d / latency$, where d is the distance between the electrodes, and the latency was recorded from the onset of the stimulus to the peak of the major deflection of the CNAPs.

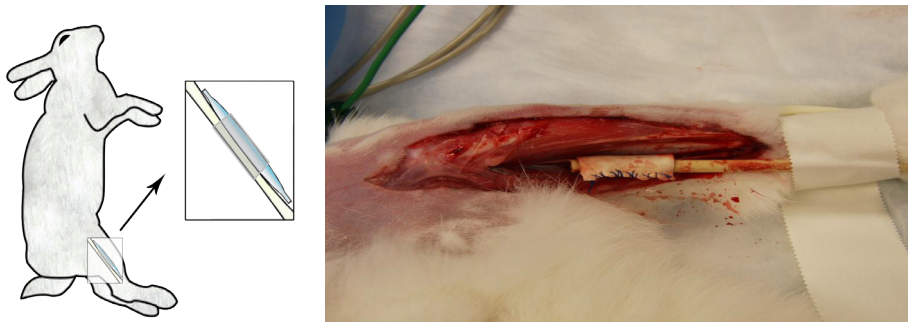

(a) **(b)**

Fig 1. (a) the diagram and (b) the photo of the balloon-sleeve compression system.

Results: The commercially available software Chart Scope 7 (AD Instruments, Bella Vista, N.S.W., Australia) was set to deliver a single square wave pulse with stimulus duration of 0.1 millisecond (msec) and a stimulus intensity of 3 mA. The amplitude of CNAPs was recorded at different compression pressure levels. Fig. 2 summarizes the results obtained from which we can see that the amplitude of CNAPs goes down remarkably in 4 out of 6 experiments as the compression pressure goes up.

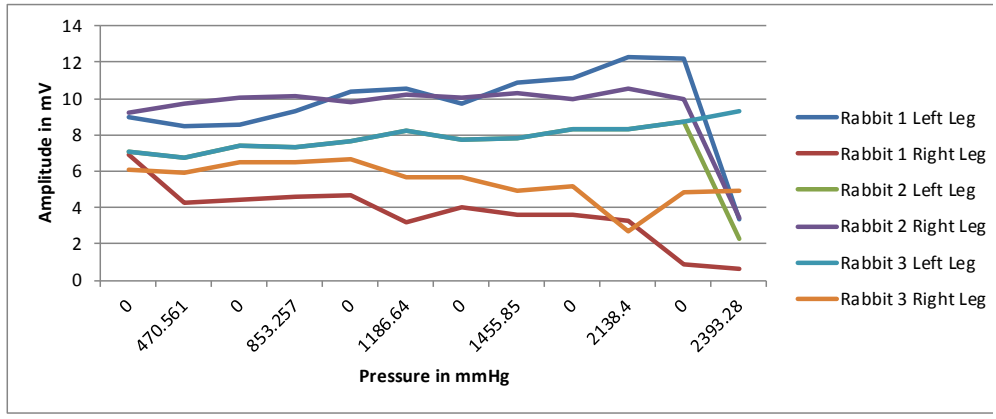

Fig 2. Curve of amplitude of CNAPs as the compression pressure goes up.

Conclusion: Preliminary results show the amplitude of CNAPs decreases as the compression pressure is increased in most of the cases that demonstrates the feasibility of using the balloon-sleeve system to perform the designed nerve compression study. Future studies will demonstrate the relationship between repetitive compression and amplitude/velocity of nerve conduction.

ABSTRACT 35

EVALUATION OF A NEW 240 µm SINGLE-USE HOLMIUM:YAG OPTICAL FIBER FOR FLEXIBLE URETEROSCOPY

David M Shore[1], Michael Antiporda[1], Joel M Teichman[2], Bodo E Knudsen[1]

[1] *Department of Urology, The Ohio State University Medical Center*
[2] *Department of Urologic Sciences, The University of British Columbus*

Introduction: Numerous holmium:YAG optical laser fibers are available commercially for flexible ureteroscopy. Fiber performance and durability can vary widely among different manufacturers and their product lines. Differences in performance characteristics with a single product line have been reported. We sought to determine the performance characteristics of a newly developed non-tapered, single-use 240 micron fiber, the Flexima (Boston Scientific, Natick, MA), during both clinical use and in a bench-test model.

Methods: One hundred single-use fibers were used in 100 consecutive ureteroscopy procedures. Pulse energy, frequency, and total energy delivered were recorded. The amount of fiber burn back from the tip was measured with a digital micrometer. Following their use in clinical cases, the fibers were evaluated for energy transmission in both straight and 180° bent configuration using an energy detector with settings of 400 mJ at 5Hz. Fifty pulses were recorded for each trial. Failure threshold was evaluated by bending the fibers to 180° with an initial bend radius of 1.25 cm. The laser was activated with a setting of 1200 mJ at 10Hz for 30 seconds. If the fiber did not break, the radius was reducing in 0.25 cm increments and the testing repeated until a radius of 0.5 cm was reached. Three trials for each fiber were performed.

Results: The mean energy transmitted was 451 mJ and 441 mJ in a straight and 180° bend configuration, respectively. 80% of fibers transmitted at least 400 mJ; 13% of fibers fractured at a bend radius of 0.5 cm with energy transmission. No fibers failed at larger bends. No fibers failed at the connector end. During clinical use, fiber tips burnt back an average length of 1.664 mm, but the amount of burn back was highly variable. No correlation with laser settings or total energy transmission was identified. 67% of fibers had greater than half of the maximal tip length remaining following their clinical use. No fibers fractured during clinical use.

Conclusion: Fiber performance between fibers was consistent in terms of energy transmission and resistance to fracture when activated in a bent configuration. Fiber burn back during clinical use showed significant variation amongst the fibers that did not correlate with settings used or energy delivered. This suggests possible mechanical damage to the fiber tip during manufacturing. The lack of fiber fracture during clinical use may reduce the risk of flexible endoscope damage.

ABSTRACT 36

NOVEL INSTRUMENTATION FOR DAVINCI™ ROBOTIC LAPAROENDOSCOPIC SINGLE-SITE SURGERY: EARLY LABORATORY EXPERIENCE

Georges-Pascal Haber, Riccardo Autorino, Michael A. White, Rakesh Khanna, Shahab Hillyer, Gregory Spana, Wahib Isaac, Julien Guillotreau, Raschid Yakoubi, Bo Yang, Fatih Altunrende, Humberto Laydner, Robert J. Stein, and Jihad H. Kaouk

Glickman Urological and Kidney Institute, Cleveland Clinic, Cleveland, OH

Introduction: Herein we describe our initial laboratory experience with VeSPA robotic instruments and assess their feasibility and efficiency for urological application.

Methods: The VeSPA surgical instruments (Intuitive Surgical, Sunnyvale, CA) were designed to be used with the daVinci Si surgical system. A multichannel port and curved cannulae were inserted through a single 3.5-cm umbilical incision. The port allowed 1 scope, 2 robotic instruments, and a 5- to 12-mm assistant instrument. Four pyeloplasties (right 2, left 2), 4 partial nephrectomies (right 2, left 2), and 8 nephrectomies (right 4, left 4) were performed in 4 female farm pigs (mean weight, 34.5 kg). Technical feasibility and efficiency were assessed in addition to perioperative outcomes.

Results: All 16 R-LESS procedures were performed successfully without the addition of laparoscopic ports or open conversion. There were no intraoperative complications. No robotic system failures occurred, and robotic instrument clashing was found to be minimal. One needle driver malfunctioned and assistant movement was limited.

Procedure	No. of Procedures	Operative Time (min)*	Estimated Blood Loss (mL)*	Warm Ischemia Time (min)*	Conversion	Intraoperative Complications
Pyeloplasty	4	55 (40-65)	<20	—	0	0
Partial Nephrectomy	4	37.5 (34-40)	30 (30–60)	14.8 (12–20)	0	0
Radical nephrectomy	8	16.8 (8-27)	50 (50–100)	—	0	0
Total	16	110.6 (82-127)	30 (<20–100)	—	0	0

* Values expressed as means (range).

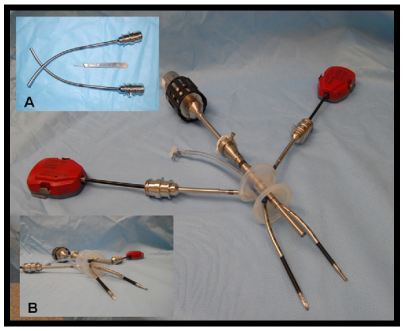

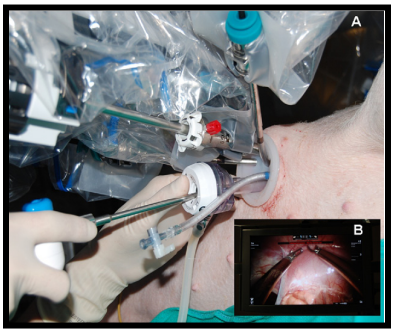

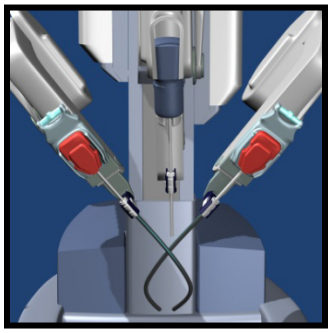

Conclusion: R-LESS kidney surgery using the VeSPA instruments is feasible and efficient in the porcine model. The system offers a wide range of motion, instrument and scope stability, improved ergonomics, and minimal instrument clashing. Although preliminary experience is encouraging, further refinements are expected to optimize urological applications of this robotic technology.

ABSTRACT 37

LASER PROBE FOR LAPAROSCOPIC NEPHRON SPARING SURGERY

Timothy Munuhe, John Eifler, Chunwoo Kim, Yihe Zuo, Doru Petrisor, Dan Stoianovici, Ronald Rodriguez
Robotics Laboratory, Brady Urological Institute, Johns Hopkins University, Baltimore, Maryland
http://urobotics.urology.jhu.edu/

Introduction: Laparoscopic partial nephrectomy typically requires clamping the renal vessels to prevent hemorrhage during excision of the renal masses. This warm ischemia time may damage healthy renal tissue during surgery and contribute to postoperative decline in glomerular filtration rate. Laser technologies may improve renal functional outcomes and reduce operating time by eliminating the need to clamp the renal vessels. Also, intraoperative bleeding may be reduced by the known coagulative benefits of laser technology.

Methods: To employ lasers in laparoscopic partial nephrectomy, the vaporized kidney must be evacuated from the abdomen to maintain surgeon's view of the kidney, and a support of the slender fiber must be provided to use it as a laparoscopic instrument. Also, the probe must not outpace the CO_2 used to distend the abdomen or the abdomen will collapse. A laparoscopic probe adapter for a side-fire GreenLight™ laser was designed and built. This type of laser is used frequently in laser prostate photovaporization.

Results: The probe presents a slender tubular construction through which the laser fiber is placed and securely attached at its head, as shown in the Figure 1. The side-fire tip of the fiber protrudes at the tip of the probe. The diameter of the fiber, inner, and outer diameters of the probe are 1.7 mm, 4 mm, and 5 mm respectively. The length of the probe under its handle is 283 mm. A guide is placed at the tip of the probe to center the fiber. A connection attaches the GreenLight™ at the head of the probe. To provide suction to extract the vaporized kidney tissue concurrently while lasing, several orifices are provided at the probe tip, right next to the side-fire laser output. To maximize airflow, these are built within the tip guide and also laterally within the barrel of the probe next to the tip. Two valves and corresponding buttons are placed at the head of the probe. One is connected to a vacuum source, and the other could be used for irrigation, as needed. To operate the laser probe the surgeon uses the GreenLight as usual but simultaneously depresses the vacuum valve to evacuate vapors during and after lasing. The direction of the side-fire laser can be adjusted relative to the probe from a knob behind the connection.

Bench tests of the probe show that components can easily be assembled for the procedure. Fume suction experiments show that the vacuum extraction is functioning well. The balance between the flow of CO_2 and the outflow of the suction will be addressed in animal experiments to determine if the vapors can be effectively eliminated without collapsing the abdomen. The tip guide is expected to concentrate suction at the place where kidney vapors are produced, thus extracting with low vacuum flow. Institutional Animal Care and Use Committee protocols are approved, and porcine experiments are expected to commence soon.

Conclusion: A new probe adapter was designed and built to use a GreenLight laser for laparoscopic laser vaporization of renal tissue. We believe this strategy may be a useful adjunct for nephron sparing surgery.

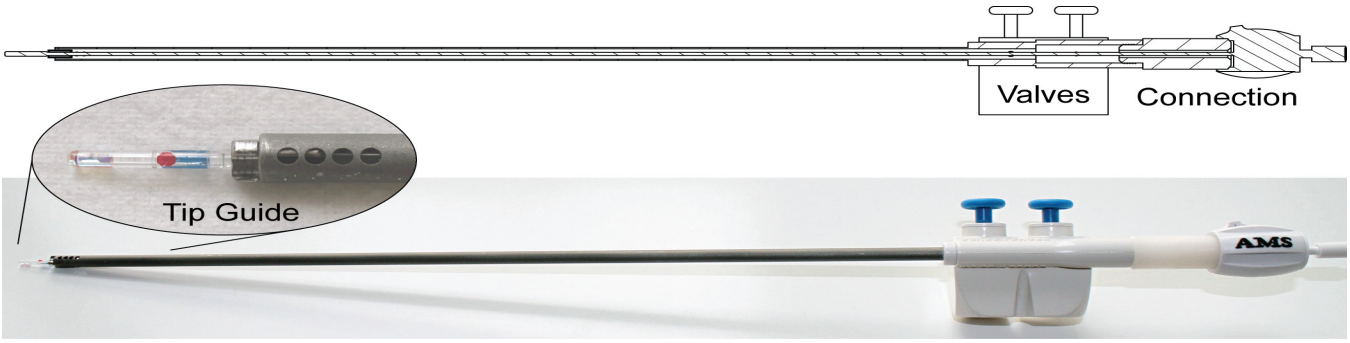

Figure 1. Laser probe with GreenLight™ laser

ABSTRACT 38

ENDOSCOPIC SNARE RESECTION OF BLADDER TUMORS

Maurice MJ[1,2], Vricella GJ[1,2], Ponsky LE[2]
[1]*Case Western Reserve University*
[2]*University Hospitals Case Medical Center*

Introduction: Transurethral resection (TUR) with a resectoscope (rTUR), the gold standard of bladder tumor management for 80 years, is flawed. rTUR violates the cardinal oncologic principle of *en bloc* resection, scattering and potentially seeding tumor throughout the bladder. This shortcoming may explain the high rate of tumor recurrence after rTUR. We describe endoscopic snare resection of bladder tumors (ESRBT), a safe *en bloc* method of TUR, and specimen retrieval using an electrosurgical colonic polypectomy snare and endoscopic net. We present our initial experience with 9 patients.
Methods: Under cystoscopy, a colonic snare was lassoed around the tumor base. Cutting current was applied to the snare, severing the tumor at its base and achieving hemostasis. The tumor was secured in the snare or in a mesh net and then removed. Deep resection of the tumor base was performed. Efficacy of the snare resection was evaluated by pathologic assessment. Safety was evaluated by clinical assessment.
Results: 11 bladder tumors in 9 patients (mean age: 65 years) were treated, with tumor sizes of: 2 small, 6 medium, and 3 large. All papillary TCC tumors were non-muscle-invasive, including 5 high-grade, 2 low-grade, and 1 nondiagnostic. Location: 6 lateral wall, 2 dome, 2 trigone, and 1 posterior wall. All tumors were resected *en bloc*. Muscle was present in 50% of specimens. There were no immediate or early post-operative complications at 2-week follow up.
Conclusion: We have shown that ESRBT is a technically easy, safe, and effective technique for TUR of pedunculated bladder tumors using currently available equipment. ESRBT limits tumor dispersal and provides excellent pathologic specimens. ESRBT may decrease morbidity and lower recurrence rates. Given our promising initial results, we foresee ESRBT as an emerging alternative treatment modality for the TUR of certain bladder tumors.

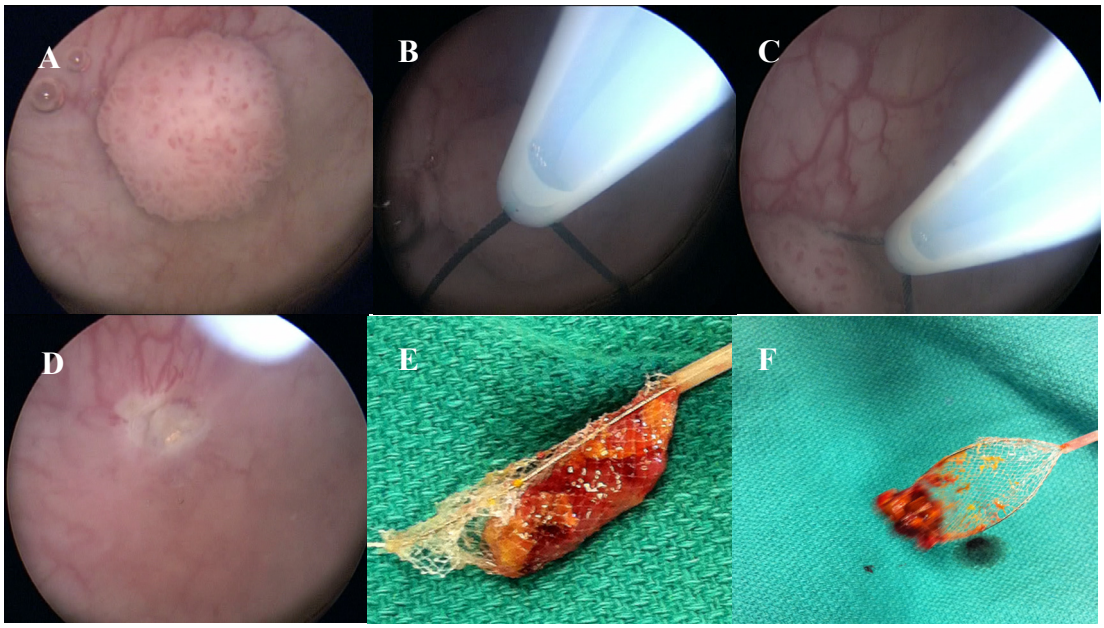

Figure 1: *The bladder tumor was identified (A), encircled with the snare (B, C) and resected en bloc with cutting current, leaving a small electrocautery footprint (D) with excellent hemostasis. The specimen was retrieved en bloc within an endoscopic net, preserving tumor architecture and limiting tumor dispersal (E, F).*

ABSTRACT 39

MR-TRUS Registration Accuracy for Targeted Biopsy of the Prostate

Shyam Natarajan[1], Ram Narayanan[4], Dinesh Kumar[4], Daniel J. A. Margolis[2], Aaron Ward[5], Aaron Fenster[5], Leonard S. Marks[3]

[1] *Biomedical Engineering IDP, University of California, Los Angeles, CA 90095*
[2] *Department of Radiology, University of California, Los Angeles, CA 90095*
[3] *Department of Urology, University of California, Los Angeles, CA 90095*
[4] *Eigen, Grass Valley, CA 95945*
[5] *Robarts Research Institute, University of Western Ontario, London, Canada*

Introduction: Image-guided prostate biopsy through fusion of multi-parametric MRI with real-time transrectal ultrasound (TRUS) offers the promise of improved cancer diagnosis. Accurate image registration of MR and TRUS is necessary to target areas of suspected cancer reliably. We performed preliminary clinical validation of the MR-TRUS registration accuracy in a 3D imaging and biopsy-tracking device (Artemis, Eigen). Prior validation of MR-TRUS registration has been performed only on phantoms.

Methods: Five patients with internal gold bead fiducials (3 per patient), previously inserted to guide radiation therapy, were imaged using multi-parametric MRI and 3D transrectal ultrasound. The fiducial locations were identified by a uro-radiologist and imaging scientists on MRI and TRUS. Prostates were then outlined using a semi-automatic segmentation method in both modalities. For each case, three users (SN, RN, DK) performed manual alignment and automatic registration independently. Segmentations in TRUS and MRI were kept constant across users per study. Registration was performed on both segmented surfaces with a user defined rigid alignment followed by an automatic non-rigid surface registration of corresponding segmentations from MR and TRUS followed by elastic interpolation. Target registration error (TRE), *i.e.*, the distance between corresponding points on MR and TRUS, was averaged across users and fiducials in a study. The error associated with selecting a fiducial, or fiducial localization error (FLE), was normalized across users, and calculated as the mean norm of the resulting error vectors.

Results: 10 of the 15 fiducials were found with certainty on both modalities. We found an average target registration error (TRE) of 3.23 mm, with a fiducial localization error (FLE) of 0.53 mm in TRUS and 0.44 mm in MRI. When all observers agreed upon an alignment for registration, a TRE of 3.08 mm was found.

Conclusion: Registration accuracies in men agreed with values previously obtained in phantoms (Narayanan *et al*, IEEE Biomed Imag, 2009). FLE contributions to TRE were minimal. Increases in both the dataset size and TRUS scan quality are necessary for improved estimation of error. Segmentation variability in TRUS and MR and its contribution to TRE are also necessary for an accurate measure of error sources. These preliminary data indicate that MR-TRUS fusion, for the purpose of targeted prostate biopsy, may be performed with accuracy.

Case	# of Fiducials	Segmented TRUS Vol. (mL)	Segmented MR Vol. (mL)	Difference in Vol. (%)	Max Fiducial Distance(mm)	Target Registration Error (mm)
1	2	20.25	24.85	+20.40	27.67	4.91
2	2	25.83	28.00	+8.06	27.20	4.15
3	2	39.67	41.16	+3.69	15.65	2.17
4	1	45.98	55.74	+19.19	-	2.30
5	3	134.70	107.43	-22.53	45.05	3.01
TRUS Fiducial Localization Error (FLE)			0.53 mm			
MR Fiducial Localization Error (FLE)			0.44 mm			
Average Target Registration Error (TRE)			3.23 mm			

ABSTRACT 40

EX VIVO MODEL FOR RENAL FRACTURE IN CRYOABLATION

Cervando G Ortiz-Vanderdys

Introduction: Renal fracture is a recognized complication of cryoablation. In some series it comprises 4% of the complications associated with the procedure. Factors that have been associated with the occurrence of parenchymal fracture include the usage of larger cryoprobes and the use of the guillotine technique. Several investigators have proposed different mechanisms for the formation of these fractures. Our objective was to demonstrate in a controlled lab setting the formation of fractures due to cryoablative therapy.

Methods: Endocare Perc-17 probes and Galil 17 gauge IceRod probes were selected because they are of similar diameter (1.7 mm and 1.47 mm respectively) and reported ice ball size. Cryoablation was performed with one or two probes of either Galil 1.47 mm IceRods or Endocare Perc-17. Freezes were first done in water and subsequently in the *ex vivo* renal model. The *ex vivo* model used here is a kidney obtained at the butcher or supermarket which was subsequently bivalved. One kidney that was used was fresh harvested and had a capsule. However this proved not to be essential for modeling renal fractures. The cryoprobe or probes are placed parallel and just underneath the cut surface, inserted through the lateral surface of the kidney towards the medial surface of either upper or lower pole to avoid the pelvis and major calyces and involve the most parenchyma. Freeze-thaw-freeze cycles of various durations were performed. Two IceRods and two Perc-17s were frozen individually and parallel to each other at a distance of 3 cm. Freezing was done in normal saline solution, ultrasound gel, and kidney obtained from butcher shop. These kidneys are readily available, however they are provided with the renal capsule removed.

Results: No fractures were noted in the IceRod freezes. Fractures were noted in the Perc-17 freezes, either singly or together forming one large iceball. A popping sound was noted during thaw both in the saline model and in the *ex vivo* hemisected porcine kidney. When there was audible cracking sound during thaw, a visible crack became evident during the second freeze in the kidney (Figure 1). Cracks were noted to extend from the probe through parenchyma. In multiple probe freezes the zone of merging of two ice balls has smooth ice and the fractures that appear there originate at the probe and extend through this area. We only observed fracture formation with the Endocare probes. We also observed more effective, faster ice ball formation with the Endocare probes.

Conclusion: Of the proposed mechanisms of fracture generation, thermal shock fit our data best. The bivalved *ex vivo* kidney is a good model for study of fracture during cryoablation.

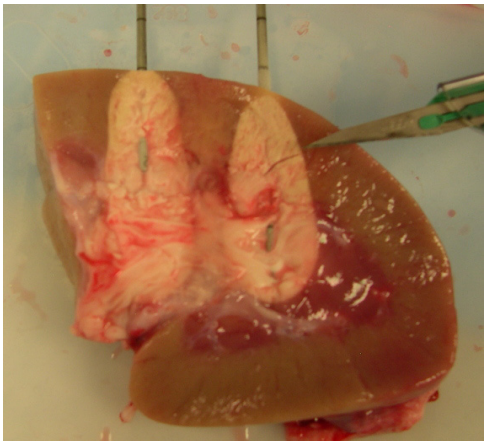

Figure 5: Fracture in the model with Perc-17 second freeze

ABSTRACT 41

LAPAROENDOSCOPIC SINGLE-SITE SURGERY FOR RENAL CANCER: ONCOLOGICAL OUTCOMES

Humberto K Laydner; Riccardo Autorino; Michael A White; Rakesh Khanna; Fatih Altunrende; Bo Yang, Wahib Isac, Gregory Spana, Shahab Hillyer, Julien Guillotreau, Rachid Yakoubi,
Georges-Pascal Haber; Robert J Stein; Jihad H Kaouk
Cleveland Clinic, Cleveland, OH

Introduction: Despite advantages of better cosmesis and potentially less surgical trauma, concerns have arisen about oncological efficacy of LESS. Our objective was to evaluate the oncological outcomes of Laparoendoscopic single-site surgery (LESS) for renal tumors in the short to mid-term.

Methods: At our center, since 2007, 34 patients have undergone LESS procedures for renal tumor, including partial nephrectomy (PN) (11), radical nephrectomy (17), cryoablation (5), and metastectomy (1). Articulating and straight laparoscopic instruments were used for standard LESS procedures (22) and the da Vinci system for robotic LESS procedures (12). Surgical, functional, and oncological outcomes were evaluated.

Results: Mean operative time was 189 ± 51.8 minutes and mean blood loss was 252 ± 305 milliliters. Tumors for PN procedures had median PADUA and RENAL nephrometry scores of 7 and 6, respectively; with a mean warm ischemia time of 20.2 ± 7.1 minutes. Overall, mean visual analog pain scale at discharge was 1.5 (1-10). Mean length of stay was 3.4 days. One focally positive margin was noted after a PN, with negative intraoperative frozen section. Mean decrease of glomerular filtration rate was 15.9%. Postoperative complications included retroperitoneal abscess (Clavien IIIa) in 1 patient, and bleeding (Clavien II) in 6 patients, treated conservatively. Most of the transfusions occurred in the PN subgroup. There were 2 conversions to standard laparoscopy and 2 to open surgery. Overall, recurrence-free, and cancer specific survival were 98%, 100%, and 100%, respectively, with a mean follow-up of 26 months.

Conclusion: LESS is feasible for treatment of renal cancer in selected patients. Initial results of oncological adequacy are similar to published standard laparoscopy series; however, longer follow up is awaited.

Table I. LESS for renal cancer – main outcomes

Procedure	N of tumors	Mean size (cm)	Mean OR time (min)	Mean EBL (mL)	Conversion	Complications	Grade*	PRBC Transfusion	Mean VAPS	Mean LOS (days)	Histology	Margins	Mean % variation of GFR	% Disease-free survival	% Overall survival	Mean Follow-up (months)
RN (17)	19	5	182	137	1 to lap	-	-	0	2.3	2.5	Clear cell: 13 Papillary: 3 Others: 3	neg (17)	-34.6	100	100	18
PN (11)	11	2.2	213	491	1 to open 1 to lap	bleeding (4) sepsis (1)	II IIIa	4	0.7	5.3	Clear cell: 4 Papillary: 3 Other: 4	neg (10) pos† (1)	+4.2	100	100	35
MXT (1)	1	1.2	120	150	-	-	-	0	0	1	Clear cell: 1	neg (1)	+0.3	100	100	42
CRYO (5)	5	3	174	90	1 to open	bleeding (2)	II	2	1.2	2.8	Clear cell: 3# Papillary: 1#	N/A (5)	-3.5	100	80	35
TOTAL (34)	**36**	**3.7**	**189**	**252**	**2 to open 2 to lap**	**7**	**II/IIIa**	**6**	**1.5**	**3.4**	**Clear cell: 21 Papillary: 7 Others: 8**	**neg (28) pos† (1) N/A (5)**	**-15.9**	**100**	**98**	**26**

RN: Radical nephrectomy, PN: partial nephrectomy, MXT: metastectomy, CRYO: cryoablation, R-LESS: robotic LESS, WIT: warm ischemia time, EBL: estimated blood loss, PRBC: packed red blood cells, VAPS: visual analog pain scale (at discharge), LOS: length of stay, GFR: glomerular filtration rate, *Clavien classification, †focally positive, with frozen section negative, N/A: not applicable, #based on biopsy

ABSTRACT 42

RENAL NEPHROMETRY SCORE IS ASSOCIATED WITH COMPLICATION RATE AFTER ROBOTIC PARTIAL NEPHRECTOMY

Fatih Altunrende, Humberto K Laydner, Riccardo Autorino, Bo Yang, Michael White, Rakesh Khanna, Wahib Isac, Shahab Hillyer, Gregory Spana, Julien Guillotreau, Rachid Yakoubi, Sylvain Forest, Adrian V Hernandez, Georges-Pascal Haber, Jihad Kaouk, Robert J Stein

Introduction: Recently, the RENAL nephrometry score (RNS) was developed to standardize the description of renal tumors anatomy in a quantifiable manner. The aim of this study was to evaluate the RNS as a predictor of postoperative complications related to robotic partial nephrectomy (RPN).

Methods: We reviewed the image exams of 187 consecutive patients who underwent RPN at our institution. For each patient RNS was determined. RNS consists of R: radius (tumor size), E: exophytic/endophytic properties of the tumor, N: nearness of the tumor to collecting system/or sinus, A: anterior/posterior location, L: location relative to polar lines. We evaluated the relation between the complication rate and each component of the RNS using logistic regression analysis.

Results: Mean patient age, body mass index (BMI), and tumor size were 59.6 years, 30.6 Kg/m2, and 3.15 cm, respectively. Tumor was located in the upper pole in 22%, interpolar or hilar region in 46%, and lower pole in 32% of the patients. The mean warm ischemia time was 18.3 min. The overall RNS was categorized as low complexity (4-6) in 84 patients (45%), moderate complexity (7-9) in 80 (43%), and high complexity (10-12) in 23 (12%). Larger tumors were associated with a higher frequency of complications (Chi-square test p=0.005). Forty six percent of the patients with tumors > 4 cm had complications, against 21.3% of the patients with tumors ≤ 4 cm (Fisher exact test, p=0.0021). There was no relation between E (p=0.8), N (p=0.2), A (p=0.8), L (p=0.3) components and complications. Complications were significantly associated with more complex tumors, according to the total RNS (Chi-square test p=0.003). There was no correlation between grade of complications and complexity of the tumor, according to RNS (Chi-square test p=0.252).

Conclusion: Higher RNS is associated with increased risk of perioperative complications. Of all RNS categories, larger tumor size has the highest correlation with complication incidence.

RNS	Complication			Grade*
	No (137)	Yes (50)		
4 – 6 (Low complexity)	65	19	Hypokalemia (2)	1
			Atelectasis (2)	1
			Fever (2)	1
			Ileus (2)	1
			Back pain (1)	1
			Gout crisis (1)	2
			Suicidal ideation (1)	2
			T wave inversions (1)	2
			↓ Hemoglobin requiring transfusion (6)	2
			DVT requiring IVC filter (1)	3a
7 – 9 (Moderate complexity)	62	18	Hypokalemia (1)	1
			Fever (2)	1
			Ileus (2)	1
			Lymph leak with prolonged JP drain (1)	1
			Bladder infection (1)	2
			Pneumonia (1)	2
			↓ Hemoglobin requiring transfusion (8)	2
			Pulmonary edema (1)	2
			Reintervention due to bleeding (1)	3b
10 – 12 (High complexity)	10	13	Urine leak (2)	1
			↓ Hemoglobin requiring transfusion (7)	2
			Rhabdomyolysis (1)	2
			Pneumonia (1)	2
			Pneumothorax (1)	3a
			Pulmonary edema (1)	3a

RNS: RENAL nephrometry score, *Clavien classification, DVT: deep vein thrombosis, IVC: inferior vena cave

ABSTRACT 43

EARLY TREATMENT OF HORMONE-REFRACTORY NON-METASTASIZED PROSTATE CANCER (HRPCa) WITH ROBOTIC HIGH INTENSITY FOCUSED ULTRASOUND (rHIFU)

Chaussy Christian[1,3] , Thueroff Stefan[2,3]
[1]*Dept. of Urology University of Regensburg,*
[2]*Dept. of Urology Klinikum Muenchen,* [3]*Harlachinger Krebshilfe e.V.*

INTRODUCTION AND OBJECTIVES: Treatment of hormone-refractory prostate cancer (HRPCa) is challenging and rewarding at the same time. The early onset of androgen deprivation therapy (ADT) and the longer patient survival lead to an increase in the number of patients requiring post-hormonal therapy. We analyzed how local tumor ablation with rHIFU may influence progression of the disease.

METHODS: 56 patients with locally, non-metastasized, biopsy proven PCa who showed triple PSA progression under long term ADT were included in the study. The age was 74 (55-88), staging was T2: 29%, T3-4: 71%; Gleason: 7.5 (4-9); N0/M0; ADT before: mean 5.1 years; mean PSAtr (at HIFU therapy) 13.8 (7%>50ng/ml). rHIFU combined with TURP was performed under spinal anaesthesia in one session using Ablatherm® (EDAP-TMS, Lyon) at 3 MHz. Efficacy and side effects have been analyzed during a follow-up of maximum of 9.5 years.

RESULTS: Efficacy: mean PSA Nadir: 0.9 (0-69) ng/ml (0-148): of those 71% <4ng/ml and 10% >20mg/ml. time to Nadir (months): 1.7(0.3-8.6). median PSA reduction by 84%. Mean follow-up time 26 months; mean last PSA: 4.9 ng/ml. Survival rate was 66% at a mean time of 27 months. 34% of the patients died during follow-up: in 11% death was PCa related, in 18% not PCa related, in 5% unknown. **Side effects** : perioperative side effects according Clavien Classification: 23% (Clavien 1-3 only). Any side effect in further follow up: 38.6% (of those 50% caused by local obstructive reasons, 45% by UTI and one case of fistula)

CONCLUSIONS: Early local adjuvant tumor ablation of non-metastasized HRPCa with "TURP & rHIFU" reduced PSA by 84% and resulted in a mean PSA velocity of 2.95 ng/ml/year. This new minimal invasive, single session, adjuvant concept in early treatment of HRPC showed its high efficacy as additional therapy in prostate cancer treatment in this unfavourable patient group. Two-thirds of the patients were still alive after a follow-up of 2 years with a PSA below entry PSA at treatment inclusion. This single-session therapy showed only moderate side effects. It preserved ADT and more invasive or systemic therapies for later use.

Source of Funding:
Harlachinger Krebshilfe e.V., Lingen Stiftung
Thanks to Ms. Regina Nanieva for database management

ABSTRACT 44

INTRAPROSTATIC CANCER TOPOGRAPHY AND DETECTION RATE IN 963 CASES

Chaussy Christian[1,3] , Thueroff Stefan[2,3]
[1]*Dept. of Urology University of Regensburg,*
[2]*Dept. of Urology Klinikum Muenchen,* [3]*Harlachinger Krebshilfe e.V.*

OBJECTIVE: Before the onset of any therapy, prostate cancer (PCa) has to be confirmed histologically. Visually guided or random biopsies and TURP can provide material for histological determination of tumor location (topography), tumor volume (No. of positive biopsies), and aggressiveness (Gleason score). As with all diagnostic methods, there are significant limitations. We analyzed the unilateral detection rate from a prospective series of transrectal ultrasound guided biopsies. In a second step, we combined the analysis with TURP results from the same patients.

METHODS: Data analysis was from a prospective, monocentric HIFU database for T1-2, N0, M0 patients. All patients had 6-24 TRUS-guided transrectal prostate staging biopsies. All biopsies were correlated to 6 major topographic locations (right/left/apex/middle/base). Furthermore, patients with TURP and biopsies were analyzed accordingly. Results were compared.

RESULTS:

A) Prostate Volume (cc)	< 11	11-30	31-50	51-70	71-90	>90
n	4	342	392	137	54	34
%	0,5	35,5	41	14	5	4

B) TUR gr	**No PCa**	< 10% PCa	11-40%PCa	>40%PCa	TOTAL
< 15	217 (45%)	126 (25%)	92 (18%)	62 (12%)	497 (100%)
16-25	64 (30%)	72 (34%)	36 (17%)	40 (19%)	212 (100%)
26-35	49 (43%)	29 (25%)	23 (20%)	14 (12%)	115 (100%)
36-50	20 (27%)	22 (30%)	18 (25%)	13 (18%)	73 (100%)
>50	23 (35%)	20 (30%)	13 (25%)	10 (15%)	66 (100%)

C) Intrabioptic PCa volume:	< 1mm	1-3 mm	>3mm	**TOTAL**
1: R base (n / %)	136 (14%)	110 (11%)	147 (15%)	393 (41%)
2: R middle	210 (22%)	152 (16%)	178 (18%)	540 (56%)
3: R apex	167 (17%)	105 (11%)	135 (14%)	407 (42%)
4: L apex	184 (19%)	94 (10%)	143 (15%)	421 (44%)
5: L middle	217 (23%)	162 (17%)	169 (18%)	548 (57%)
6: L base	144 (15%)	83 (9%)	174 (18%)	401 (42%)

CONCLUSION:

- Prostate cancer detection rate by TURP in a cohort of 963 patients with biopsy proven PCa (100%) was between 55% and 73%. The resected tissue volume was 71% of the initial prostatic volume.
- Transrectal bioptic prostate cancer distribution showed a slight prevalence to the lateral middle zones of the prostate.
- No differences in primary PCa localisation between apex and base, right or left was found.
- Regarding tumor volumetry, we did not find any prevalence in tumor size or tumor location.

ABSTRACT 45

DEFINING OPTIMAL LASER FIBER SWEEPING ANGLE FOR EFFECTIVE TISSUE VAPORIZATION USING A 180 W, 532 nm LITHIUM TRIBORATE LASER

Woo Jin Ko[1], Hyun Wook Kang[2], Danop Rajabhandharaks[2], Matthew Rutman[3], Osterberg E. Charles [4] and Benjamin B. Choi[4]

[1]Department of Urology, National Health Insurance Corporation Ilsan Hospital, Goyang, South Korea, [2]American Medical Systems, San Jose, CA, USA, [3]Department of Urology, Columbia University Medical Center, New York, NY, USA, [4]Department of Urology, New York Presbyterian Hospital-Weill Cornell Medical Center, New York, NY, USA

Background: A side-to-side, rotational laser fiber sweeping motion during photoselective vaporization of the prostate (PVP) is considered standard technique contrary to axial (in and out) motions seen in traditional TURP. Scientific validation of the optimal laser fiber sweeping techniques currently is lacking.

Objective: To identify the most efficient tissue vaporization sweeping angle (SA) during PVP.

Design, Setting and Participants: Experiments were conducted with the GreenLight XPS^{TM} laser system with Moxy^{TM} fiber technology (American Medical Systems, Inc.) at 120W and 180W. Ten 2.5 x 2.5 x 1.5 cm blocks of porcine kidney were used for each SA (n=140). Specimens were placed in a chamber equipped with computer-assisted sweeping motion at variable SAs (0, 15, 30, 45, 60, 90, and 120°).

Measurements: Vaporization efficiency was assessed by the amount of tissue removed per time. The coagulation zone (CZ) thickness also was measured. Statistical analysis was performed with the two-sample Student's t-test ($p < 0.05$).

Results and Limitations: Maximal vaporization rate (VR) was achieved at SA 15 and 30°. Irrespective of power, VR increased and CZ decreased linearly with decreasing SA from 120° to 30°. Across all SA, 180W achieved at least a 60% greater VR versus 120W. Specifically, the percentage difference of VR was statistically significant for 15° and 30° when compared to 60° for both 120W and 180W. The CZ was the thinnest at SA 30°. This study used an *in vitro* model that may restrict its clinical translation.

Conclusions: Optimal vaporization, regardless of the laser power, occurred at a SA of 15° and 30° with the lowest CZ at 30°. Contrary to anecdotal recommendations for a wider SA, a narrower SA (30°) achieved the maximal tissue vaporization efficiency. Collectively, these data highlight the capability to test PVP technique in a scientific manner, identifying the optimal surgical parameters to aid practicing urologists to achieve desired clinical outcomes.

ABSTRACT 46

PROSPECTIVE, RANDOMIZED USE OF THE BARBED VLOC SELF-RETAINING SUTURE TO FACILITATE VESICOURETHRAL ANASTAMOSIS DURING ROBOT ASSISTED RADICAL PROSTATECTOMY: TIME REDUCTION AND COST BENEFIT

Kevin C. Zorn[1,2], Quoc-Dien Trinh[1], Hugues Widmer[1], Jean-Baptiste Lattouf[1], Dan Liberman[1], Maxine Sun[1], Pierre I. Karakewicz[1], Ronald Denis[1], Gagan Gautam[2], Assaad El-Hakim[1]

[1] Section of Urology, University of Montreal Hospital Center, Sacre-Coeur de Montreal Hospital Montreal, QC, Canada , [2] Section of Urology, University of Chicago Medical Center, Chicago, IL, USA

Introduction: Robotic vesicourethral anastomosis (VUA) using the Van Velthoven technique has improved urinary reconstruction significantly during robot-assisted radical prostatectomy(RARP). Recent case series have suggested that the use of barbed polyglyconate suture may facilitate VUA. Compared to standard monofilament posterior reconstruction (PR) and VUA technique, we sought to evaluate the effectiveness of VLOC 180 suture (Covidien, Mansfield, MA) for urinary reconstruction.

Methods: A prospective, randomized study was conducted in 70 consecutive RARP cases by a single surgeon (KCZ). Standard VUA was performed using three, 4-0 Monocryl sutures all secured with LapraTy clips (1 single 6 inch for PR and 2 attached 6 inch for VUA). The study group involved two, 3-0 6-inch VLOC 180 sutures, loop-interlocked and used for knotless PR and VUA. Assurance of watertight closure with a 300mL saline visual cystogram intraoperatively was performed in all cases. Time to complete the suture setup by the nursing personnel, anastomosis time, and need to adjust suture tension were recorded. Suture-related complications, validated-questionnaire continence and a cost analysis were also analyzed.

Results: Compared to our conventional reconstruction technique, there was a significant reduction in mean nurse setup time of suture material (31 vs 294sec; $p<0.01$) and reconstruction time (13.1 vs 20.8min ; $p<0.01$). Need to readjust suture tension or place additional LapraTy clips to establish a watertight closure was observed in 8 (24%) vs 2 (6%) of cases ($p=0.03$). A cost reduction was also seen at our institution (48.05$ vs. 70.25$CAN) with the use of the interlocked VLOC technique. Time to foley removal was comparable between groups (4.1 vs. 4.2 days, $p=0.87$). With a mean follow-up of 6.2 months, no delayed clinical anastomotic leaks or bladder neck contractures were observed in either group. Pad-free continence outcomes at 1 (64%vs69%, $p=0.60$), 3 (76%vs81%, $p=0.54$) and 6 months (88% vs. 92%, $p=0.67$) were also comparable.

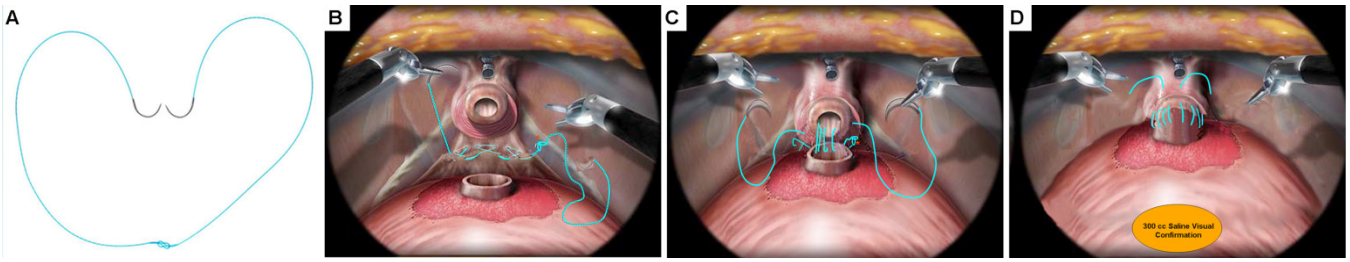

Figure 1. Interlocked VLOC configuration for PR and VUA. Note the use 2 six-inch sutures in which the loops of both suture are threaded by the opposite needles. As such, an efficient, knotless setup which allow efficient PR and simultaneous VUA closure. Upon completion of VUA, the integrity is always assessed with 300c NS bladder instillation.

Conclusions: Compared to standard monofilament suture, the unidirectional barbed VLOC suture appears to provide a safe, more efficient, and cost effective PR and VUA during RARP. Use of the interlocked VLOC suture technique prevents slippage, precluding the need for assistance, knot tying, and constant reassessing of anastomosis integrity.

ABSTRACT 47 **OUTSTANDING PAPER AWARD**

COMPUTER SIMULATIONS OF THERMAL DAMAGE TO THE HUMAN VAS DEFERENS DURING NONINVASIVE LASER VASECTOMY

Gino R. Schweinsberger, Christopher M. Cilip[1], Nathaniel M. Fried[1,2]
[1] *Department of Optical Science and Engineering, University of North Carolina at Charlotte, NC*
[2] *Department of Urology, Johns Hopkins Medical Institutions, Baltimore, MD*

Introduction: Successful noninvasive laser thermal coagulation of the canine vas deferens, *in vivo*, has been reported previously both with and without the use of optical clearing agents (to make the scrotal skin more transparent). However, there are significant differences between the tissue properties of canine and human skin. Since the matrix of laser and cooling parameters is too large to completely explore in experiments, it is important to use computer simulations to predict the optimal set of treatment parameters. In this study, a standard three-stage (optical, thermal, and tissue damage) computer model was used to explore the feasibility of noninvasive laser vasectomy in humans.

Methods: Part 1 (optical) of the model consists of a Monte Carlo model of light transport in tissue to determine the spatial distribution of absorbed photons in the major tissue layers (epidermis, dermis, and vas). The scrotal fold anatomy in the vas ring clamp makes it necessary to include skin layers on the top and bottom of the model. An index of refraction, absorption and scattering coefficient, and anisotropy factor (direction of scattering) was assigned to define the optical properties of each tissue layer. Part 2 (thermal) of the model consisted of using the MC results as the spatial heat source for the heat transfer model. Each tissue layer was assigned a value for the density, specific heat, and thermal conductivity. Part 3 (tissue damage) of the model used the temperature-time data from Part 2 as the input in a standard Arrhenius integral model for irreversible thermal tissue denaturation. In this model, tissue damage is treated as a first order rate process (based on chemical reaction kinetics) that is exponentially dependent on temperature and linearly dependent on time. Tissue damage is defined by a single parameter (Ω), where a value of $\Omega > 1$ results in irreversible tissue damage. Multiple treatment parameters were studied, including laser output power (5-9 W), cryogen pulse duration (60-100 ms), cryogen cooling rate (0.5-1.0 Hz), and increase in optical transmission (0-50 %) through skin due to application of optical clearing agents. The parameters were chosen based on those used successfully in a canine model.

Results: After application of an optical clearing agent to increase skin transmission by 50%, an average laser power of 6 W, cryogen pulse duration of 60 ms, and cryogen cooling rate of 1 Hz, resulted in vas wall temperatures of approximately 58 °C, sufficient for thermal coagulation ($\Omega > 1$), while 1 mm of the skin surface remained at a safe temperature of approximately 45 °C with $\Omega < 1$ (Figure 1). A critical temperature above 52 °C would result in undesirable thermal coagulation of skin.

Conclusion: A computer model including Monte Carlo, heat transfer, and thermal damage simulations, indicates that it is possible to noninvasively thermally coagulate the human vas deferens without adverse side-effects (*e.g.*, scrotal skin burns) if an optical clearing agent is applied to the skin prior to the procedure.

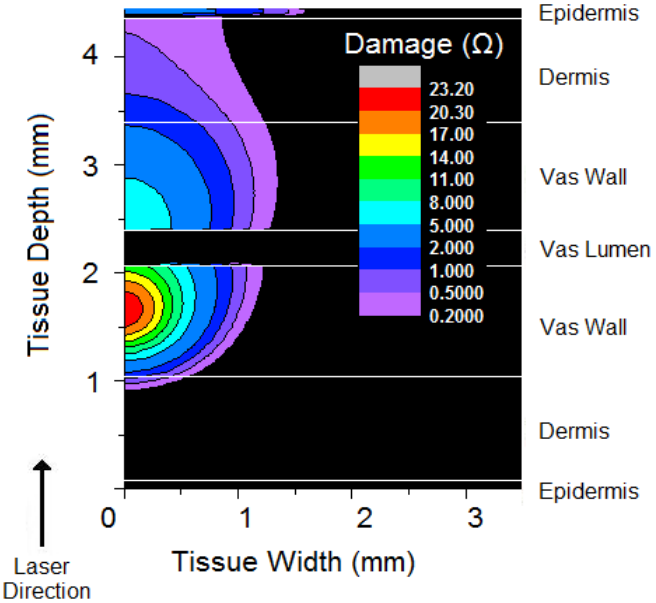

Figure 6. Map of accumulated thermal damage after 60 sec of laser irradiation and 6 W of average laser power. The vas wall is thermally coagulated ($\Omega > 1$) while the skin remains undamaged ($\Omega < 1$).

ABSTRACT 48

DECREASED OPERATIVE INTERRUPTION USING FloShield TO KEEP THE LAPAROSCOPE CLEAN

Wayne Poll, M.D., Caroline Crisafulli
Minimally Invasive Devices, Inc.

Introduction: Laparoscopic surgery and the ability of the surgeon to focus are benefited by a clear and uninterrupted view of the patient's anatomy. However, laparoscopic video images often are obscured and/or interrupted by the accumulation of debris on the end of the laparoscope or condensation. This is particularly true with smoke or plume from modern energy coagulation techniques. This study examines the use of FloShield™, a novel device that uses insufflation airflow to prevent debris accumulation on the end of the laparoscope, to decrease operative interruption during laparoscopic cholecystectomy.

Methods: 28 consented patients scheduled to undergo laparoscopic cholecystectomy were randomized to have their surgery performed with or without the FloShield device. An observer in the room was tasked with recording how many times during each procedure the surgeon interrupted surgery to clean the end of the laparoscope in order to restore adequate vision. These results were tabulated and compared.

Results: In the 14 laparoscopic cholecystectomy cases not using FloShield, surgery was interrupted an average of 2.96 times per case. In the 14 procedures using FloShield, surgery was interrupted an average of 0.26 times, a 90% reduction.

Conclusion: FloShield is a novel device that fits over the shaft of the laparoscope and utilizes principles of fluid dynamics to flow CO2 over the end of the laparoscope to prevent debris from attaching to the surface of the lens. FloShield prevents condensation and "spins" particulate matter away from the optics of the laparoscope. This study supports the observation in over 2,000 cases since commercial launch that FloShield significantly reduces the need to interrupt surgery to clean the laparoscope.

Figure: Demonstrated is a smoke tube (bottom part of screen) blowing onto a 30-degree laparoscope that has the FloShield™ sheath over it. When CO2 is blowing through FloShield™ (left), the smoke is pushed away from the lens. When CO2 is not flowing through FloShield™ (right), smoke contacts the lens.

ABSTRACT 49

SUBMILISIEVERT COMPUTED TOMOGRAPHY FOR THE EVALUATION OF UROLITHIASIS

Brian Eisner[1], Naveen Kulkarni[2], Daniella Pinho[2], Guarav Desai[2], Raul Uppot[2], Dushyant Sahani[2]

[1] Department of Urology, Massachusetts General Hospital, Harvard Medical School
[2] Department of Radiology, Massachusetts General Hospital, Harvard Medical School

Introduction: To evaluate feasibility and diagnostic performance of submillisievert computed tomography (CT) examinations reconstructed with iterative reconstruction (IR) techniques in patients with urinary stone disease.

Methods: 26 patients (mean age 38 years) with diagnosed urolithiasis, treated and on follow-up underwent submillisievert dose unenhanced scan on 64 MDCT (Discovery CT750 HDCT, GE Healthcare) and 128 MDCT (Somatom Definition Flash, Siemens Health care) for evaluation of stone disease. The scan protocol included 80 kV, auto mA 75-150 or Ref mA - 80, slice thickness 5mm for < 200 lbs and 100 kV, auto mA 75-150 or Ref mA - 80, slice thickness 5mm for > 200 lbs. Images were reconstructed using filtered back projection (FBP) and IR [ASIR(GE) 60% & 80% and IRIS (Siemens)]. Images of 2-3 mm were reconstructed in the coronal and sagittal planes in all cases. All the image data set axial (FBP, IR) coronal and sagittal images were reviewed for image quality (scale 1-5), noise (scale 1-3), number & size of calculi and confidence in diagnosis of urolithiais as well as urologic or non-urologic diagnosis (scale 1-3) other than calculi on PACS work station. Comparison was made with the prior low dose FBP baseline CT scan. The radiation dose (CTDI, DLP and mSv) were recorded and compared with baseline CT studies. Analysis of data was performed by using Wilcoxon signed rank sum test and Student's t-test.

Results: All 34 stones, mean size 6.4 mm (range 4-15 mm), were diagnosed confidently by two readers, yielding 100% sensitivity and accuracy. In 8 patients, stones had passed/resolved after treatment. In giving a differential diagnosis, IR images were rated better than FBP (2.8 vs. 1.7). The mean CTDI, DLP and mSv for submillisievert protocol was 1.2, 65.3, and 0.86, respectively, in comparison to 10.6, 363.4, and 5.4, respectively for our baseline low dose exam, with 82-88% dose reduction (p=0.0013).

Conclusion: Submillisievert unenhanced CT is feasible clinically for diagnosis of urinary tract stone disease with 82% to 88% dose reduction. This study suggests that submillisievert dose CT with new iterative reconstruction technique is adequate in the assessment of urinary tract stone and enables significant reduction in radiation dose when compared with the standard, low-dose stone protocol CT.

ABSTRACT 50

THE SPEAR-HEADED LITHOTRIPTOR: AN INEXPENSIVE ALTERNATIVE FOR HARD STONES

Rawandale AV, Kurane CS, Patni LG
Institute of Urology, Dhule, India

Objectives: To describe a novel modification of the lithotriptor head in order to make intracorporeal lithotripsy for hard calculi fast, safe, and inexpensive.

Methods: The "Spear-headed lithotriptor" was fabricated, patented, and used for percutaneous nephrolithotripsy at the Institute of Urology. It has a pointed tip in contrast to the flat disc-shaped tip of a conventional probe (Figure 1).

Results and Discussion: Although conventional probes are excellent for stone fragmentation, they are not universally fast and efficient, especially in the setting of hard urinary stones. Another disadvantage in these clinical scenarios is stone chipping and tangential probe slippage, making it difficult to pin down the stone. This results in involuntary application of excessive axial pressure on the probe with the possible potential of renal trauma. The impact pressure generated at the tip of the probe is directly proportional to the pressure transferred along the shaft of the probe from the lithotriptor handpiece and inversely proportional to the area of the tip of the probe. At the generator settings of 4 bars; the probe tip impact pressure is 16 bars when the probe tip diameter is 3 mm (a conventional probe). On reducing the tip diameter to 0.5 mm (the Spear-headed lithotriptor) the probe tip impact pressure increases to 575 bars. Thus at the "First Hit" (*i.e.*, on point contact of the probe with the stone), a highly focused impact force is generated (Figure 2). As fragmentation progresses, cracks and uneven surfaces cause more area of the probe tip to come into contact with the stone (Figure 3), increasing the effective probe tip area and causing a drop in the impact pressure of subsequent strikes. This creates the graduated impact force. The lateral vectors of force and mechanical separation also come into play at this stage (Figure 4) leading eventually to bivalving of the stone; the end point of the fragmentation process. The safety profile of the spear-headed lithotripter is likely to be similar to that of other pneumatic devices. As a universal precaution it should be used only under direct vision, keeping away from the mucosa. One should judge the depth of the stone to avoid injuries caused by the tip boring through the distant end of the stone. It should be fairly easy to learn and master, but it may be difficult to pin down a stone at the contact hit (*i.e.*, prior to the creation of the first dent).

Conclusions: The Spear-head creates highly focused impact forces, graduated impact forces, centrifugal vectors of force, larger stone fragments, augmented mechanical separation of the fragments, decreased lateral displacement of probe, decreased stone migration, and reduced generator pressure settings, thus improving stone pulverisation.

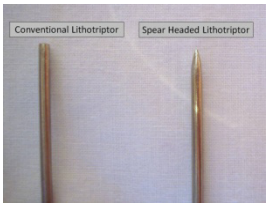

Figure 1

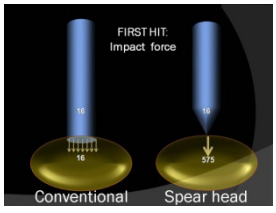

Figure 2

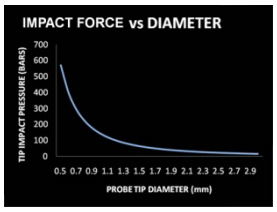

Figure 3

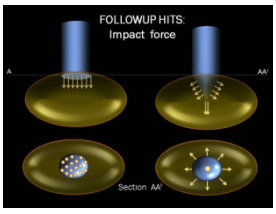

Figure 4

ABSTRACT 51

"STAGHORN MORPHOMETRY": A NEW TOOL FOR CLINICAL CLASSIFICATION AND PREDICTION MODEL FOR PCNL MONTHERAPY

Mishra S[1], Sabnis RB[2], Desai MR[1]

[1] *Muljibhai Patel Urological Hospital, Nadiad, Gujarat, India. Pin 387001*

Introduction: Staghorn stone volume and its distribution within the collecting system, "staghorn morphomerty," predicts the requirement of tract and stage for percutaneous nephrolithotomy (PCNL) monotherapy. Our objective was to develop a CTU staghorn morphomerty-based prediction algorithm to predict tract(s) and stage(s) for PCNL monotherapy and classify staghorn stones accordingly.

Methods and Results: A retrospective case-control design of 94 units was used. CT software calculated the total stone volume (TSV) with absolute volume and percentile volume in the pelvis, planned entry calyx, and favorable and unfavorable calyx. Entry calyx was the optimum calyx chosen, keeping the relations of the ribs and adjoining viscera that could clear maximum stone volume. Unfavorable calyx was defined as having acute angle from the entry calyx and infundibular width of 8 mm. A prediction model with OR (95 % CI) was constructed on univariate and multivariate regression factors.

Conclusion: The model predicts the tract and stage for PCNL monotherapy. Staghorn morphometry differentiates staghorn into type 1 (single tract and stage), type 2 (single tract-single/multiple stage or multiple tract-single stage), and type 3 (multiple tract and stage).

ABSTRACT 52

WEB-ACCESSIBLE 3D ANATOMY SOFTWARE OF UROLOGIC PATHOPHYSIOLOGICAL CONDITIONS AND PROCEDURES FOR PATIENT EDUCATION

D. Burke[1,2], X. Zhou[1,2], V. Rotty[2], B. Konety[1], R. Sweet[1,2]

[1] *Urologic Surgery, Medical School, University of Minnesota, Minneapolis, MN*
[2] *Center for Research in Education and Simulation Technologies (CREST), University of Minnesota, Minneapolis, MN*

Introduction: The poor transfer of knowledge to patients with standard informed consent is well documented. Providing easy-to-use, web-accessible tools for clinicians and patients should enhance informed consent. While passive 2-D animation models exist on the Internet, it has been shown that interactivity and the use of 3-D virtual models enhances understanding of anatomic structures and relationships. Our goal was to provide a detailed anatomy guide, tailored to displaying specific ailments and common procedures in urology with an easy-to-use interactive 3D web format.

Methods: Using current WebGL software, we access and display our library of 3D human anatomical structures. Models are derived from real human MRI/CT, and built under the guidance of consulting physicians. Users move and rotate models, remove layers and isolate areas of interest in finer detail, and even replace anatomy with available, diseased versions using a simple point-and-click interface. There is also the option to view animations of actual procedures for specific ailments. We utilize several drop-down commands and anatomy lists.

Results: A screen shot of the web-based 3-D model is shown in Figure 1. A high-quality model is displayed over the Internet in realtime. The user can strip layers off the model from skin to bone with an infinite number of viewpoints. Disease specific applications have been developed for BPH and prostate cancer. The user is able to continue interacting with the models during the procedures. This system has been deployed in the Urologic Clinic at the University of Minnesota for pilot testing.

Conclusion: The web-based anatomy viewer can be used online in real-time and warrants study as to the ability to enhance informed consent about urologic diseases and procedures to patients.

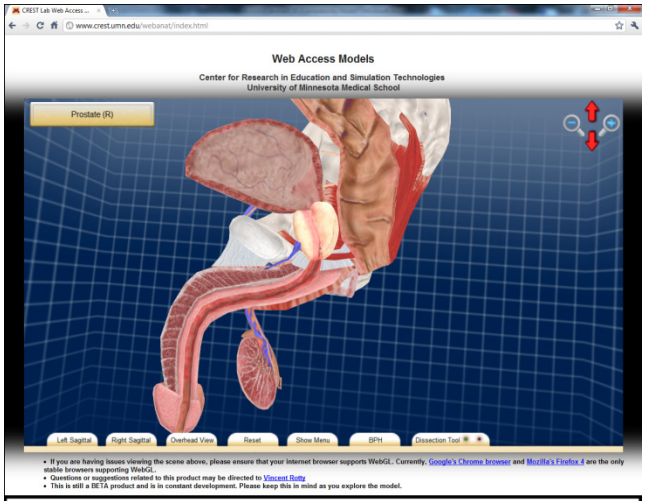

Figure 1: 3D gross anatomy of male pelvis, available for individual dissection.

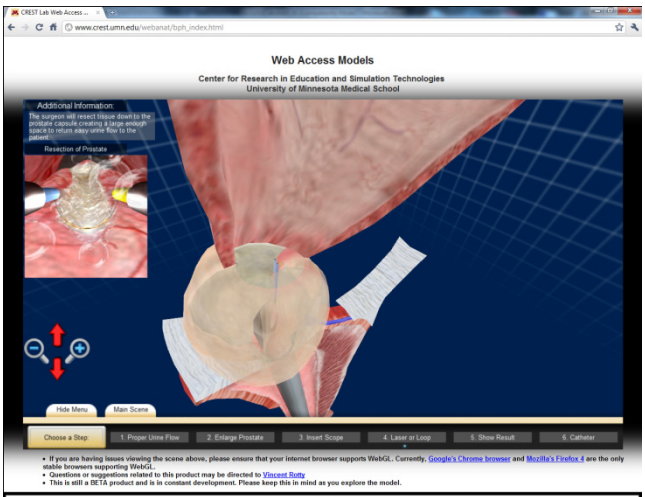

Figure 2: Resection step of BPH treatment animation, with additional information and internal view.

ABSTRACT 53

FACTORS DERERMINING STONE-FREE RATE IN SHOCK WAVE LITHOTRIPSY USING THE STANDARD FOCUS OF STORZ MODULITH SLX-F2 LITHOTRIPTER

Mohamed A. Elkoushy, Jacob A. Hassan, Douglas D. Morehouse, Maurice Anidjar, and Sero Andonian

Department of Surgery, Division of Urology, McGill University Health Center, McGill University, Montreal QC, Canada

Introduction: Since its invention, shock wave lithotripsy (SWL) remains one of the first line options for management of upper urinary tract calculi. However, the latest generation of electromagnetic (EM) shockwave lithotripters with smaller focal areas and higher peak pressures has been criticized for lower stone-free rates and higher retreatment rates due to difficulty in keeping the stone in the smaller focal zone. Whereas the Efficiency Quotient (EQ) of the original electrohydraulic (EH) Human Model 3 (HM3) lithotripter is between 0.64 and 0.67, there is a wide variation among the reported EQs of the latest generation of EM Storz Modulith lithotripters (0.57-0.67). Therefore, the objectives of the present study was to calculate the EQ of the latest fourth generation mobile Storz Modulith SLX-F2 lithotripter and to determine factors affecting stone-free rate.

Methods: A retrospective review of a prospectively collected database of the first consecutive 533 patients undergoing SWL between June 2009 and February 2010. A total of 16 patients with radiolucent stones and 46 patients with incomplete follow-up were excluded. To minimize radiation, patients were followed with plain radiography to assess stone-free status. While success was defined as absence of residual fragments or presence of fragments < 4 mm, stone-free was defined as complete absence of radio-opaque stone fragments. Retreatment was considered when a repeat SWL was performed for the same stone. Patients requiring post-SWL curative auxiliary procedures, such as ureteroscopy, were considered SWL failures and were not included in the stone-free rate. Univariate and multivariate analyses were performed to identify factors determining stone-free rates.

Results: Follow-up was complete for 474 patients with a mean age of 54.2 ± 14.5 years. Mean stone size was 9.51±3.87 mm, with 248 (52.3%) being left-sided and 270 (57.0%) located in the kidney. Renal stones were significantly larger than ureteral stones (10.5±3.5 vs. 8.7±1.62 mm, p=0.001). Overall success rate after a single SWL session was 82.7% (renal 82.2% and ureteral 83.3%; p=0.81). Retreatment rate was 14.7% (renal 15.2% and ureteral 14.2%; p=0.79). Stone-free rate was 77% (renal 74.1% and ureteral 80.9%; p= 0.10). Forty-three patients had pre-SWL ureteral stents, whereas 13 patients required post-SWL ureteral stenting. Thirty-five patients required post-SWL curative procedures. The EQ was 0.66 and the modified EQ was 0.62. On multivariate analysis, stone-free patients were associated with significantly smaller stone size (9.5 vs. 10.3 mm, p=0.02), younger age (53.1 vs. 58.0 yrs; p=0.002), right-sided stones (83.6% vs. 71.0%; p=0.001) and absence of a ureteral stent (78.7% vs. 64.3%; p= 0.001).

Conclusions: The mobile Storz Modulith SLX-F2 lithotripter has an acceptable EQ of 0.66. In the present study, smaller stones (<10 mm), younger age, right-sided stones, and absence of ureteral stents were associated with significantly higher stone-free rates.

ABSTRACT 54

IN VIVO TESTING OF THE SECOND GENERATION SPIDER LAPAROENDOSCOPIC SINGLE-SITE SURGICAL SYSTEM

Vladislav Gorbatiy[1], Michael A. Gorin[1], Scott M. Castle[1], Watid Karnjanawanichkul[1], Kenneth D. Fernandez-Prada[1,2], Nelson Salas[1,2], Raymond J. Leveillee[11]

[1]*Joint Bioengineering and Endourology Developmental Surgical (JBEDS) Laboratory, Division of Endourology, Laparoscopy, and Minimally Invasive Surgery, Department of Urology, University of Miami Miller School of Medicine, Miami, Florida*
[2]*Department of Biomedical Engineering, University of Miami, Coral Gables, Florida*

Introduction: The Single Port Instrument Delivery Extended Reach (SPIDER) surgical system (Figure 1A) was developed by TransEnterix Inc. (Durham, NC) for improved ergonomics and instrument control during laparoendoscopic single-site surgery (LESS). The system's flexible vertebral design eliminates instrument collision during LESS (Figure 1B). This study aimed to compare the second generation SPIDER device to a currently available multichannel LESS system during renal surgery in a porcine model.

Methods: Two experienced laparoscopic surgeons tested the SPIDER in comparison to an existing multichannel LESS port with articulating instruments. Each surgeon performed a dismembered pyeloplasty with both surgical platforms in an adult pig. The two systems were compared for total procedure time, knot-tying time, degree of instrument collision/crossing, and overall ease of use.

Results: Both surgeons completed the procedures without intraoperative complications. Pyeloplasty completion times were 36 and 40 minutes with the SPIDER versus 70 and 82 minutes with the comparison system. The average time to tie three standard intracorporeal surgical knots was 24 minutes with the SPIDER as compared to 55 minutes with the other device ($p = 0.029$). A significantly greater degree of instrument crossing and collision was experienced with the multichannel platform resulting in a subjectively inferior surgical experience. Both surgeons reported the SPIDER to be of greater ease of use.

Conclusions: The main advantages of the SPIDER surgical system include the elimination of instrument collision/crossing and improved ability to tie intracorporeal knots. These features translated to significantly shorter procedure times and an overall superior operative experience to currently available multichannel LESS systems.

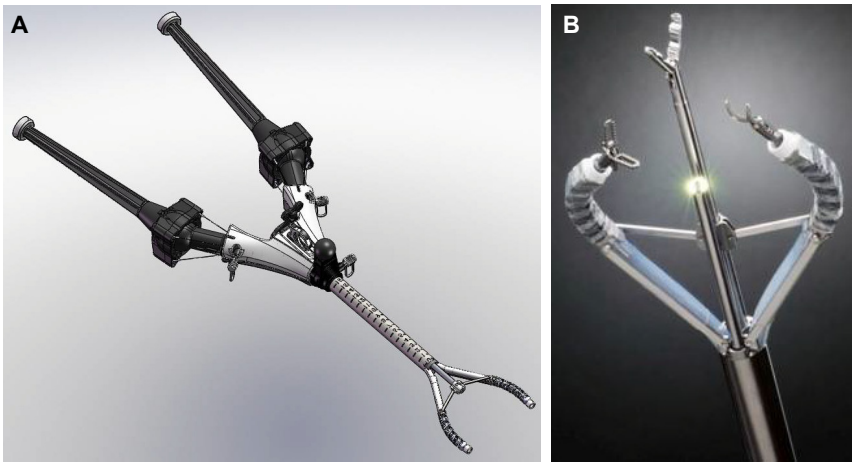

Figure 7: (A) Schematic drawing of the SPIDER surgical system.
(B) Photo of the system's flexible end-effectors.

ABSTRACT 55

NOVEL OFFICE-BASED RAPID UTI DETECTION SYSTEM

Joseph V. DiTrolio, MD[1], Eric Levy[2], Michael D. LaSalle, MD[3]

[1] *Department of Urology, UMDNJ/New Jersey Medical School, Newark, New Jersey*
[2] *UMDNJ/New Jersey Medical School, Newark, New Jersey*
[3] *Department of Urology, St. Barnabas Medical Center, Livingston, New Jersey*

Introduction: Rapid assessment of microbial activity in a urine sample is critical in the care of medicine in the 21st century. Over or inappropriate antibiotic use is a major factor in the cost of medical management of urinary tract symptoms and will lead to an increase in super-resistant bacterial populations. Therefore, an office-based mechanism that evaluates the potential for an active urinary tract infection would greatly enhance office-based management of this disease entity. Using the MicroBionetics CultureStat Urinary Detection System, a physician should be able to determine the potential of an active UTI or the success of a previously treated UTI within 30 to 150 minutes.

Methods: Thirty (30) patients were evaluated with lower urinary tract symptoms or a recently suspected UTI with antibiotic therapy already initiated, pending culture results. Using the CultureStat aspiration tube, 7ml of freshly collected urine is allowed to incubate for 30 minutes, followed by a spectroscopy reading looking for both turbidity (cell mass) and increased metabolic activity causing a change in TTC Level (bacterial respiration). Suspicious specimens were incubated an additional two hours to plot bacterial activity.

Results: CultureStat was able to identify 100% of the appropriately treated urinary tract infections, and was 85% accurate in identifying those patients where symptoms would require antibiotic therapy immediately.

Conclusion: Urinary tract infections are a log phase bacterial event. An increase in turbidity (cell mass) and bacterial respiration allows for a rapid assessment of active bacterial growth in the collected specimen. When incorporated with the clinical history, this can either confirm appropriate treatment of an already treated patient, or the need to start antibiotic therapy in those with a high level of bacterial activity. In an era of cost containment and efficient use of antibiotic therapy, this office-based test mechanism deserves further evaluation.

ABSTRACT 56

COST ANALYSIS OF METAL URETERAL STENTS WITH 12 MONTHS OF FOLLOW-UP

Eric R. Taylor, Aaron Benson, Bradley Schwartz
Division of Urology, Southern Illinois University, Springfield, IL

Introduction: The metallic ureteral stent was developed for patients with ureteral obstruction related to malignant disease, but it can be used in all patients requiring chronic indwelling ureteral stents for ureteral obstruction. The traditional method of polymer stent management requires 3 to 6 exchanges per year depending upon patient and logistical factors. This has significant direct financial cost associated with it. We report our experience with the placement of the Resonance metallic stent for benign and malignant ureteral obstruction focusing on comparative hospital charges to polymer based ureteral stents.

Methods: A prospective database of patients undergoing metal stent placement from February 2008 to present was reviewed. Mean charges for a single, traditional non-metal and metal stents insertion was calculated. Cost was based on direct hospital charges related to stent cost and surgery.

Results: 21 patients underwent metal stent placement at our institution. Of these, 3 traditional stent placements were omitted from analysis due to charges for ureteroscopy at the same setting. Mean charges per single traditional and metal stent placement was $6,853.16 and $9,699.73, respectively. The estimated annual cost of traditional stents (3-6 exchanges) would be $18,218.25 to $36,436.50. Based on three, four, or six polymer stent exchanges per year, the annual cost reduction compared to a metal stent would then be 48.02%, 61.02% and 74.01%. No patient required early discontinuation of his or her metal stent due to LUTS or gross hematuria.

Conclusions: For patients not fit for definitive surgical intervention regarding their ureteral occlusive disease the metal stent is a financially advantageous and well-tolerated option. Compared to traditional polymer stents, the metal stent has a significant financial benefit, with an estimated cost reduction of 48% to 74%.

ABSTRACT 57

3D-TRUS MAPPING FUSION FOR SECOND LOOK PROSTATE BIOPSIES

Pierre Mozer[1], Michael Baumann[2,3], Gregoire Chevreau[1,2], Vincent Daanen[3],Jocelyne Troccaz[2]

[1] *Department of Urology, Pitié-Salpêtrière Hospital, Pierre et Marie Curie University (Paris VI) Paris, France.*
[2] *TIMC Laboratory, IN3S, Faculté de Médecine, Domaine de la Merci, 38706 La Tronche Cedex, France.*
[3] *KOELIS SAS - www.koelis.com*

Introduction: We present a new imaging technology dedicated to prostate biopsy management. 3D transrectal ultrasound (3D TRUS) and elastic image fusion should allow one to import and display previous biopsy mappings as planning information for second look targeted biopsies in recurring patients.

Methods: The method is based on full 3D TRUS and image fusion software. We use a 3D TRUS probe on a Medison scanner, connected to the Urostation software platform from KOELIS. The 3D tracking and mapping is based on an automatic registration method described previously[1]. Whereas the clinical workflow of transrectal biopsy is unchanged, the system records biopsy locations on a single TRUS volume of the prostate. In this work, we have performed retrospective elastic fusion of prostate TRUS volumes[2] from two consecutive biopsy sessions in 8 patients. The aim was to visualize the biopsy locations from both series in the same 3D reference prostate volume. We have evaluated the delay and accuracy of image registration, and the feasibility of the method integrated in the 3D biopsy workflow for planning purposes.

Results: The automatic elastic registration of prostate volumes succeeded in every case in 5 to 12 seconds. The accuracy of the fusion visually evaluated from image superimposition in 3 planes is millimetric, including in the anteroposterior axis which usually shows most deformations. The two biopsy sets mappings could be displayed in 3D in a single reference image (Figures 1 to 3).

Conclusion: Automatic elastic fusion of two 3D biopsy mappings is fast and accurate. Preliminary results encourage the use of the method in planning and targeting second look biopsy, as well as for better documented cancer extension and patient management in active surveillance or treatment strategies.

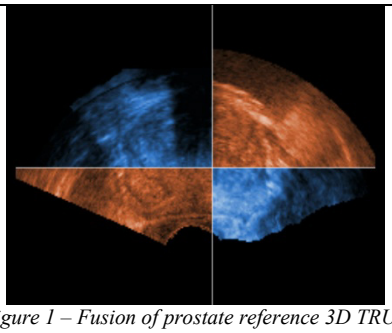

Figure 1 – Fusion of prostate reference 3D TRUS images (transverse view) from biopsy series 1 (blue) and 2 (orange), after elastic registration.

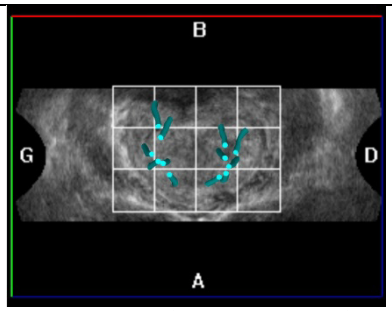

Figure 2 – First Look 3D TRUS 12-core biopsy mapping (coronal view). All biopsies are free of cancer.

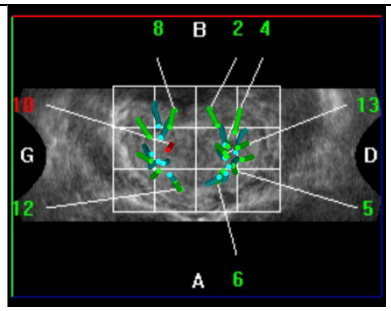

Figure 3 – Second Look 3D biopsy mapping. Biopsies in green were targeted to free areas. Biopsy N°10 in red contains cancer tissue.

[1]. Mapping of transrectal ultrasonographic prostate biopsies: quality control and learning curve assessment by image processing. *Mozer P, Baumann M, Chevreau G, Moreau-Gaudry A, Bart S, Renard-Penna R, Comperat E, Conort P, Bitker MO, Chartier-Kastler E, Richard F, Troccaz J, Journal of Ultrasound in Medicine 2009 28(4):455-60.*
[2]. Prostate Biopsy Assistance System with Gland Deformation Estimation for Enhanced Precision *Baumann M, Mozer P, Daanen V and Troccaz J, Medical Image Computing And Computer-Assisted Interventions – Miccai 2009 Vol 5761/2009:67-74*

ABSTRACT 58

RADIOSURGICAL ABLATION OF RENAL TUMORS: EVALUATION OF SAFETY

Oussama M. Darwish and Lee E. Ponsky

Urology Institute, University Hospitals Case Medical Center, Cleveland, OH

Introduction: A variety of minimally invasive, energy-based modalities has been and continues to be investigated for the treatment of renal tumors. The goal of any such technique is definitive destruction of the lesion, preservation of the normal surrounding parenchyma, and minimal morbidity. It is the intent of this study to determine the optimal dose and safety of radiosurgical ablation of renal tumors.

Methods: Patients who were considered to be poor surgical candidates were offered radiosurgical ablation of the renal tumor. Patients underwent renal biopsy and fiducial marker placement under computed tomography (CT) guidance with local anesthesia. A CT and/or magnetic resonance imaging (MRI) were obtained and the tumor and surrounding structures were contoured. The physicists then determined the ideal number of radiosurgical beams that would be needed to ablate the tumor and the direction of the beam. Escalating doses from 2400 cGy up to 4800 cGy were used. Patients were monitored for any adverse events; a follow-up biopsy was performed at 6 months, and serial imaging performed at 6-month intervals.

Results: A total of 19 patients have been treated to date, with a mean age of 80 years. The mean tumor size was 3.42 cm and all patients were stage T1a. Four patients received 600 cGy x 4 fractions, 4 patients received 800 cGy x 4 fractions, 4 patients received 1000 cGy x 4 fractions, and 7 patients received 1200 cGy x 4 fractions. Of the patients treated, 1 patient reported a grade 2 serious adverse event (nose bleed) and there was 1 death from lung cancer, both of which were determined to be unrelated to treatment.

Conclusion: In our initial dose escalation study to determine ideal dosing and toxicity, we reached no dose limiting toxicities. We intend to extend our study with a dose escalation over 3 fractions. Once we reach the optimum ablative dose regarding toxicities, we plan to determine the efficacy. We anticipate that radiosurgical ablation of renal tumors will prove to be a safe and efficacious non-invasive option for the management of renal masses.

ABSTRACT 59

TRUS PROSTATE BIOPSIES PIERCED AREA CAN IMPACT CANCER RATE DETECTION

G Coffin[1,2], C Torterotot[1] ,M Baumann[3] , M.A Vitrani[1], G Morel[1], G Chevreau[2], P.C Mozer[1,2]
[1] *ISIR laboratory, University Pierre and Marie Curie, CNRS-UMR7222, Paris, France*
[2]*Department of Urology, La Pitié-Salpêtrière hospital, Assistance-Publique Hôpitaux de Paris, Paris, France*
[3]*TIMC-GMCAO laboratory (CNRS-UMR 5525), Domaine de la Merci, Grenoble, France*

Introduction: Some studies have already shown that the number of biopsy cores and biopsy scheme can have an influence on cancer rate. We wanted to know if the *pierced area* of each prostate lobe could impact cancer rate detection in each lobe.

Methods: The Urostation (Koelis, France) provides 3D mapping of transrectal prostate biopsies. With this device, we were able to estimate the pierced area of the posterior prostate capsule for each lobe (Figure 1). We retrospectively reviewed prostate biopsies that were realized with the Urostation® ultrasound system in our department. All patients laid on lateral decubitus position, and 6 biopsies were performed for each prostate lobe. *We define the cancer in each lobe as one or more positive core in the lobe*. We only included patients without history of prostate cancer, PSA < 20ng/ml. We analyzed the following criteria: age, PSA level, DRE, prostate volume, and left and right prostate pierced area. Significance of results was assessed with χ^2 tests for qualitative values (cancer rate in each lobe) and Student's t-Test or ANOVA tests for quantitative measures (pierced area of each lobe).

Results: Between October 2008 and January 2011, 789 biopsy procedures were done in our department; 158 patients were eligible for the study. Mean age was 65 years (47.3, 85.6), anormal DRE was found in 36 patients (26 nodules on right side, and 10 on left side), mean PSA level was 8.21ng/mL (0.62, 17.3), mean prostate volume was 50.34g (17, 138). Mean pierced area was 104.79mm^2 (27.42, 231.05) in the right lobe and 116.55mm^2 (31.43, 309.98) on the left lobe with a significant difference (analysis of variance, p=3,03.10^{-19}). Cancer rate detection was 29.1% in the right lobe and 40.5% in the left lobe with a significant difference (p=0.00671) for prostate volume <80g (Figure 2). Differences between the right and the left lobes were also significant according to prostate volume.

Conclusion: There are significant differences between right and left lobe cancer detection rate and pierced area. These differences may impact on clinical decision.

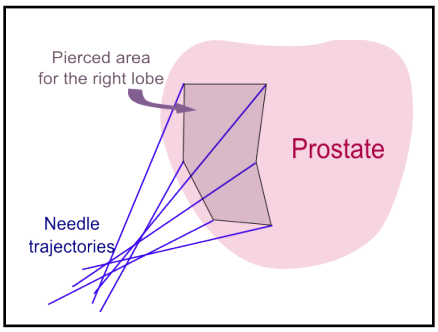

Figure 1: Pierced area in the prostatic capsule for the right lobe

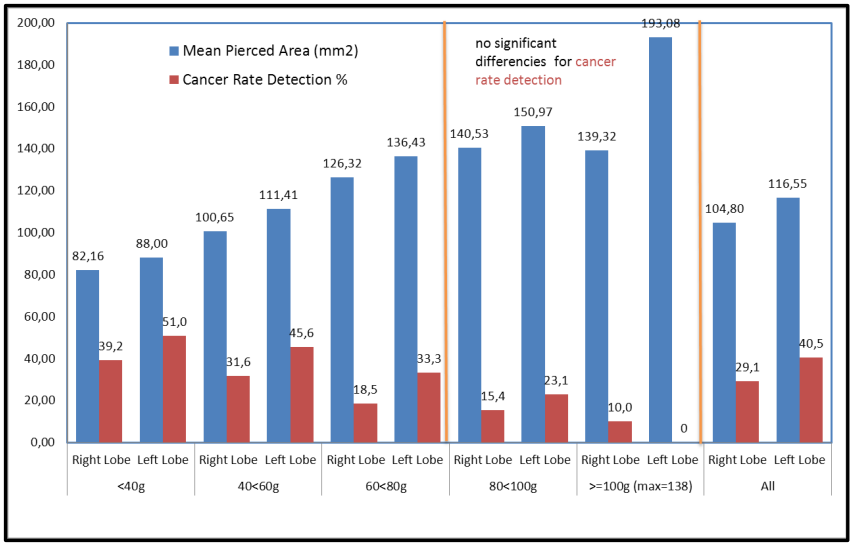

Figure 2 Variation of pierced area and cancer detection rate according to prostate volume and lobe side

ABSTRACT 60

INITIAL HUMAN LAPAROENDOSCOPIC SINGLE SITE PYELOPLASTY USING THE SPIDER SURGICAL SYSTEM: FEASIBILITY AND SAFETY

Scott M. Castle[1], Vladislav Gorbatiy[1], Michael A. Gorin[1], Nelson Salas[1,2], Raymond J. Leveillee[1,2]
[1]*Joint Bioengineering and Endourology Developmental Surgical (JBEDS) Laboratory, Division of Endourology, Laparoscopy, and Minimally Invasive Surgery, Department of Urology, University of Miami Miller School of Medicine , Miami, Florida*
[2]*Department of Biomedical Engineering, University of Miami, Coral Gables, Florida*

Introduction: Laparoendoscopic Single Site Surgery (LESS) has been applied to several urologic procedures. However, currently available systems are somewhat limited in their utility. The Single Port Instrument Delivery Extended Reach (SPIDER) surgical system was developed by TransEnterix Inc. (Durham, NC) for improved ergonomics and instrument control during LESS. The flexible design of the SPIDER system allows for continuous instrument triangulation and eliminates instrument collision during LESS. We present our initial clinical experience performing a LESS Pyeloplasty (LESS-Pp) with the SPIDER surgical system.

Methods: Following informed consent, a 40-year-old female underwent a right-sided dismembered LESS-Pp using the SPIDER surgical system for the management of a urinary obstruction. All portions of the procedure were performed using the SPIDER system with the aid of a 5-mm assistant port entering the skin < 1 cm away from the SPIDER entry site.

Results: The case was completed without an intraoperative complication. The length of surgery was 423 minutes and the length of hospital stay was 4 days. An elevated JP creatinine on post-op day #2 was managed conservatively and resolved.

Conclusion: LESS-Pp with the SPIDER surgical system can be safely performed following careful patient selection. This system allows for excellent surgical triangulation without instrument crossing or clashing. However, its ultimate application in LESS-Pp remains to be proven as our experience showed an increased procedure time. Also at present, the assistant port may be required to pass suture needles as these cannot be passed through the instrument ports. Nonetheless, LESS-Pp is a safe and feasible option using the SPIDER system.

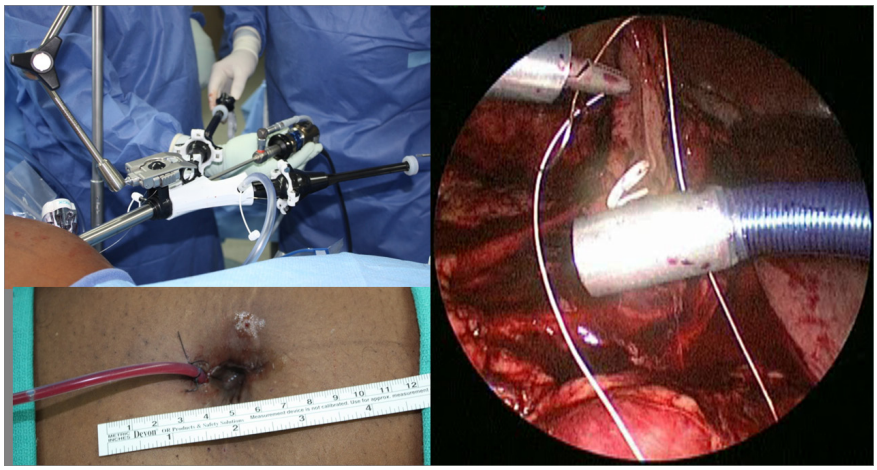

Figure: [Top Left] Extracorporeal view of SPIDER and assistant port. [Bottom Left] Skin Incision with blake drain. [Right] Intracorporeal view of SPIDER arm triangulation during suturing

ABSTRACT 61

A 3D ELASTROGRAPHY-GUIDED SYSTEM FOR LAPAROSCOPIC PARTIAL NEPHRECTOMY

Phillip M. Pierorazio[1], Philipp J. Stolka[3], Mathias Keil[3], Emad Boctor[2], and Mohamad E. Allaf[1]
[1]Brady Urological Institute, [2]Department of Radiology; [3]Johns Hopkins University, Baltimore, MD

Introduction: Laparoscopic partial nephrectomy (LPN) is the traditional approach to minimally invasive nephron-sparing surgery; however, it can be challenging technically and relies on resection without visible landmarks in a limited field of view, especially when tumors are endophytic. Ultrasound elastography, relying on the elastic properties of tissues, can discriminate and classify lesions in a number of tumor models. In order to improve the safety, applicability and dissemination of LPN and related surgeries, a real-time, image-guided intervention system using 3D elastic imaging (EI) registered to preoperative CT was created.

Methods: The strain computation process of 3DEI is optimized using dynamic programming algorithms and electromagnetic tracking of the US probe to create a 3D volume reconstruction with few low-quality frames. EI stiffness values are registered to CT density information using Mattes Mutual Information (Equation 1) as the metric for registering two distinct modalities. Three landmarks are chosen in US and CT and registered via optimization algorithms. The tumor is outlined on 2D imaging by the user, then scaled and stored into 3D by the navigation part of the system. Using electromagnetic (EM) sensors in the tumor, US probe, laparoscope and instruments, a 3D "tumor" is overlaid into the live video stream. Porcine-based and synthetic kidney phantoms with tumors were used for all experiments.

$$S(\mu) = -\sum_{\iota \in L_T} \sum_{\kappa \in L_R} p(\iota,\kappa;\mu) \log \frac{p(\iota,\kappa;\mu)}{p_T(\iota;\mu)\, p_R(\kappa)}$$

Equation 1. Similarity metric according to Mattes Mutual Information (MMI) comparing two images with histograms *LT*, *LR*, with one image experiencing displacement μ, and joint and marginal probability distributions *p*, *pT*, and *pR*.

Results: Registration of the volume of interest was complete in 5 to10 seconds for three translational degrees of freedom. With high quality, robust strain imaging, kidney tumors were imaged reliably in an interventional setting. Using EM sensors, real-time motion tracking was achieved (Figure 1).

Conclusions: Through real-time elastrography, fast 3DEI/CT registration and intraoperative tracking, kidney tumors could be located and tracked in a phantom model for laparoscopic partial nephrectomy.

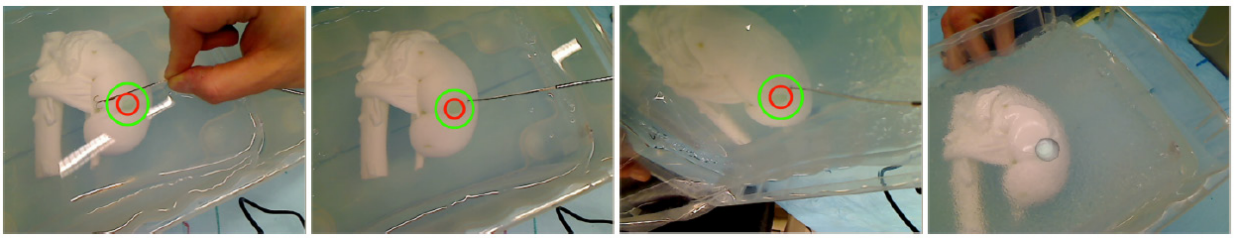

Figure 8. Real-time "augmented reality" overlay of tracked target region onto intra-operative video stream from a tracked webcam. An EM sensor (left) was manually inserted under US guidance into the tumor ROI after 3D US acquisition, with its position projected back into camera coordinates (left center and right center). The same position can be used to overlay a 3D surface model of the segmented tumor region (right).

Acknowledgements: IGT-JHU Grant, Georg Sakas, Professors Russell Taylor and Elliot McVeigh.

ABSTRACT 62

DEVELOPMENT OF A RENAL PHANTOM MODEL FOR IMAGE-GUIDED LAPAROSCOPIC PARTIAL NEPHRECTOMY

Phillip M. Pierorazio[1], Philipp J. Stolka[3], Emad Boctor[2], and Mohamad E. Allaf[1]
[1]Brady Urological Institute, [2]Department of Radiology; [3]Johns Hopkins University, Baltimore, MD

Introduction: Laparoscopic partial nephrectomy (LPN) is the traditional approach to minimally invasive nephron sparing surgery; however, it can be challenging technically and relies on resection without visible landmarks in a limited field of view, especially when tumors are endophytic. Advances in intra-operative imaging, navigation and registration with preoperative imaging may improve the safety, applicability and dissemination of LPN and related surgeries. We describe the creation and use of renal phantoms for the use in the creation of image-guided LPN.

Methods: *Ex vivo* phantoms (animal tissue preparations exhibiting structures resembling actual in-vivo conditions) were based on porcine kidneys (extracted shortly after exitus) due to their similarity to the human organs. The kidneys were treated partially with arterially and per urethra applied CT contrast agent (5% suspension of TiO powder (5m) in agar solution), and embedded in a stabilizing porcine gelatin mold. Additional fiducials were inserted into the phantoms to facilitate later registration. Pseudotumors were created with radiofrequency ablation and alginate injection. Using a novel system based on 3D-US elasticity imaging (EI) registration with CT imaging, pseudo-tumor containing phantoms were tested for ability to identify, register and track tumors for intra-operative motion tracking.

Results: Porcine phantoms were created by the above methods (Figure 1). Renal parenchyma, blood vessels, the collecting system, pseudo-tumors and fiducials (Figure 2) were visualized using CT and US. With high quality, robust strain imaging (through a combination of parallelized 2D-EI, optimal frame pair selection, and optimized palpation motions), kidney tumors that were previously unregistrable or sometimes even considered isoechoic with conventional B-mode ultrasound were imaged reliably.

Conclusions: Porcine-based renal phantoms with tumor models are easily produced viewable in US and CT imaging. The transformation of planning CT data to the intra-operative setting with a markerless mutual-information-based registration and intraoperative tracking, using these phantoms is feasible.

Figure 9. Porcine kidney phantom embedded in gelatin**.**

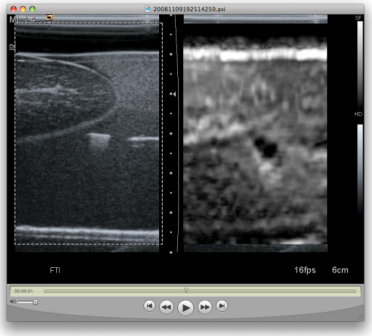

Figure 10. US (left) and CT (right) images of the kidney phantom. The fiducials are visible in both images. The pseudotumor is visible in the CT image.

Acknowledgements: IGT-JHU Grant, Georg Sakas, Professors Russell Taylor and Elliot McVeigh.

ABSTRACT 63

FLOW CHARACTERISTICS OF A NOVEL SPIRAL CUT URETERAL STENT

Phillip Mucksavage, Mohammed Etafy, Donald Pick, David Kerbl, Jason Lee, Cervando Ortiz-Vanderdys, Stephanie Olamendi, Michael K Louie, Ralph V. Clayman, Elspeth M McDougall

Introduction: Ureteral stents are one of the most commonly used implants in urology. Different designs and materials have been created to decrease the morbidity associated with an indwelling stent. We characterized the flow of a novel spiral cut flexible stent in a porcine model.

Methods: Flow characteristics of the novel stent were determined in an acute and chronic swine model and compared to a standard Percuflex stent. The flow characteristics in the model were determined after ligating the renal vessels and after establishing an nephrostomy tube delivering a standard rate of 0.9% saline at 35 cm H_20. Flows in the unobstructed ureter, normal stent, intraluminally obstructed stent, extraintrinsically obstructed stent and both intraluminally and extrainsically obstructed stent were determined. In the chronic animals (animals with indwelling stent for 10 days), flow was determine in the normal stent and after stent removal

Results: The novel stent performed as well as the standard Percuflex stent in all flow characteristics in the acute animals. Antegrade nephrostograms revealed that the novel stent appeared to conform subjectively better to the shape of the ureter. Flows were also similar in the chronic animals. Size and weight of the kidney, degree of hydronephrosis as determined on nephrostogram, and presence of urinary tract infection were also similar between stents in the chronic animals. The sectioned diameter of the mid ureter was slightly smaller in the novel stent compared to the standard stent (11.8 ± 1.21 mm vs. 15.7 ± 0.89 mm, $p=0.032$); however, other ureteral measurements did not differ significantly.

Conclusion: This novel stent with spiral cuts appears to perform as well as the standard Percuflex stent; however, the spiral cut shape of the stent seems to allow it to better conform to the ureter. Clinical trials will be necessary to determine if this characteristic will impact stent-related morbidity.

ABSTRACT 64

LOCALLY ADVANCED NON-METASTAIC PROSTATE CANCER (T3-4, N0, M0) TREATED WITH ROBOTIC HIGH INTENSITY ULTRASOUND (rHIFU)

Thueroff Stefan[2,3], Chaussy Christian[1,3]

[1]Dept. of Urology University of Regensburg,
[2]Dept. of Urology Klinikum Muenchen, [3]Harlachinger Krebshilfe e.V.

INTRODUCTION AND OBJECTIVES: We analyzed efficacy and side effects of local single session prostate cancer therapy with robotic HIFU during a maximum follow-up of 9 years in subgroup of patients.

MATERIAL & METHODS: A subgroup of the prospective Munich HIFU database (n = 2,300) was analyzed. This subgroup summarizes 146 patients with locally advanced PCa and a negative systemic staging. At study entry, the patients were stratified into three groups according to their PSA at inclusion (PSAi): Group A: PSAi<20 (n=89); Group B: PSAi 21-50 (n= 39); and Group C: PSAi >50 ng/ml (n= 18). Mean follow-up was 3 years (0.3-9), staging: T3: 90%, T4: 10%, age: 70 (49-84). Mean PSAi was 26.5 ng/ml (0.6-211). Mean PSA at treatment was 12.4 ng/ml (0-131) because of short-term neoadjuvant androgen deprivation therapy (ADT) (<3months: 38%). 62% had no ADT. All patients were treated with HIFU (Ablatherm®, EDAP-TMS,Lyon) after debulking TUR. The majority of patients received spinal anaesthesia combined with analgosedation. Mean 662 HIFU lesions were applied in 111 minutes. Withdrawal of the urethral catheter was at day 2.

RESULTS: Mean follow-up time was 36 (4.4-108) months. ADT adjuvant in follow-up: without ADT: 95.9%, ADT > 3 months 6.1 %. **Efficacy:** Median PSA Nadir: 0.28 ng/ml (mean 2.05), time to Nadir: 2.5 months. Median last PSA 1.1ng/ml (mean 9.9): of those 77% <10 ng/ml and 5% >50 ng/ml. Median last PSA after 2 years was in 93 % (Group A: 95; Group B: 94; Group C: 92) below PSAi levels. PSA velocity was median 0.26 ng/ml/year (mean 8.9): in Group A: 0.14, in Group B: 0.5 and in Group C: 0.93 ng/ml. Deaths in follow-up: 16/133 (12%) 4 PCa related, 12 other reasons. **Side effects:** perioperative (Clavien1-5): 10.3 % only Clavien 1-3. Any side effect in follow-up: 24.7 % (only low grade): of those 60% intermittent micturition problems.

CONCLUSION: Analysis of minimal invasive local tumor ablation (TURP + robotic HIFU) in a prospective consecutive monocentric T3-4, N0, M0 PCa cohort of 146 patients resulted in a PSA Nadir of 0.28 ng/ml 2 months after HIFU treatment and a median PSA velocity (ng/ml/year) of 0.26. Until a mean follow-up of 3 years, 94 % of the patients were without ADT. The concept of minimal non-invasive tumor ablation in locally advanced PCa showed favourable results with minimal side effects. ADT / radiation was preserved for cases with later progression.

Source of Funding: *Harlachinger Krebshilfe e.V, Lingen Stiftung*
Thanks to Ms. Regina Nanieva for HIFU database management and analysis

ABSTRACT 65

5-PART PERCUTANEOUS ACCESS NEEDLE WITH GLIDEWIRE (5-PANG) TECHNIQUE FOR PERCUTANEOUS NEPHROLITHOTOMY: TECHNIQUE AND OUTCOMES

Rawandale AV, Kurane CS, Patni LG
Institute of Urology, Dhule, India

Introduction: Initial tract creation and dilatation during percutaneous nephrolithotomy (PCNL) still remains a challenging step as the traditionally described techniques have their own shortcomings. We describe our 5-part Percutaneous Access Needle over Glidewire (5-PANG) technique in an attempt to make PCNL tract creation and dilatation a fast, safe, and less cumbersome procedure.

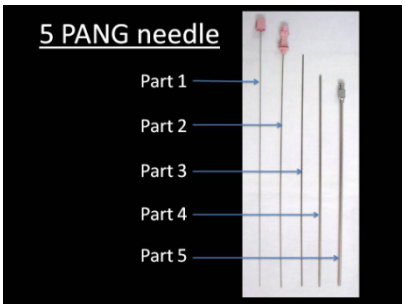

Methods: The 5-PANG needle was designed, fabricated, patented, and published by our institute. During PCNL the initial puncture and tract dilatation was done with the 5-PANG needle, followed by rigid telescopic metal dilatation. 364 renal units evaluated for PCNL from April 2005 to Oct 2010 were considered suitable candidates for the study. 5-PANG technique was performed at the hands of a single attending surgeon and the patients followed up to 5 years. The data were analyzed prospectively. The technique was evaluated with emphasis on the safety, efficacy, conversion rate, and associated complications. The video describes the procedure and results in detail.

Results:
Average time calculated from successful puncture to rod placement was 51.32 seconds with an average radiation time of 3.31 seconds. No failure, limitations, early or late complications or sequelae related to the procedure were observed. Conversion to the conventional technique was not needed in any instance. Learning curve in different hands needs to be evaluated.

Conclusion: 5-PANG makes PCNL tract creation and dilatation, safe, fast, effective, and inexpensive. It is easy to learn and master.

PATIENT DATA		5-PANG
Renal units		364
Mean age in years		35.55 (2-65)
Sex - M:F		1.9:1
History of previous renal surgeries		42 (11.54%)
Time:Puncture to Rod placement (secs)		51.32 (26-453)
Time: Rod placement to sheath placement (secs)		72.33 (35-300)
Radiation Time:Puncture to Rod placement (secs)		3.31 (.01-30)
Radiation Time: Rod placement to sheath placement (secs)		10.24 (0.01-17)
Ease of puncture	1st attempt	299 (82.14 %)
	2nd attempt	59 (16.21 %)
	> 2 attempts	6 (1.65 %)
Calyx punctured	Upper	38 (10.44 %)
	Middle	101 (27.75 %)
	Lower	225(61.81 %)
Tract size	20Fr	7 (1.92 %)
	22Fr	10 (2.75 %)
	24Fr	69 (18.96 %)
	26Fr	28 (7.69 %)
	28Fr	135 (37.09 %)
	30Fr	115 (31.59 %)
Visual clarity	Good	316 (86.81 %)
	Tolerable	43 (11.81 %)
	Bad	5 (1.37 %)
Intra op complications	Minor	5 (1.37 %)
	Major	7 (1.92 %)
Conversion to conventional method		0
Post operative complications		0

ABSTRACT 66

5-PART PERCUTANEOUS ACCESS NEEDLE OVER GLIDEWIRE - SUPRAPUBIC ACCESS TECHNIQUE (5-PANG-SAT): A MINIMALLY INVASIVE SOLUTION FOR SUPRAPUBIC VESICAL ACCESS: OUR INITIAL EXPERIENCE

Rawandale AV, Kurane CS, Patni LG
Institute of Urology, Dhule, India

Introduction: Describe and evaluate our 5-part Percutaneous Access Needle over Glidewire-suprapubic access technique (5-PANG-SAT) for easy suprapubic access of the bladder

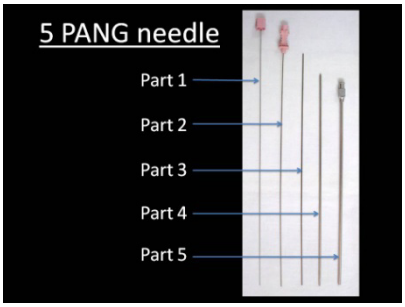

Methods: A 5-PANG access needle (Figure 1) designed, fabricated, and published by our institute was used for suprapubic access during suprapubic cystostomy (SPC) and percutaneous cystolithotomy (PCCL).
Procedure: Supine position under local (for SPC) and regional / general anaesthesia (for PCCL).
Step 1: Ultrasound guided vesical puncture- with inner 3 parts of the needle. Part 1 and 2 are withdrawn. Urine flow out of part 3 confirms the puncture. A wire is parked into the bladder through part 3.
STEP 2: The 4th and 5th part are then telescoped over the part 3 till the markings. The 3rd and 4th parts are removed.
STEP 3: For SPC – An infant feeding tube is parked in the bladder through part 5 and part 5 removed.
For PCCL -Alkens rod is passed through part 5 and part 5 withdrawn. Alkens dilatation till desired size is followed with sheath placement.
Prospective collection of data from June 2009 to May 2011; was evaluated. Safety, potential strengths and weaknesses were assessed.

Results:
All punctures were successful in the first attempt. Results not altered by the status of bladder fullness.
Advantages: Less exchange of dilators makes it a fast and painless procedure. Low chance of the wire slipping into the retropubic space. Easily done in partially full bladders. "Give away" sensation on entering bladder with USG guidance makes "controlled puncture" possible.
Eliminates posterior bladder wall injury. Drainage during SPC can be controlled allowing "slow decompression" if desired.
Cheap alternative for the commercially available SPC sets
Learning curve: easy

PATIENT DATA	5-PANG-SAT
Number of patients	21
Suprapubic cystostomy	11
Percutaneous cystolitholapaxy	10
Mean age in years	43.5 (35-57)
Sex	All males
History of previous vesical surgeries	4
Partially full bladder	3
Mean time: SPC(min)	4.56
Mean time: PCCL (min)	7.35
Conversion to conventional methods	0
Complications	0

Conclusion: The 5-PANG-SAT allows "controlled vesical puncture" and "controlled slow decompression." It is a safe, fast, inexpensive, and effective technique in an emergency as well as elective setup. It is easy to learn and master.

ABSTRACT 67

ABLATION OF SMALL RENAL MASSES: PRACTICE PATTERNS AT ACADEMIC INSITUTIONS IN THE UNITED STATES

Sutchin R. Patel, E. Jason Abel, Sean P. Hedican, Stephen Y. Nakada
University of Wisconsin School of Medicine and Public Health, Madison WI

Introduction: The purpose of our study was to determine the current practice patterns at academic institutions in the use of ablative technologies for the management of small renal masses.

Methods: Mail surveys were sent to 124 academic institutions in the United States. The survey consisted of 12 questions pertaining to the institutional use of ablation technology for treatment of small renal masses and the role of the urologist in evaluation and treatment.

Results: The overall response rate for the survey was 52% (64/124). Ablation was offered by all of the responding academic centers and included: percutaneous cryoablation (75%), percutaneous RFA (52%), laparoscopic cryoablation (83%), and laparoscopic RFA (19%). Eighty-eight percent of institutions performed 1 to 5 total ablation procedures each month. The procedure was performed primarily by radiologists alone (45%) or a combined approach with both urologist and radiologist present (42%). In combined procedures, the urologist was present at the time of ablation in 59% of institutions and placed the ablation probes in only 32% of institutions. Pre-ablative biopsy of the mass was performed at 89% of academic institutions, with 67% performing a core biopsy. Biopsy was performed prior to the day of the procedure so that the pathology was known prior to ablation in only 19% of responding institutions.

Conclusions: Ablative technologies are widely utilized for the treatment of small renal masses at current academic institutions with urologists participating in the ablation procedure in half of the institutions. While pre-ablation biopsy is common, pathology is known rarely prior to ablation.

ABSTRACT 68

PROSPECTIVE RANDOMIZED EVALUATION OF GELMAT FOOT PADS IN ENDOSCOPIC SUITE

Joseph A. Graversen,[b] Ruslan Korets,[b] Adam C. Mues,[b] Hiroshi K. Katsumi,[b] Ketan K. Badani,[b] Jaime Landman,[c] Mantu Gupta[b]

[b]*Department of Urology, Columbia University Medical Center, New York, NY, USA*
[c]*Department of Urology, University of California in Irvine, Orange, CA, USA*

Introduction: Ironically, the same advancements in surgical technology that have led to significant improvements in patient outcomes compromise surgeon comfort, leading to reports of tremors, muscle aches, and joint pain. The use of gelmats in the laparoscopic setting has been associated with improved surgeon comfort and fatigue levels. However, the endoscopic suite poses several distinct challenges not faced during laparoscopy. The purpose of the study was to expand on previous work and evaluate whether the use of gelmat foot pads (GelPro® Austin, TX) would benefit the surgeon in the singular environment of the endoscopic suite.

Methods: Between April and August 2010, 100 varied endoscopic procedures were prospectively randomized into being performed with a gelmat (*n*=50) or without (*n*=50). All subjects in the study completed a pre-, intra-, post- and 24-hour post-operative questionnaire. An independent observer recorded the number of stretches and postural changes due to discomfort during the procedure. The questionnaires evaluated baseline metrics and utilized a numeric pain scale to quantify discomfort in various muscle groups and joints. Procedures then were stratified further into those ≤60 minutes and those >60 minutes. The results were tabulated and univariate analysis was performed.

Results: The mean preoperative metrics for the gelmat and no gelmat groups were similar, with the exception of the ≤60 minute group which found the gelmat group starting with greater overall discomfort (1.7 vs. 1.3, p=0.0273). In the ≤60 minute group, gelmat use decreased post operative discomfort significantly (p=0.0435) and improved post operative energy (p=0.0411). In those procedures >60 minutes, the gelmat not only demonstrated improvements in post operative discomfort and energy, but also in the number of stretches and postural changes during the procedure.

Conclusion: Gelmat use in the endoscopic setting improves surgeon overall post-operative discomfort and energy in all cases. For cases >60 minutes duration, gelmats also decrease the number of stretches and postural changes due to discomfort. Some of these salutary effects may translate into more efficient surgery and better outcomes, particularly for longer and more challenging endoscopic surgical procedures.

Procedures ≤60 min			
	No Gelmat	**Gelmat**	**p-value**
OR Time	42.08	40.50	0.8989
Post-op Discomfort	2.06	1.58	0.0435
Post-op Energy	7.14	7.42	.0411
Procedures >60 min			
	No Gelmat	**Gelmat**	**p-value**
OR Time	107.21	109.50	0.8479
Posture Changes	3.5	2.0	0.0385
Stretches	1.93	0.65	0.0235
Post-op Discomfort	2.21	1.81	0.0480
Post-op Energy	6.36	6.73	0.0493

ABSTRACT 69

NOVEL ROBOT FOR TRANS-PERINEAL PROSTATE NEEDLE INTERVENTION: PHANTOM STUDY

Andrew J. Hung, Osamu Ukimura, Henry Ho, Christopher Cheng, Inderbir S. Gill, Mihir M. Desai

USC Institute of Urology, Keck School of Medicine, University of Southern California and Singapore General Hospital, Singapore

Purpose: To evaluate in phantom prostates the accuracy of a novel robotic ultrasound-guided intervention device, which may be utilized for active surveillance and focal therapy of prostate cancer in the near future.

Materials and Methods: The BioXbot (Biobot Surgical, Singapore) is an automated robotic intervention delivery device that utilizes 2D ultrasound imaging to create 3D planning models for needle delivery. Once the targets are designated in the 3D model, the robotic positioning system serially positions the delivery arm for each target. Needle is delivered transperineally with conformation to a dual-cone template in which a maximum of two skin puncture sites are required to cover the entire prostate. We first targeted the center of pre-made hypoechoic lesions randomly distributed within three commercially available prostate phantoms (Model 053MM, CIRS, Norfolk, Virginia). As we retracted the needle from each target, we injected colored dye to mark the needle tracts. After targeting and delivering the needles to the center of the hypoechoic lesions once, we re-positioned the BioXBot device and re-captured the images of the phantom prostate to create a new planning model. Re-targeting of the hypoechoic lesion centers was then performed a second time, and the needle tracts were inked as described. Additionally, we also targeted and delivered needles to additional areas of the phantom prostate away from the pre-made hypoechoic lesions following a sextet template. The first and re-targeted sextet needle tracks were all inked. Finally, we acquired 1-mm step MR imaging of the phantom prostates and utilized the images to measure the spatial distance between tips of the needle tracts and their intended targets.

Results: Each hypoechoic lesion was targeted twice (six needle tracts per phantom x three phantoms = 18 needle tracts) with the average distance from needle tip to lesion center being 3.81 ± 1.25 mm. Of note, the needle tip was successfully placed within all nine pre-made lesions in both rounds. The tips of the sextet-based needle tracts (18 additional needle tracts) were each re-targeted by ultrasound imaging with the average distance between the first and second needle tips 4.68 ± 1.18 mm (targeting hypoechoic lesions versus sextet biopsy tracts, $p = 0.06$. Some difficulty was encountered in visualizing the tips of the first sextet needle tracts by ultrasound and likely contributed to an increased error in accuracy.

Conclusions: The BioXBot allows automated delivery of intervention needles, robotically targeting and re-targeting lesions within the prostate currently with reasonable accuracy. Although presently limited by its lack of real-time imaging during targeting to confirm actual needle location (versus planned target), this device has a promising future for the management of low-risk prostate cancer by active surveillance or focal therapy.

ABSTRACT 70

A NOVEL 3.0 FR URETERAL STENT WITH DRAINAGE CHARACTERISTICS OF A 4.7 FR JJ STENT

Dirk Lange, Nathan Hoag, Beow Kiong Poh, Ben H. Chew

Department of Urologic Sciences, University of British Columbia, Canada

Introduction: Double J (JJ) stents are used to manage ureteric obstruction from urolithiasis. Because the majority of flow past the obstruction is extra-luminal, a newly developed 3.0 Fr cannula with a film occlusion mechanism on the proximal end (MicroStent, PercSys) is hypothesized to provide similar drainage as a 4.7 Fr stent. Anchoring of the stent proximally to the stone within the ureter may have minimal effects on peristalsis and the smaller stent may improve patient comfort. We sought to determine whether the overall flow past the 3 Fr MicroStent is comparable to conventionally used 4.7 Fr JJ stents.

Methods: An *in vitro* silicone ureter model and *ex vivo* porcine kidney/ureter model were used to measure the overall flow through obstructed and unobstructed ureters in the presence or absence of a 3.0 Fr JJ stent (Cook), 3.0 Fr MicroStent (PercSys), or 4.7 Fr JJ stent (Cook). Six measurements in two stone positions were performed and mean flow rates were compared with descriptive statistics.

Results: Mean flow rates (mL/min) through the obstructed silicone ureter (12 mm stone) for the 3.0 Fr MicroStent, 3.0 Fr JJ Stent, and 4.7 Fr JJ Stent were 326.7±13.3, 283.3±19.2, and 356.7±14.1, respectively. Flow as a percentage of obstructed flow in the *ex vivo* porcine ureter model was 60%, 53%, and 50%, respectively. In both ureteric models, differences in flow rates were not significant statistically between the 3 Fr MicroStent and the 4.7 Fr JJ stent.

Conclusion: The 3.0 Fr MicroStent provides drainage equivalent to a 4.7 Fr JJ stent, in both the *in vitro* silicone and *ex vivo* porcine urinary models. We have demonstrated the crucial first step that this 3.0 Fr stent employing a novel anchoring device has similar if not improved drainage compared to its larger counterpart.

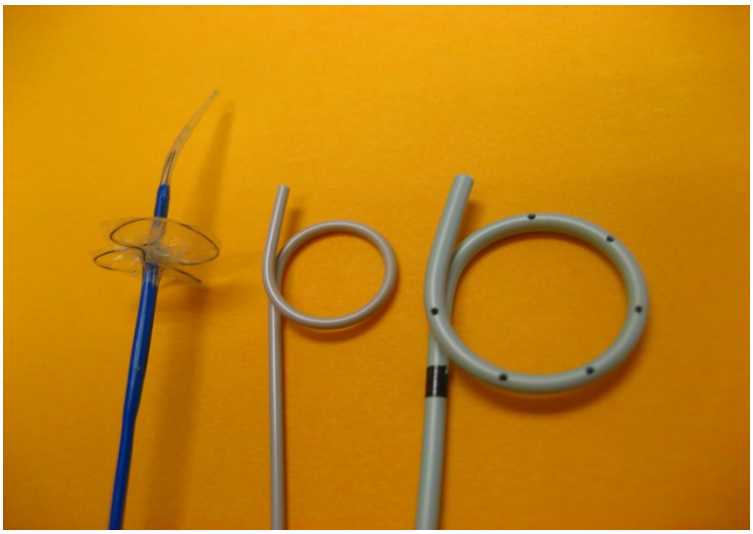

Figure 1. 3.0 Fr MicroStent (left), 3.0 Fr JJ stent (center), and 4.7 Fr JJ stent (right).

ABSTRACT 71

MINNESOTA ONLINE SURGICAL LEARNING MANAGEMENT PLATFORM FOR MULTI-INSTITUTIONAL VALIDATION STUDIES AND SKILLS ASSESSMENT

Yunhe Shen [a,b] , Divya Ambadipudi [a,c], Saurabh Jain [a,c], Vamsi Konchada [a,c], Carson Wong [d], Culley Carson [e], Claus Roehrborn [f] and Robert Sweet [a,b]

[a]*Center for Research in Education and Simulation Technologies, Univ. of Minnesota*
[b]*Department of Urologic Surgery, University of Minnesota*
[c]*Department of Computer Science and Engineering, University of Minnesota*
[d]*Department of Urology, University of Oklahoma Health Sciences Center*
[e]*Department of Surgery, University of North Carolina*
[f]*Department of Urology, University of Texas Southwestern Medical Center at Dallas*

Introduction: Virtual reality (VR)-based simulation training tools are an attractive training solution that provides objective, performance-specific data to the user and the proctor. Validation studies of residents on the learning curve have been limited in urology due to low subject numbers at individual institutions. In order to address this issue, we designed a web-based learning management platform (LMP) that facilitates instantaneous, coordinated data acquisition, access, display, and analysis across institutions worldwide.

Methods: Requirements of the LMP include online access for demographic registration, account management for individual users vs. individual sites vs. a central-administrator level management of curricula and simulation settings, and instantaneous performance-metrics acquisition, analysis, and display for numerous real-time surgical simulators. Figure 1 demonstrates the LMP software framework with a client-server structure that collects data over the internet/intranet or locally. A client-side agent program connects and interfaces specific surgical training software, and communicates with a standardized data-server via network protocols. A front-end web application on a web-server interfaces user access to the LMP database.

Results: We have completed, integrated and tested the design of the LMP and implemented the first proof-of-concept example with the GreenLight SIM™ laser simulation curriculum to support multi-institutional studies.

Conclusion: This represents the first web-based LMP for a specific VR simulation platform in surgery. The LMP has demonstrated the aforementioned functionalities, and can be integrated as a common module with our existing and future simulation-development projects.

Sources of Funding: University of Minnesota Vincent Johnson Breakthrough Fund and sponsored research from American Medical Systems.

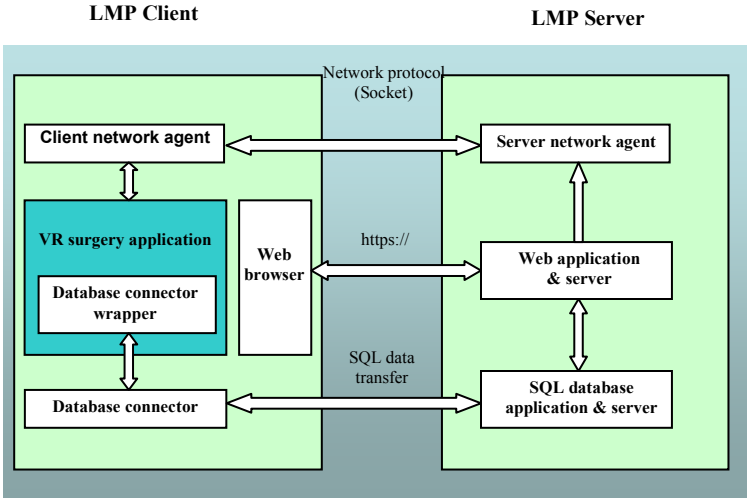

Figure 1. Client-Server framework for the Learning Management Platform

ABSTRACT 72

INFLUENCE OF HO:YAG PULSE MODIFICATION ON *IN VITRO* STONE DISINTEGRATION

Felix Pohl, Christopher Netsch, Andreas J. Gross, Thorsten Bach

Asklepios Hospital Barmbek, Hamburg, Germany

Introduction: Depending on size and density, Holmium:YAG laser disintegration of calculi can be a time consuming procedure. Therefore, strategies to improve stone disintegration are of major interest. We evaluated the effect of modifications in pulse sequence during Holmium:YAG laser lithotripsy in an *in vitro* model, using artificial calculi of varying densities.

Methods: Lithotripsy was conducted using 3 different types of artificial stones consisting of soft stone (plaster of Paris) and hard stone composition (Fujirock dental plaster grade 3 and 4). Ho:YAG laser stone fragmentation efficiency was evaluated *in vitro* at different pulse sequences at a standardized power output of 12 Watts (energy: 1.0 J, Pulse length 350 microsec.). Delivered energy was standardized to 750 Joule. Pulse sequence was modified. Therefore standard pulse sequence (A: 12 pulse/sec, pulse width 80 ms) was compared to modified sequences (B: 6 doublets/sec; C: 4 triplets/sec; D: 2 x 6 pulses/sec; E: 3 x 4 pulses/sec). All measurements were carried out 5 times. The volume was weighed by filling the resulting crater with fine granulated sand.

Results: With growing stone density, the volume of stone fragmentation decreased. The highest efficacy (ml/750 Joule) was achieved by standard pulse sequence (A) (see Table).

Mean [ml/750 J]	A	B	C	D	E
Sequence	IIIIIIIIII	II II II II II II	III III III III	IIIII IIIII	IIII IIII IIII
Plaster of Paris	0.52	0.25	0.31	0.34	0.37
Dental plaster Grad 3	0.37	0.23	0.27	0.27	0.39
Dental plaster Grade 4	0.33	0.16	0.24	0.27	0.29

Conclusion: Modifications in pulse sequence do not lead to improved stone disintegration.

ABSTRACT 73

DETERMINATION OF RENAL STONE COMPOSITION IN PHANTOM AND PATIENTS USING SINGLE SOURCE DUAL-ENERGY CT

Brian Eisner[1], Naveen Kulkarni[2], Daniella Pinho[2], Avinash Kambadakone[2], Mukta Joshi[2], Dushyant Sahani[2]

[1] *Department of Urology, Massachusetts General Hospital, Harvard Medical School*
[2] *Department of Radiology, Massachusetts General Hospital, Harvard Medical School*

Introduction: To characterize the urinary tract stones in phantom and patients using single source dual-energy CT (SS DECT).

Methods: Twenty stones of pure crystalline composition [Uric acid (UA), struvite, cystine, and calcium oxalate monohydrate (COM)] were assessed in a phantom and 11 patients (age 39-67 years) with urinary tract stones were evaluated. A low dose unenhanced CT (kVp-120, mA-150-450, NI-26, slice thickness -5 mm) was performed first followed by a targeted DECT acquisition on a SS DECT (Discovery CT 750 HDCT, GE). UA and non-UA stones were defined using a two-material decomposition (MD-Iodine/Water) algorithm. The stone effective atomic number (Zeff) was used to sub classify non-UA stones. The stone HU was also studied to determine its performance in predicting the composition. Ex-vivo chemical analysis of the stone served as a gold standard.

Results: Of the 59 verified stones (phantom=20 and patients=39, mean size- 6 mm) there were 16 UA and 43 non-UA type. The MD-DE images were 100% sensitive and accurate in detecting UA and non-UA stones. The Zeff accurately stratified struvite, cystine and calcium (COM) stones in the phantom. In patients, Zeff identified 100% UA (n=10) and 83% of calcium stones (n=24) as well as the dominant composition of 2 mixed stones (one 80% COM and 20% UA, the other 80% UA and 20% COM). The HU measurements alone were 71% sensitive and 69% accurate in detecting the UA stones.

Conclusion: SS DECT can predict UA and non-UA stone composition accurately *in vitro* and *in vivo*. Sub-stratification of non-UA stones of pure composition can be made *in vitro* and *in vivo*. In stones of mixed composition, the Zeff values reflect the dominant composition

ABSTRACT 74

JET EVACUATION TECHNIQUE (JET) FOR CALCULI EXTRACTIONDURING URETEROSCOPY

Rawandale AV, Kurane CS, Patni LG
Institute of Urology, Dhule, India.

Objectives: We describe an innovative "Jet Evacuation Technique (JET)" for easy and fast extraction of calculi during ureterorenoscopy.

Methods: Includes description of the JET and study of the advantages and pitfalls.
During ureteroscopy the "JET" is carried out as follows:
1. Place the ureteroscope in the bladder so that the orifice is seen in the centre of the field
2. Forcefully inject irrigating fluid through the sideport of the ureteroscope in 5-10 second pulses
3. Minor adjustments of the position of the scope may be required
4. See the fragments ejecting out of the orifice

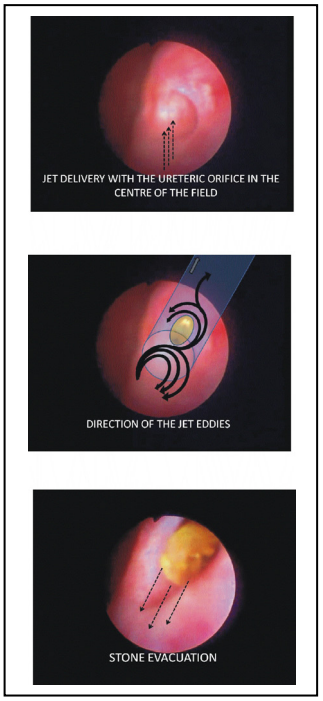

JET DATA	
Number	25
Mean age	33.52 (8-52)
Male : Female	4:1
History of previous surgery	1(4%)
Left	18
Right	7
Avg. stone size	11.6 mm
Fragments evacuated	21 (84%)
JET abandoned	4(16%)
Intra op complications	0

Results: Ureteroscopy for large calculi is associated with a large ureteric stone fragment load. Stone fragment evacuation at times may be tedious. The JET facilitates fragment evacuation without increasing the risk of fragment migration. Forceful jet of saline through the ureteroscope abuts on the posterior wall of the ureter causing a whirlpool effect just outside the ureteric orifice. Some whirls enter the ureteric orifice causing eddies with exponentially decreasing diameters in the ureter proximal to the calculi. This combination of whirls and eddies help calculi evacuation and prevents proximal migration by virtue of their circular direction and decreasing magnitude in the proximal ureter. The whirlpool effect is augmented in cases of complete ureteric obstruction due to an impacted proximal calculus making the evacuation of distal calculi easier.

Conclusion: We find the JET technique fast, safe, effective, inexpensive, and easy to learn and master. This is a standard fragment evacuation technique at our institute.

ABSTRACT 75

COMBINING SUBJECT-SPECIFIC PELVIC MODELING AND AMBULATORY MONITORING APPROACHES IN ASSESSING FEMALE SUI

Yingchun Zhang[1], Gerald W Timm[1], Nissrine A Nakib[1], Robert Sweet[1], Arthur G Erdman[2]
[1] Urologic Surgery, [2] Mechanical Engineering, University of Minnesota

Introduction: A subject-specific pelvic modeling approach has been developed to non-invasively assess urethrovaginal support function, which is an etiologic factor associated with stress urinary incontinence (SUI) in females. A validation study has been conducted to evaluate the performance of this approach in preparation for applying it to clinical population.

Methods: A 22-year-old female subject was recruited to participate in this University of Minnesota IRB approved study. Axial proton density and coronal T2-weighted high resolution MR images were obtained on the subject with a 3.0 Tesla scanner using a commercially available combined body-spine coil array for reception. The subject's specific pelvic model was constructed from her MR images using the subject-specific FE pelvic mesh model generation procedure. The BTS SMART-e motion capture system (BTS SMART, BTS S.p.A.) as shown in Fig 1 (a) and (b) was used to simultaneously measure dynamic biomechanical response and landing impact of her pelvis when she lands a jump. Reflective markers were fixed over the lower back to measure the landing impact of the pelvic bones (Fig 1 (e)) and other markers were fixed over other points of her pelvis to measure the induced biomechanical response (Fig 1(d)). The subject jumped off from a 0.5 feet-high table. The motion of each reflective marker was captured and corresponding landing velocities and accelerations were calculated. The dynamic structure-fluid interaction finite element (FE) analysis was performed using velocities of the left back marker to simulate dynamic biomechanical response of the pelvis. The simulated dynamic biomechanical responses were compared with the simultaneous recordings at same markers to evaluate the proposed pelvic modeling approach.

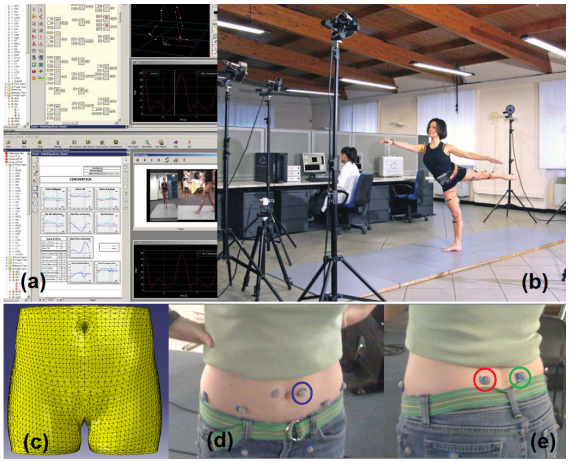

Fig 1. Validation protocol using the BTS SMART-e motion capture system. (a) SMART Analyzer, (b) motion capture system, (c) pelvic model of the 21-year-old female subject, (d) and (e) show the tracking marks on the female pelvis (marker in red, green and blue cycles indicates Left Back, Right Back and Left Belly marker respectively)

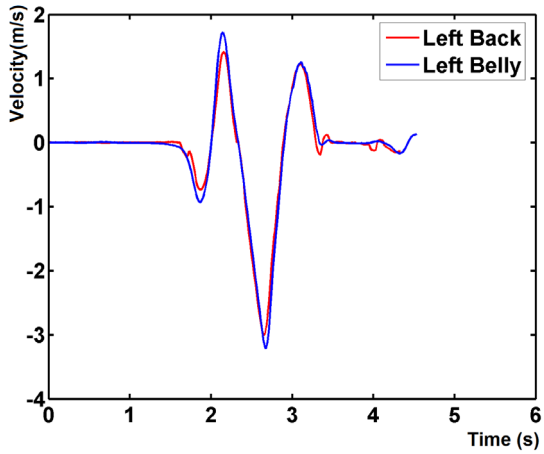

Fig 2. Velocity recordings of Left Back and Left Belly markers on the subject.

Results: The female pelvic FE model developed in this study consists of 35 anatomical parts including 10 pelvic muscles, 10 pelvic ligaments, 6 pelvic bones, skin, fat tissues, bladder, urethra, uterus, vagina, colon, rectum and anus. Figure 2 shows the velocity recordings of two markers of the pelvis, and we can clearly see the deference of dynamic measurements between the pelvic bone (Left Back Marker) and other soft organs (Left Belly marker). These measurements will be used to evaluate the performance of our pelvic modeling approach.

Conclusion: Evaluation results will be presented at the conference upon the completion of this study.

ABSTRACT 76

TARGETED IMAGING OF BLADDER CANCER WITH CANCER-SPECIFIC MOLECULAR CONTRAST AGENTS

Jen-Jane Liu[1,3], Ying Pan[1,3],Jens-Peter Volkmer[2] Katherine E. Mach,[1,3] Irving Weissman[2], Kristin Jensen[3], Joseph C. Liao[1,2]

[1]Department of Urology and [2]Institute for Stem Cell Biology and Regenerative Medicine, Stanford University and [3]Veterans Affairs Palo Alto Health Care System, Palo Alto, USA

Introduction: Current diagnosis of bladder cancer is by white light cystoscopy, which has suboptimal specificity for differentiating non-papillary cancer from inflammation. Probe-based confocal laser endomicroscopy (CLE) provides dynamic *in vivo* imaging of the endoluminal tracts with micron-scale resolution. Real-time analysis of confocal images remains challenging with non-specific contrast agents such as intravesical fluorescein. Tumor imaging specificity may be enhanced by coupling CLE with fluorescently labeled tumor-specific antibodies or peptides. We report our preliminarily efforts of *ex vivo* bladder tumor imaging by CLE using an antibody against a known human tumor-specific surface biomarker and a peptide that binds human epidermal growth factor receptor (EGFR) as contrast. Studies have shown that both the antibody and peptide bind surface markers abundant in cancer but absent on the surface of normal urothelium.

Methods: The tumor-specific antibody or the EGFR-binding 12-amino acid peptide was labeled with fluorescein isothiocyante (FITC) and instilled intravesically into a fresh cystectomy specimen (n=4 for antibody; n=1 for peptide). For a negative control, tumor-specific antibody was instilled into the renal pelvis of a radical nephrectomy specimen removed for RCC. After 15-30' incubation at 37^{o}C, the bladder was drained, opened, and imaged with a CLE system (Mauna Kea Technologies, Paris, France). Imaging was performed of normal-appearing, tumor, and suspicious areas, followed by excision of imaged tissues for histopathology with H&E. Tumor-specific staining with the antibody was further confirmed with immunofluorescence.

Results: All bladders had high-grade urothelial carcinoma on pathology. The tumor-specific antibody consistently showed greater fluorescent staining with CLE in areas of tumor, compared to normal urothelium in all 4 bladders (Figure 1). An erythematous area was not stained by the antibody and was confirmed to be inflammation by pathology. Immunofluorescence showed tumor-specific antibody on the most superficial layer of tumor but not on normal urothelium. Similarly, preferential staining of tumor compared to normal urothelium was observed when using the EGFR-binding peptide as a contrast agent. Imaging with tumor-specific antibody on normal urothelium from the renal pelvis of a nephrectomy specimen also did not show any fluorescent signal on CLE.

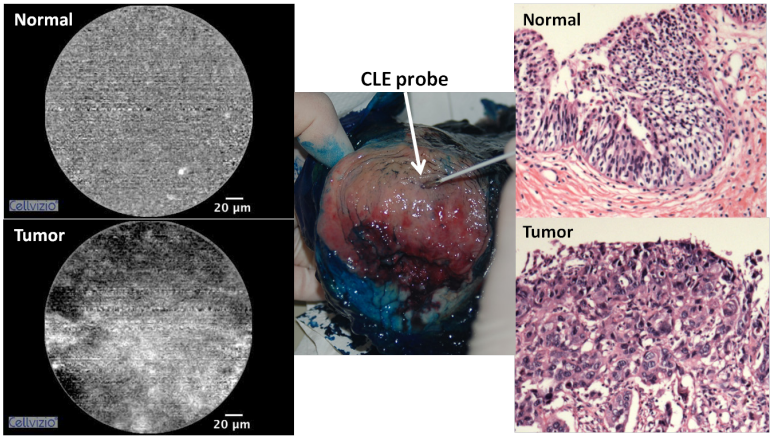

Figure 11: CLE of normal and tumor areas after administration of tumor-specific antibody. Corresponding H&E confirmed pathology.

Conclusion: Both the known tumor-specific antibody and EGFR-specific peptide show specificity for bladder cancer by CLE, *ex vivo*. Our study shows the feasibility of optical imaging of bladder cancer with CLE and tumor-specific contrast agents and raise the possibility of using intravesical molecular contrast agents for *in vivo* endoscopic targeted imaging of bladder cancer.

ABSTRACT 77

PROSTATE TUMOUR IDENTIFICATION USING A FORCE-SENSITIVE ROLLING INDENTATION PROBE

Pardeep Kumar[1], Jichun Li[2], Hongbin Liu[2], Ben Challacombe[1], Ashish Chandra[1], Lakmal Seneviratne[2], Kaspar Althoefer[2], Prokar Dasgupta[3]

[1] *Departments of Urology and Histopathology, Guys and St Thomas Hospital, London, UK*

[2] *Department of Mechanical Engineering, King's College, London, UK,* [3] *MRC Centre for Transplantation, NIHR Biomedical Research Centre, King's Health Partners, Guy's Hospital, London, UK*

Introduction: Dynamic force feedback is integral to traditional open surgical practice. Minimally invasive techniques reduce this sense of touch and in the case of robotic-assisted surgery, remove it altogether. We have developed a lightweight and potentially minimally invasive probe which provides haptic feedback. The probe has the potential to discriminate between malignant and benign prostatic tissues and has been validated in the *ex vivo* setting on the human prostate.

Methods: The rolling probe consists of a spherical metal roller and an ATI Nano 17 six-axis force/torque sensor (resolution 0.0003N). It is connected to a position-sensing device. This is currently a PHANTOM Omni (SensAble), which provides 6 degrees of freedom position sensing (Figure 1). Patients undergoing robotic-assisted radical prostatectomy were recruited with full ethical approval. Immediately following prostate removal, real time data were collected by the passage of the haptic probe over the excised specimen in a standardised manner covering all aspects of the perimeter (Figure 2). During the rolling indentation, the measured tissue reaction forces along the rolling paths are fused together to generate a map showing the stiffness distribution using Matlab software (Figure 3). The force feedback maps were correlated with pre-operative clinical examination, ultrasound guided prostate biopsies, staging MRI, and the final histopathology.

Results: As generally tumors are stiffer than the surrounding tissue, the tumor areas were indicated as higher stiffness, red colored areas. There was good correlation with clinical data, in particular for index lesions.

Conclusion: This is a new method to augment haptic feedback during robotic-assisted radical prostatectomy. It seems able to discriminate pathological tissue variations and could be used in a variety of settings. This may eventually reduce positive margins and allow more accurate nerve sparing to be performed. *In vivo* laparoscopic testing is planned.

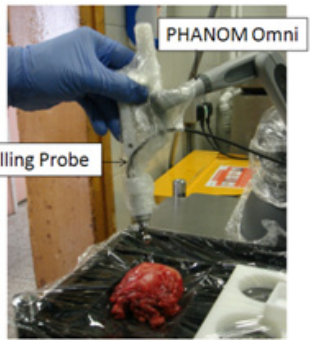

Fig. 1: Rolling probe and position sensing device set up for testing

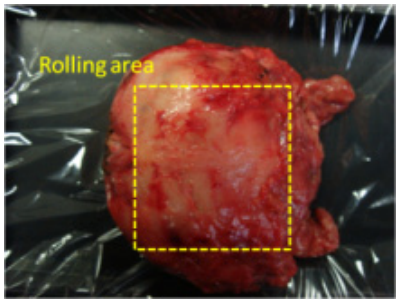

Fig. 2: Base of prostate prepared for rolling probe examination

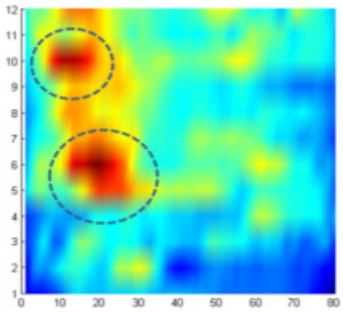

Fig. 3: Typical 2D map on excised human prostate identifying 2 apical index lesions

ABSTRACT 78

NOVEL ROBOTIC-ASSISTED PERCUTANEOUS ABLATION SYSTEM

Julien Guillotreau[1], Shahab Hillyer[1], Riccardo Autorino[1], Humberto Laydner[1], Rachid Yakoubi[1], Jérémy Guerin[2], Charles O'Malley[3], Mike White, Greg Spana, Robert Stein[1], Jihad Kaouk[1] Georges Haber[1]
1. Department of Urology, Glickman Urological and Kidney Institute, Cleveland Clinic 2. Medtech Innovative Surgical Technology. 3. Department of Radiology, Cleveland Clinic

Introduction: Ablative treatments are playing an increasingly important role in the management of small renal masses. Percutaneous image-guided tumor ablation has demonstrated low morbidity with encouraging renal function and oncological outcomes. ROSA™ is a new robotic system, initially developed for neurosurgical treatments, which has shown precision in instrument guidance. The aim of this study was to evaluate the feasibility and accuracy of this platform for percutaneous renal focal therapy.

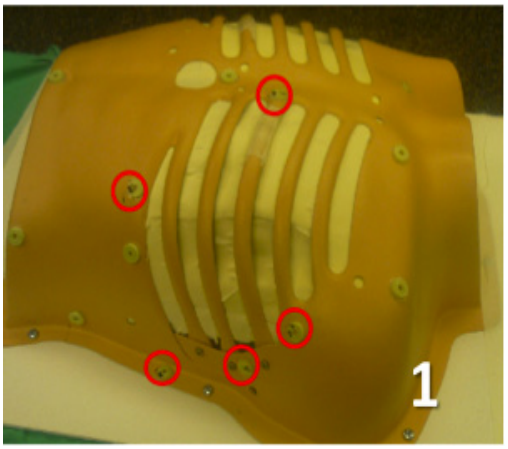

Methods: Incremental targets were placed inside a body model. Fiducial markers were subsequently placed at time of the 3D CT scan acquisition (Figure 1). DICOM data were transferred to the ROSA™ system. After synchronization, preplanification consisted of defining the entry point, trajectory and target point (Figure 2).
The robotic arm steered into position allowing manually insertion of the probe into the target (Figure 3). Accuracy then was evaluated.

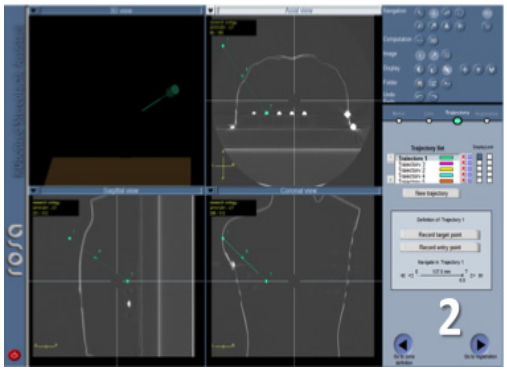

Results: 10 targets were used. Average targets volume and size were 1.15 ± 0.7 ml and 11.3 ± 4.3 mm. Preplanification was successful in all cases. Synchronization was obtained with a registration error of 2.23 mm. Median trajectory length was 142 mm (range 115-201 mm). All probes successfully reached the planned target (Figure 4).

Conclusion: Herein, we present the first urological application of the ROSA™ platform. Robotic assistance for percutaneous ablation of renal tumors is feasible and offers precise guidance for probe positioning in preclinical studies. Clinical evaluation is ongoing.

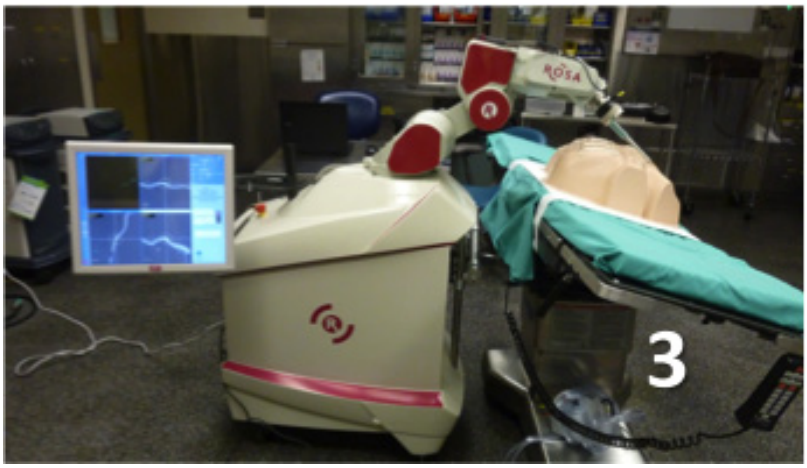

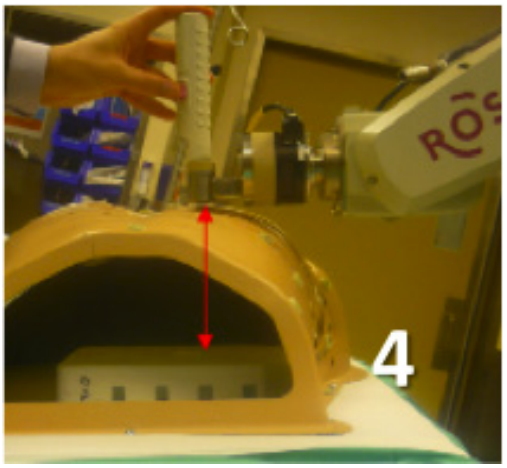

ABSTRACT 79

INFLUENCE OF ULTRASOUND SYSTEM SETTINGS ON KIDNEY STONE DETECTION

JC Kucewicz[1], B Dunmire[1], MR Bailey[1]
[1] *Center for Industrial and Medical Ultrasound, Applied Physics Laboratory, University of Washington, Seattle, Washington, USA*

Introduction: The twinkling artifact (TA) is the rapidly changing, random pattern of colors on and deep to kidney stones often observed during ultrasound color Doppler imaging. The potential clinical benefit of TA to urology and other medical specialties is well documented, but the use of TA is not without limitations. The origin of the artifact is not well understood, it appears to be influenced by multiple system settings, and without a specific knob to control it, twinkling can be intermittent. Furthermore, twinkling can be misinterpreted as true blood flow reducing its sensitivity to the detection of stones. Color Doppler imaging consists of the transmission and reception of a sequence of ultrasound pulses followed by a series of signal processing and imaging processing steps that are optimized to detect blood flow and that are often outside of the control of the clinical user. In order to better understand the origin of TA and further the development of a stone-specific ultrasound imaging method, "raw" ultrasound data were collected, processed, and analyzed to determine the influence of acoustic output and amplifier gain on TA and to determine the differentiability of twinkling and blood flow.

Methods: A tissue phantom containing both a human *ex vivo* kidney stone and 5 mm flow channel was constructed. Water with cellulose was pumped through the flow channel to simulate blood flow under normal and turbulent flow conditions. Ultrasound data prior to any color Doppler-specific signal and image processing were collected with an Ultrasonix RP (Ultrasonix Medical Corporation, Canada) while varying acoustic output and two parameters related to amplification of the received ultrasound signals. Twinkling was measured using an autocorrelation Doppler method and an autoregressive Doppler method. Discriminate analysis was used to test the differentiability of twinkling and blood flow.

Results: Twinkling was correlated directly with both acoustic output and amplifier gain. Both Doppler methods performed comparably with stone detection using TA and differentiating TA from blood flow (Figure 1) although the autoregressive method performed marginally better with the former and the autocorrelation method performed marginally better with the latter. Differentiability of TA and blood flow degraded under turbulent flow conditions.

Conclusion: The potential of stone detection using TA is promising but not without pitfalls. Until ultrasound systems include a stone-specific imaging method, clinical users must manually adjust system settings including maximizing both output and gain to produce TA.

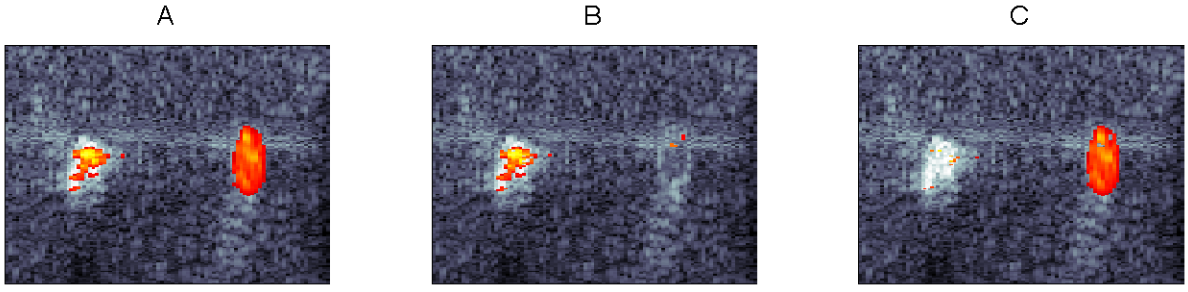

Figure 12: A) Power Doppler image of a "twinkling" kidney stone and laminar blood flow. B) Power Doppler image optimized for stone detection. C) Power Doppler image optimized for blood flow detection.

Acknowledgements: This work was supported by the National Institutes of Health (DK43881, DK86371) and the National Space Biomedical Research Institute through NASA NCC 9-58.

ABSTRACT 80

FREEHAND 3D-TRUS PROSTATE BIOPSY MAPPING : first clinical results

Mozer P[1], Baumann M[2] ,Chevreau G[1], Coffin G[1], Renard-Penna R[1], Troccaz J[2]

[1] *Department of Urology, Pitié-Salpêtrière Hospital, Pierre et Marie Curie University (Paris VI) Paris, France.*

[2] *TIMC Laboratory, IN3S, Faculté de Médecine, Domaine de la Merci, 38706 La Tronche Cedex, France.*

Objective: Primary objective was to determine the robustness of the Urostation (Koelis, France), which provides 3D mapping of transrectal prostate biopsies (Figure 2). Secondary objectives were to ensure that the device does not modify routine clinical practice and to determine the impact of performing additional biopsies in undersampled zones.

Design, Setting, and Participants: The method is based on 3D transrectal ultrasound (3D TRUS). We use a 3D TRUS probe on a Sonoace X8 scanner (Medison, Korea), linked to the computer with a network cable (Figure 1). The 3D cartography is based on an automatic registration method. The clinical workflow is unchanged, meaning that biopsies are performed under local anesthesia with the patient on the left side. An initial "reference" 3D image of the prostate is recorded before starting the biopsy sampling. After every biopsy gun shot, the needle is left in the prostate less than 3 seconds while a 3D TRUS image is transferred to the computer, and displayed in 3D on the reference prostate. The clinician may rotate, zoom or reslice the 3D prostate and biopsies using a trackball. Alternatively, a 3D TRUS image may be transferred before a biopsy shot in order to check the actual biopsy target, that can be reached afterwards providing the probe is unmoved. 222 patients requiring prostate biopsies either for the diagnosis of prostate cancer or to detect recurrence following external beam radiotherapy or HIFU were included. All biopsies were performed by a single operator. All patients were biopsied according to a protocol of 12 biopsies. Additional biopsies were performed when the operator considered that a zone was undersampled at the end of protocol. Robustness was defined as the number of correctly positioned biopsies divided by the total number of biopsies performed. The absence of modification of routine clinical practice was determined by the procedure time and the pain experienced by the patient scored on a visual analogue scale between 0 and 10.

Figure 1 - Left : Laptop, Middle : UltraSound, Right : Patient

Results and Limitations: A total of 3,246 biopsies were performed. Robustness was 96% and was not modified in patients previously treated by external beam radiotherapy or HIFU. The mean time required to perform a series of 12 biopsies was 13 minutes. Additional biopsies were performed in undersampled zones in 55 patients (25%) and were positive in 7 patients (13%). Two (29%) of these patients had negative standard biopsies.

Conclusions: The Urostation provides precise transrectal prostate biopsy mapping with no significant modification of routine clinical practice. The potential of this system is above all the possibility to create for each patient a precise map of sampled areas without significant change in routine clinical practice. Moreover, it can be used in the near future in order to merge repeated biopsy sessions or to plan an accurate focal therapy treatment.

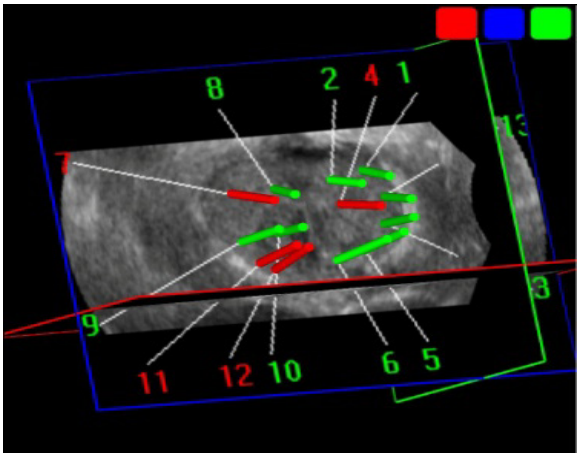

Figure 2 : Representation of the prostate showing 12 biopsies from a posterior view. Green biopsies are negative and red biopsies are positive.

ABSTRACT 81

RAPIDLY DEPLOYABLE TELEROBOTIC SLAVE FOR TRANSURETHRAL EXPLORATION AND INTERVENTION

Roger E. Goldman[1], Lara K. Suh[2], Andrea Bajo[3], Mitchell C. Benson[2], Nabil Simaan[3]
[1] *Department of Biomedical Engineering, Columbia University, New York, NY*
[2] *Department of Urology, Columbia University Medical Center, New York, NY*
[3] *Department of Mechanical Engineering, Vanderbilt University, Nashville, TN*

Introduction: Bladder cancer, a significant cause of morbidity and mortality worldwide, presents a unique opportunity for aggressive treatment due to the ease of accessibility for visualization and resection. While the location affords advantages, transurethral resection of bladder tumors (TURBT) is limited by current instrumentation posing difficult challenges for surgeons. We are developing a rapidly deployable telerobotic slave to improve intravesicular visualization, dexterity and accuracy of resection with the aim of reducing complication rates for TURBT procedures.

Methods: A novel TURBT device must meet the clinical requirements of the current procedures while extending capabilities toward improving current techniques and providing instrumentation for novel procedures. The development has focused on combining new imaging capabilities and dexterity for en-bloc resection of bladder tumors. Kinematic analysis was performed in the Matlab computing environment to assess the workspace of the prototype design for resection throughout the bladder.

Results: The proposed telerobotic slave uses a snake-like continuum robot providing intravesicular dexterity and compatibility with a standard resectoscope (Figure 1). Instrument lumens provide working channels for light-based imaging, wire or laser resection instrumentation and novel imaging devices. Analysis shows the device is capable of visualizing and reaching throughout the bladder, including anterior aspects. A cross section of the reachable workspace is shown in Figure 2.

Conclusion: A novel telerobotic slave is under development for precision resection during TURBT procedures. The platform provides capability of delivering simultaneous visualization and precision resection in a telerobotic slave system that can be rapidly deployed in transurethral urologic procedures. Computer assistance, augmented visualization and intravesicular dexterity will assist in improvement of TURBT procedures.

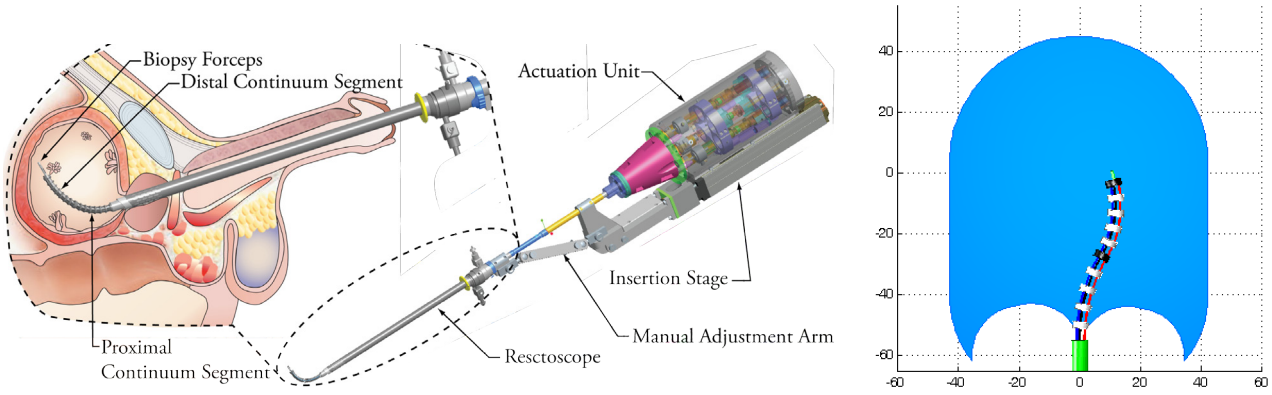

Figure 1: Telerobotic slave for TURBT: Design and cross section of the reachable workspace

ABSTRACT 82

USE OF THE ROBOTIC BOWEL CLAMP FOR RENAL HILAR CONTROL

Aria A Razmaria[1], Pablo E Marchetti[1], Sergey Shikanov, Arieh L Shalhav[1]
[1] *University of Chicago Medical Center*

Introduction: We sought to evaluate the effectiveness of the da Vinci® bowel clamp EndoWrist® instrument compared to routinely used bulldog clamp for renal hilar control in an experimental setting.

Methods: The study was performed on the porcine animal model. The standard da Vinci system was used for the series of experiments. The robotic bowel clamp has a 4 cm long tip with coarsely ribbed and centrally fenestrated grip panel. Under general anesthesia and in flank position the kidney was exposed through a subcostal flank incision and renal hilum skeletonized. As the first experiment the renal artery was clamped directly with the robotic instrument, an upper pole partial nephrectomy performed and hemostasis assessed. As a subsequent experiment, the renal artery while clamped was directly transected and bleeding evaluated. To assess and compare potential direct mechanical tissue damage by the clamp to the vessel wall, in series of experiments renal artery and vein separately as well as *en bloc* were clamped for 20 and 40 minutes. Vessel segments then were harvested and examined histologically by a "blinded" pathologist. The contralateral kidney with the hilum being controlled by the bulldog clamp served as control in all experiments.

Results: Adequate hemostasis comparable to the bulldog clamp was achieved by the robotic instrument in all experiments. The robotic bowel clamp allowed also for a scaled vessel occlusion according to the degree of instrument closure. In the histologic examination assessing specifically direct tissue crushing effects, no differences between the specimens of different clamping techniques were observed. Accordingly, in tissue specimens clamped for increasing time intervals similar findings between the two groups were observed.

Conclusion: The robotic EndoWrist® bowel clamp demonstrated effective renal vascular clamping properties in this study. Due to the significantly enhanced degrees of movement, the robotic instrument may allow for easier and faster clamp placement and removal facilitating more selective renal vascular occlusion compared to bulldog clamps.

Figure 1: Comparison of the Bulldog clamp with the robotic EndoWrist® bowel clamp. Harvested renal artery segments for histological assessment are demonstrated.

ABSTRACT 83

VISUAL MEASUREMENT OF SUTURE STRAIN FOR ROBOTIC SURGERY

Aria Razmaria[1], Young Soo Park [2], Nachappa Gopalsami[2], Gregory Zagaja[1], John Martell[1]
[1] University of Chicago, Department of Surgery, [2]Argonne National Laboratory

Introduction: A limitation of the DaVinci surgical system is a lack of direct sensory feedback to the operative surgeon. Experienced robotic surgeons use visual interpretation of tissue and suture deformation as a surrogate for tactile feedback. One of the difficulties encountered during robotic surgery is maintaining adequate suture tension while tying knots or following a running anastamotic suture. Measuring and displaying suture strain in real time has potential to decrease the learning curve and improve the performance and safety of robotic surgical procedures. Conventional strain measurement methods involve installation of complex sensors on the robotic instruments. This study presents a non- invasive image processing video-based method to determine strain in surgical sutures.

Methods: To measure suture strain, we employed a suture that was pre-marked with a set of dark markers at regular intervals. Shown in Figure 1 is a marked suture held between the two grippers of a surgical robot. The suture strain is measured by video detection of the displacement of these markers upon tension. The image processing algorithm is composed of image enhancement (color channel selection), edge detection, line detection (Hough transform), line profiling and marker detection, marker tracking (quadratic regression), and strain computation. The video analysis method was developed and validated using video of suture strain standards on an Instron 8500 + servo-hydraulic testing system. Strain calculations were implemented in two ways: one point tracking and two point tracking.

Results: These tests showed a minimum detectable strain of 0.2% for one marker tracking on stationary suture and 0.5% for the more clinically relevant two-marker tracking on moving suture. These minimum detectable strains are two orders of magnitude smaller than the known strain to failure of most suture materials (20+%), allowing a large margin of safety in the clinical setting.

Conclusion: This study presents a non-invasive method based on a video algorithm to calculate suture strain from the surgical video images, thus avoiding the complex installation of strain sensors.

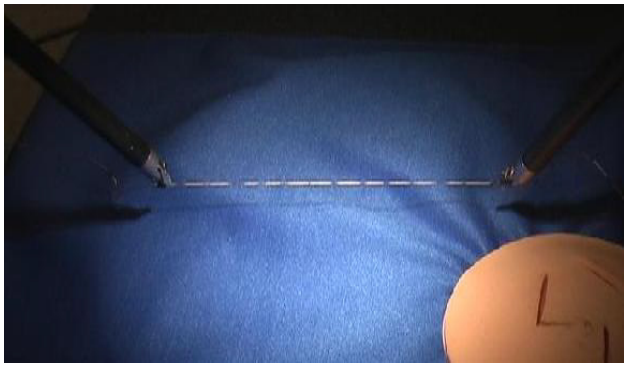

Figure 1. Marked 2.0 Dexon II suture held by the two robotic needle holders

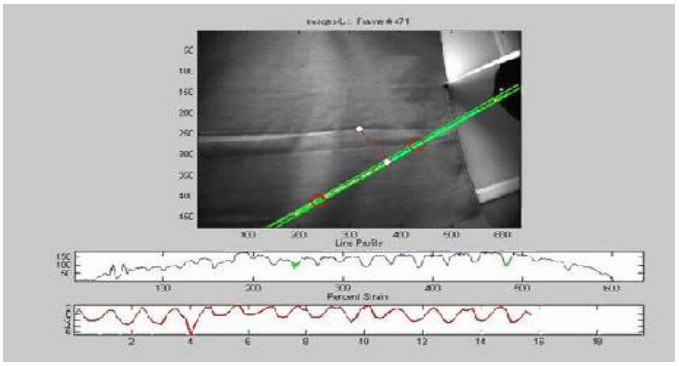

Figure 2. Snapshot of the video processing for strain measurement display

SOCIETY OFFICERS:

George Nagamatsu, M.D.
Society Founder

President
Manoj Monga
Hessel Wijkstra

Vice-President
Stephen Nakada
Sean Hedican

Secretary
Jack Vitenson

Treasurer
John Denstedt

Councilor
Louis Kavoussi

Executive Director
Dan Stoianovici

ADVISORY BOARD

Jeffrey Cadeddu

Ralph Clayman

Jean de la Rosette

John Denstedt

Thomas Lawson

Pierre Mozer

Stephen Nakada

Koon Ho Rha

William Roberts

Arthur Smith

Li-Ming Su

Gerald Timm

AWARDS:

Best Paper Award:

MODELING OF MAGNETIC TOOLS FOR USE WITH SUPERPARAMAGNETIC PARTICLES FOR MAGNETIC STONE EXTRACTION

YK Tan[1], Raul Fernandez[2], Sara L Best[1], Ephrem O Olweny[1],Stacey L McLeroy[3], Bruce E Gnade[3], Margaret S Pearle[1], Jeffrey A Cadeddu[1]

[1]University Texas Southwestern, [2]University of Texas at Arlington, [3]University of Texas at Dallas

Outstanding Paper Awards:

COMPUTER SIMULATIONS OF THERMAL DAMAGE TO THE HUMAN VAS DEFERENS DURING NONINVASIVE LASER VASECTOMY

Gino R. Schweinsberger, Christopher M. Cilip[1], Nathaniel M. Fried[1,2]

[1] Department of Optical Science and Engineering, University of North Carolina at Charlotte, NC

[2] Department of Urology, Johns Hopkins Medical Institutions, Baltimore, MD

Top 9 Abstracts:

3. **THREE-DIMENSIONAL IMAGING OF URETER WITH ENDOSCOPIC OPTICAL COHERENCE TOMOGRAPHY,** Hui Wang, Wei Kang, Hui Zhu, Gregory MacLennan, Andrew Rollins, *Case Western Reserve University, Cleveland, OH*
4. **TARGETED IMAGING OF BLADDER CANCER WITH CANCER-SPECIFIC MOLECULAR CONTRAST AGENTS,** Jen-Jane Liu[1,3], Ying Pan[1,3],Jens-Peter Volkmer[2] Katherine E. Mach,[1,3] Irving Weissman[2], Kristin Jensen[3], Joseph C. Liao[1,2], *[1]Department of Urology and [2]Institute for Stem Cell Biology and Regenerative Medicine, Stanford University and [3]Veterans Affairs Palo Alto Health Care System, Palo Alto, USA*
5. **REAL TIME DIAGNOSIS OF BLADDER CANCER WITH PROBE-BASED CONFOCAL LASER ENDOMICROSCOPY: A PROSPECTIVE DIAGNOSTIC ACCURACY STUDY,** Jen-Jane Liu,[1,2] Shelly T. Hsiao,[2] Ying Pan,[1] Katherine E. Mach,[1,2] Alex McMillan,[3] Kristin Jensen,[2] Joseph C. Liao[1,2], *[1] Department of Urology, Stanford University, USA [2] Veterans Affairs Palo Alto Health Care System-Palo Alto, USA, [3] Department of Health Research and Policy, Stanford University, USA*
6. **WEB-ACCESSIBLE 3D ANATOMY SOFTWARE OF UROLOGIC PATHOPHYSIOLOGICAL CONDITIONS AND PROCEDURES FOR PATIENT EDUCATION,** D. B*urke*[1,2], X. Z*hou*[1,2], V. R*otty*[2], B. K*onety*[1], R. S*weet*[1,]2, *1 Urologic Surgery, Medical School, University of Minnesota, Minneapolis, MN[2] Center for Research in Education and Simulation Technologies (CREST), University of Minnesota, Minneapolis, MN*
7. **HIGH FREQUENCY ULTRASOUND IMAGING DURING NONINVASIVE LASER COAGULATION OF THE CANINE VAS DEFERENS, *IN VIVO*,** Christopher M. Cilip[1], Phillip M. Pierorazio[2], Ashley E. Ross[2], Mohamad E. Allaf[2], Nathaniel M. Fried[1], *[1] Department of Optical Science and Engineering, University of North Carolina at Charlotte, NC, [2] Department of Urology, Johns Hopkins Medical Institutions, Baltimore, MD*
8. **NOVEL ROBOT FOR TRANS-PERINEAL PROSTATE NEEDLE INTERVENTION: PHANTOM STUDY,** Andrew J. Hung, Osamu Ukimura, Henry Ho, Christopher Cheng, Inderbir S. Gill, Mihir M. Desai, *USC Institute of Urology, Keck School of Medicine, University of Southern California, Singapore General Hospital, Singapore*
9. **A NOVEL LAPAROSCOPIC CAMERA FOR CHARACTERIZATION OF RENAL ISCHEMIA USING DLP® HYPERSPECTRAL IMAGING: INITIAL EXPERIENCE IN A PORCINE MODEL,** Ephrem O. Olweny[1], Sara L. Best[1], Neil Jackson[1], Eleanor F. Wehner[1], Samuel K. Park[1], Yung K. Tan[1], Abhas Thapa[1], Karel J. Zuzak[2], Jeffrey A. Cadeddu[1], *[1]Dept of Urology, University of Texas Southwestern Medical Ctr., Dallas, TX,[2]Digital Light Innovations, Austin, TX*

AWARDS:

Best Reviewer Awards:

Thorsten Bach
(2007, 2008, 2010, 2011)

Brian Eisner
(2009, 2011)

Mohamed Elkoushy

Avinash Kambadakone

Watid Karnjanawanichkul

Bodo Knudsen

Thomas Lawson
(2009, 2011)

Sutchin Patel
(2010, 2011)

Cristian Surcel

Hessel Wijkstra

Kevin Zorn
(2007, 2008, 2009, 2010, 2011)

REVIEW COMMITTEE:

The paper review committee has been assembled by e-mail solicitation. Fifty six reviewers from around the world participated. We gratefully acknowledge their contribution to the success of the meeting and thank them for taking the time to help the society.

Fatih Altunrende
Sero Andonian
Thorsten Bach
Viorel Bucuras
G. Bumbu
Tyler Bunch
Scott Castle
Doyoung Chang
Brian Eisner
Mohamed Elkoushy
Nathaniel Fried
Michael Gorin
Andreas Gross
Boris A Hadaschik
Henry Ho
Wahib Isac
Avinash Kambadakone
Watid Karnjanawanichkul
Mathias Keil
Chunwoo Kim
Hyungjoo Kim
Bodo Knudsen
John Kucewicz
Timur H Kuru
Jaime Landman
Thomas Lawson
Humberto Laydner
Evangelos Liatsikos
Rabii Madi
Cristian Mirvald
Massimo Mischi
George Mitroi
Pierre Mozer
Shyam Natarajan
Zhamshid Okhunov
Ephrem Olweny
Villalon Oscar
Athanasios Papatsoris
Sutchin Patel
Phillip Pierorazio
Thomas Polascik
A V Rawandale
Aria Razmaria
William Roberts
Ornob Roy
Nelson Salas
George Schade
Bradley Schwartz
Dan Stoianovici
Cristian Surcel
Gorbatiy Vladislav
Hessel Wijkstra
Rachid Yakoubi
Yingchun Zhang
Hui Zhu
Kevin Zorn

Special thanks to **Dr. Thomas Lawson** for his contributions to the review process and help formatting and editing this program.

We thank **Michelle Paoli** and **Debra Caridi** for their help organizing the Annual Meeting.